

Physical Controls on Low and Mid-Latitude Marine Primary Productivity

by

Apurva Chandrakant Dave

Earth and Ocean Sciences
Duke University

Date: _____

Approved:

M. Susan Lozier, Supervisor

Richard T. Barber

Nicolas Cassar

Richard G. Williams

Dissertation submitted in partial fulfillment of
the requirements for the degree of Doctor of Philosophy
in Earth and Ocean Sciences
in the Graduate School
of Duke University

2012

ABSTRACT

Physical Controls on Low and Mid-Latitude Marine Primary Productivity

by

Apurva Chandrakant Dave

Earth and Ocean Sciences
Duke University

Date: _____

Approved:

M. Susan Lozier, Supervisor

Richard T. Barber

Nicolas Cassar

Richard G. Williams

An abstract of a dissertation submitted in partial fulfillment of
the requirements for the degree of Doctor of Philosophy
in Earth and Ocean Sciences
in the Graduate School
of Duke University

2012

Copyright by
Apurva Chandrakant Dave
2012

Abstract

Strengthened stratification of the upper ocean, associated with either anthropogenic warming trends or natural climate oscillations, is generally expected to inhibit marine primary productivity at low and mid latitudes, based on the supposition that increased water column stability will decrease vertical mixing and consequently the upward entrainment of deep nutrients into the euphotic zone. Herein, we examine the local stratification control of productivity over the subtropical and equatorial Pacific by directly comparing a wide range of contemporaneous metrics, drawn from the modern observational record, for interannual stratification and productivity variability. We find no correlation between the two in the subtropical North Pacific. In the equatorial Pacific we do observe a correlation, but find no evidence of a strong causal connection between the two—instead, our analysis suggests that both biomass and stratification in this region are impacted by changes in the westward transport, via surface currents, of relatively cold, nutrient-rich waters that have been upwelled in the eastern Equatorial Pacific. The importance of horizontal nutrient supply is further evidenced by an analysis of seasonal variability in the subtropical North Atlantic, where the annual contraction and expansion of the oligotrophic region appears to be strongly influenced by the waxing and waning, respectively, of lateral nutrient transfers from neighboring, nutrient rich waters of the subpolar gyre and the West African upwelling zone.

Dedication

To Sejal (even though she probably won't read past this page), Ishan and Anjali. This dissertation has taken up almost all of my waking hours, but my first and last thoughts every day have been of you.

Contents

Abstract.....	iv
List of Tables.....	x
List of Figures	xi
Acknowledgements	xiv
Introduction.....	1
1. Local Stratification Control of Marine Productivity in the Subtropical North Pacific.....	3
1.1 Introduction	3
1.2 Background	6
1.2.1 Controls on subtropical productivity.....	6
1.2.2 Linkages to climate.....	10
1.3 Study objectives	12
1.4 Methods	13
1.4.1 Hydrographic and Biogeochemical Data	13
1.4.2 Isotopic composition of particulate nitrogen export flux	14
1.4.3 Climate and wind data.....	15
1.4.4 Data analysis	17
1.5 Results and discussion	18
1.5.1 Seasonal variability	18
1.5.1.1 Upper layer	19
1.5.1.2 Lower layer.....	21

1.5.2 Interannual variability at Station ALOHA.....	23
1.5.2.1 Stratification and productivity in the upper and lower layers.....	23
1.5.2.2 Alternate processes and time scales.....	27
1.5.3 Linkages to climate variability	30
1.5.4 Why no interannual linkages to stratification?.....	37
1.6 Conclusions	40
2. The Role of Stratification and Advection in Driving Productivity in the Subtropical North Pacific and Equatorial Pacific	43
2.1 Introduction	43
2.2 Background	48
2.2.1 Factors controlling local nutrient supply	48
2.2.2 Equatorial Pacific.....	50
2.3 Study objectives.....	50
2.4 Comparing basin-wide measures of in situ stratification and satellite productivity.....	53
2.4.1 Linking chl- <i>a</i> and stratification	53
2.4.2 Subtropical North Pacific	55
2.4.3 Equatorial Pacific.....	58
2.5 Considering the influence of wind-driven horizontal advection on biomass variability in the equatorial Pacific	60
2.5.1 CWEPAC	61
2.5.2 EEPAC	65
2.5.3 Horizontal advection.....	68
2.5.3.1 Climatological.....	68

2.5.3.2 Interannual variability.....	74
2.6 Conclusion	80
3. The impact of seasonal variability in horizontal advection on oligotrophic geometry in the subtropical North Atlantic	83
3.1 Introduction	83
3.2 Background	85
3.2.1 Climatological geometry of the oligotrophic region in the North Atlantic	85
3.2.2 Oligotrophy and nutrient supply.....	87
3.3 Seasonal cycle in oligotrophic geometry and intensity	90
3.4 Seasonal role of advective nutrient fluxes	92
3.5 Conclusions	105
APPENDIX A (Chapter 2)	109
A.1 Data Description	109
A.1.1 Hydrographic profile data	109
A.1.2 Climatological Hydrographic Fields.....	110
A.1.3 Re-analyzed Hydrographic Fields.....	110
A.1.4 Biogeochemical Data	111
A.1.4.1 Chlorophyll.....	111
A.1.4.2 Productivity Estimates	112
A.1.4.3 Nutrient Data.....	112
A.1.5 Wind data.....	112
A.1.6 Surface Current Data.....	113

A.2 Basin-scale comparison of stratification and chl-a.....	113
A.2.1 Contemporaneous measures.....	113
A.2.1.1 Use of capture-radii	114
A.2.1.2 Whole-domain averaging.....	115
A.2.2 Calculating interannual variability	115
A.2.3 Additional comparisons of stratification and chl- <i>a</i> / productivity	116
A.3 Spatial correlations in the equatorial Pacific	117
A.4 Advective flux and divergence calculations	117
Appendix B (Chapter 3)	126
B.1 Data.....	126
B.1.1 Chlorophyll, productivity and nutrients.....	126
B.1.2 Winds and currents.....	126
B.2 Methods.....	128
B.2.1 Delineation of the oligotrophic region and the subtropical gyre	128
B.2.2 Horizontal advective nutrient fluxes	129
References.....	131
Biography.....	142

List of Tables

Table 1-1: Correlations between stratification and productivity on interannual time scales at Station ALOHA.....	26
Table 1-2: Correlations between productivity and other properties on interannual time scales at Station ALOHA.....	28
Table 2-1: Climatological scaling analysis for processes providing nitrate in the equatorial Pacific	71

List of Figures

Figure 1-1: Long term average vertical profiles at HOT Station ALOHA.....	8
Figure 1-2: Seasonal time series of average monthly upper and lower euphotic zone properties at HOT Station ALOHA.....	20
Figure 1-3: Chlorophyll- <i>a</i> (chl- <i>a</i>) and productivity versus stratification at Station ALOHA..	24
Figure 1-4: Stratification and primary productivity at Station ALOHA before and after the strong ENSO/PDO transition in July 1998.....	32
Figure 1-5: Correlation of basin-scale climate processes to ecosystem variability at HOT Station ALOHA.	33
Figure 1-6: Interannual anomalies in stratification and productivity at Station ALOHA.	39
Figure 2-1: Annual mean chl- <i>a</i> concentrations in the Pacific.	47
Figure 2-2: Climatological fields of surface biomass, nutrients, winds and temperature in the equatorial Pacific.	52
Figure 2-3: Hydrographic data coverage in the Pacific.	54
Figure 2-4: A comparison of stratification and surface chl- <i>a</i> variability over the entire subtropical North Pacific.	56
Figure 2-5: A comparison of stratification and surface chl- <i>a</i> variability over the entire equatorial Pacific.	59
Figure 2-6: Local temporal correlations between chl- <i>a</i> and wind variability in the equatorial Pacific	62
Figure 2-7: Local, temporal correlations between chl- <i>a</i> , T, stratification and winds in the equatorial Pacific.	63
Figure 2-8 Annual mean chl- <i>a</i> total surface current vectors in the equatorial Pacific.	67
Figure 2-9: Horizontal and vertical advection of mixed layer nitrate into the CWEPAC and EEPAC study regions.	75

Figure 2-10: Time series of average chl- <i>a</i> concentrations versus advective fluxes of mixed layer nitrate in the CWEPAC region.....	77
Figure 2-11 Time series of average chl- <i>a</i> concentrations versus advective fluxes of mixed layer nitrate in the EEPAC region	79
Figure 3-1: Annual mean fields of chl- <i>a</i> and nutricline depth in the North Atlantic.....	86
Figure 3-2: Summer and winter geometries of the oligotrophic region and subtropical gyre in the North Atlantic.....	88
Figure 3-3: Time series showing seasonal variability in the size and intensity of the oligotrophic region in the subtropical North Atlantic.	91
Figure 3-4: Seasonal cycle in the geometry of the oligotrophic region in the subtropical North Atlantic.	93
Figure 3-5: Seasonal cycle in the geometry of the oligotrophic region in the subtropical North Atlantic (chl- <i>a</i> difference fields).....	94
Figure 3-6: Summer and winter distributions of chl- <i>a</i> , Ekman transports and average Ekman-layer nitrate concentration.....	96
Figure 3-7: Annual mean divergence of the total (geostrophic + Ekman) horizontal advective NO ₃ flux within the Ekman layer.	98
Figure 3-8: Seasonal cycle in the divergence field of the total (geostrophic + Ekman) horizontal advective NO ₃ flux within the Ekman layer.....	100
Figure 3-9: Time series showing the seasonal variability in divergences of total horizontal advective fluxes of NO ₃ in the Ekman layer.....	102
Figure 3-10: Map of the local, seasonal correlations between anomalies in chl- <i>a</i> and anomalies in the divergence of the total horizontal advective fluxes of NO ₃	103
Figure A-1.....	119
Figure A-2.....	120
Figure A-3.....	121
Figure A-4.....	122

Figure A-5.....	123
Figure A-6.....	124
Figure A-7.....	125

Acknowledgements

No student ever accomplishes anything entirely by themselves. This has been especially true of my graduate school experience here at Duke, where I have relied heavily upon an extensive institutional and personal support system to complete my degree. It would take far more space and time than I have to properly thank everyone who has helped me, but I would like to specifically acknowledge a few people:

First and foremost, I would like to express my deepest gratitude for the support, mentoring and friendship of my advisor Susan Lozier. Over the last five and half years she has provided every conceivable form of support that an advisor could give to their student, and has helped me navigate the most intellectually and emotionally challenging period of my life. As much as I have benefited from her amazing abilities as a teacher and a scholar, I have benefited equally from her kindness and compassion, the sense of fairness with which her support has been given, her high expectation of quality in my work and her insistence that I take full responsibility for myself in everything I do. In doing so, she has provided a model for professional and personal conduct that I will attempt to follow for the rest of my life. It has been an honor to learn from her.

I would also like to acknowledge Dick Barber, Nicolas Cassar and Ric Williams for their advice and support as members of my Ph.D. committee. I am extremely lucky to have had the opportunity to work with such talented and accomplished scientists. My work has been greatly improved by their thoughtful criticism and feedback; my education has been enriched by their dedication to me as a student.

My home at Duke has been the Division of Earth and Ocean Sciences (EOS). I am grateful for the tremendous departmental support that I have received, and also for the friendship and support of the staff, faculty and all of my fellow students. Within EOS, the group that I have been closest to is the Lozier Lab. I am extremely grateful to all of its past and present members for their contributions to the general camaraderie in 333 Old Chem, as well as the hundreds of conversations over the years that have contributed to my understanding of the oceans and our world. I want to specifically acknowledge Jen Ayers and Jaime Palter for the important role each has played in my personal and academic life.

I also want to mention two very special people who have been my colleagues and friends from the very first day I arrived here: Stefan Gary and Kristin Burkholder. Just as your siblings are the only people who will ever fully understand what it was like to grow up in your family, only Stefan and Kristi know in full measure what the past 5 years of study have been like for me. To paraphrase a line from Kristi's own dissertation, we have shared all of the joys and trials of grad school. I will miss the both of them dearly.

The Graduate School at Duke has been a valuable resource and source of support. I am indebted to Doug James and the Preparing Future Faculty (PFF) program, and in particular to my PFF mentor Erin Lindquist. I will be forever grateful for the generous financial and personal support that has been offered to me and my family by the Office of Graduate Student Affairs and Lana Ben David.

My closest friends over the past five and a half years, the people who I can not imagine a happy life in Durham without, have been Mary Turnipseed, Meredith Barrett, Aaron Stoertz, Brian and Dory Lutz, and Lucas and Jamie Joppa. I look forward to many more years of our friendship.

None of the work I have completed in graduate school would have been possible without the support, at the outset when circumstances were so uncertain, of my friends Nirmish and Sandy Shah and Kinnari Desai. During that same period I received unwavering support from my parents Chandu and Nutan Dave, my sister Nomi Dave, my wife's parents Gordhan and Daxa Patel and my friend Mary Turnipseed. For this and a thousand other reasons, I love them all.

My final and most heart-felt acknowledgement goes to my wife Sejal, my greatest friend and companion, who has provided unconditional love, support and, above all, patience as I inched my way through school over the last five and a half years. Every single day, whether good or bad, has ended well because she and our children have been there to come home to. There was a time when I thought that our happiness together had come to an early end, and I am grateful beyond words that we have been granted more time together.

Introduction

Primary production at the sea surface is the foundation for nearly all life in the ocean. It is also a vital component of the biological pump that draws down atmospheric carbon into the marine reservoir and redistributes carbon, oxygen and nutrients in the global ocean. Thus, over the long term, variability in this marine productivity influences marine ecology, the climate system and ocean biogeochemistry. A key objective of ocean science, therefore, is to understand the environmental factors that control variability in marine productivity on interannual and longer time scales.

Explanations for the physical forcing of marine productivity have traditionally focused on the role of local, one-dimensional (i.e. vertical) processes. A number of recent observational analyses, for example, have ascribed historical fluctuations in global and basin-scale productivity at low and mid latitudes to climate-driven changes in upper ocean stratification. This attribution of interannual productivity variability to stratification changes is based on the supposition that long-term increases in water column stability will decrease vertical mixing and consequently the upward entrainment of deep nutrients that are vital to supporting new production in tropical and subtropical regions. The research described in this dissertation has critically examined this notion by using the modern observational record to explicitly compare a wide range of contemporaneous metrics for stratification and productivity variability on interannual time scales in the low and mid-latitude ocean, and also to explore how variability in another physical mechanism for nutrient supply, horizontal advection, might impact productivity in these regions.

The first chapter examines the stratification-productivity relationship for a 2-layer ecosystem, monitored at a time series station in the eastern subtropical North Pacific. The

analysis focuses on the temporal and vertical structure of correlations between local ecosystem properties and basin-wide climate processes that have been previously suggested to drive ecosystem variability at this location. The chapter also presents tentative evidence for a possible advective control on productivity here.

The second chapter extends the direct comparison of stratification and productivity variability performed at the time series station to the broader spatial domains of the subtropical North Pacific and equatorial Pacific. The comparison here is effected by matching satellite ocean color measurements with contemporaneous, in situ measures from hydrographic profiles. The analysis in the equatorial Pacific also considers the impact of interannual variability in the horizontal advection of nutrients and heat on the productivity and stratification signals in this region.

The final chapter shifts its spatial and temporal focus to examine seasonal variability in the geometry (i.e. size and shape) of the oligotrophic region of the subtropical North Atlantic basin. The analysis examines the connection between this oligotrophic variability and seasonal changes in the horizontal advective transfer of nutrients into the oligotrophic region from neighboring nutrient-rich areas, a mechanism that could potentially be of importance to interannual trends in oligotrophic geometry that have been previously reported.

1. Local Stratification Control of Marine Productivity in the Subtropical North Pacific

1.1 Introduction

Oceanographic literature has sustained a vigorous discussion on the physical forcing that drives spatial and temporal variability in marine primary productivity. A traditional conceptualization for the open ocean is that vertical mixing controls the availability of nutrients and light to surface photosynthesizers [Sverdrup, 1953; Lewis, 1986], and that this mixing is in turn constrained by local vertical density gradients [as described by Doney, 2006]. Changes in density stratification and mixing are also thought to impact productivity by applying physiological pressure that selects for particular species within phytoplankton communities [Karl *et al.*, 2001; Falkowski and Oliver, 2007; Dore *et al.*, 2008]. From these assessments, the expectation has arisen that local stratification control can provide a mechanistic foundation for predictions of marine ecosystem response to a changing climate [Bopp *et al.*, 2001; Boyd *et al.*, 2002; Sarmiento *et al.*, 2004; Schmittner, 2005; Cermeno *et al.*, 2008].

A number of recent observational studies have interpreted interannual and decadal variability in marine productivity within this theoretical framework [including McClain *et al.*, 2004; Gregg *et al.*, 2005; Behrenfeld *et al.*, 2006; Polovina *et al.*, 2008; Irwin and Oliver, 2009]. A commonly developed narrative in many of these studies has been that strengthened stratification of the upper ocean, associated with either secular warming trends or climate oscillations, has increased energy requirements for overturning and subsequently reduced vertical mixing. In the tropical and subtropical oceans, where there is an ample supply of solar radiation, strengthened stratification is expected to negatively

impact surface autotroph communities by decreasing the entrainment of deep, nutrient-rich water towards the surface. Two studies, in particular, present evidence for global, interannual decreases in productivity with increasing stratification. From an analysis of satellite-derived surface chlorophyll-*a* (chl-*a*), which is a widely used proxy for phytoplankton biomass, *Behrenfeld et al.* [2006] report a global decline in productivity that is associated with an increase in surface warming and stratification (measured as $\rho_{200} - \rho_0$) of tropical and subtropical waters in the aftermath of the 1997-1998 El Nino event. Similarly, *Polovina et al.* [2008] describe increases in the sea surface temperature (SST) and areal extents of the oceans' most oligotrophic regions over the period 1998-2006.

A recent examination of interannual variability in subtropical upper ocean stratification and productivity, however, suggests that the two are not strongly correlated. In an analysis of data from the Bermuda Atlantic Time Series (BATS) program in the North Atlantic, *Lozier et al.* [2011] demonstrate that local stratification (assessed as $\rho_{200} - \rho_0$ for consistency with *Behrenfeld et al.*) has essentially no correlative relationship with either surface chlorophyll concentrations or vertically integrated primary productivity on interannual time scales over the observational record, 1988–2008. In the same study, comparisons over the broader North Atlantic subtropical domain using satellite chl-*a* and historical hydrographic data yield similar results. Whether these regional observations are representative of the global subtropical ocean is not certain; to date, no similar comparisons have been made outside of the Atlantic. More importantly, the linkages between productivity and stratification variability that characterize the North Atlantic cannot be assumed to translate directly to other basins.

The subtropical North Atlantic has traditionally been viewed as a system in which annual cycles of productivity are driven by seasonal destratification and strong mixing accompanied by nutrient entrainment from depth [Menzel and Ryther, 1961; Gruber *et al.*, 2002]. In another important oligotrophic region, the vast subtropical North Pacific, the role of stratification appears to be qualitatively different. In general, the North Pacific has lower surface salinities, stronger stratification and shallower seasonal mixed layers than the Atlantic [Emery and Dewar, 1982; Lozier *et al.*, 1995; Macdonald *et al.*, 2001; Suga *et al.*, 2004]. Previous ecosystem assessments in the subtropical North Pacific, including the ongoing Hawaiian Ocean Time-series (HOT) program, demonstrate that the strong stratification restricts vertical mixing and deep nutrient inputs into the surface layer [Epply *et al.*, 1973; Letelier *et al.*, 1993]. Unlike the subtropical North Atlantic, then, the subtropical North Pacific is a region in which annual variations in productivity are not principally driven by destratification. In such a setting, the sensitivity of productivity to future long-term changes in the mean stratification state may be difficult to predict. The modern observational record is a valuable tool in this regard, since it provides direct information on the historical relationship between variability in stratification and productivity and informs our predictions of what may happen to this relationship in the future. Towards that end, this study focuses on two decades of time series data collected at Station ALOHA (A Long-term Oligotrophic Habitat Assessment), the primary field site of the HOT program. Our primary aim is to determine whether interannual variability in the density stratification of the local water column has impacted primary productivity over the observational record.

1.2 Background

1.2.1 Controls on subtropical productivity

In general, the mid-latitude upper ocean is characterized by a deep and strongly stratified euphotic zone in which a relatively shallow, nutrient-limited surface mixed layer with low levels of biomass allows enough light to pass through to support substantial photosynthesis and nutrient uptake at depth. This subsurface biological activity is evidenced by the persistent deep chlorophyll maxima (DCMs) that are ubiquitous in subtropical waters [*Fennel and Boss, 2003; Huisman et al., 2007*]. In this physical environment, patterns of productivity, nutrient cycling and phytoplankton community structure can vary significantly between the upper and lower euphotic zone [*Venrick, 1982; Venrick, 1993; Winn et al., 1995; Karl et al., 1996; Letelier et al., 2004; Corno et al., 2008*]. This vertical ecosystem structure can be destroyed by deep convective mixing during the winter and spring, which would homogenize biomass distributions and instigate blooms of phytoplankton at the surface in two ways: through entrainment of deeper, nutrient-rich waters into the upper layer, and decoupling of grazing pressure from primary producers through reduced encounter rates between planktonic organisms [*Behrenfeld, 2010*]. It would be reasonable to expect, therefore, that subtropical marine productivity would be highly sensitive to interannual variability in stratification, yet the analysis of the subtropical North Atlantic by *Lozier et al. [2011]* suggests otherwise.

What can account for the lack of a strong interannual association between subtropical stratification and productivity? One explanation is that local stratification is only one of many factors that control vertical mixing. Interannual variability in wind and buoyancy forcing, both processes that destroy stratification and provide energy for mixing,

has been shown to influence the timing and magnitude of phytoplankton blooms in the North Atlantic [Follows and Dutkiewicz, 2002 and Ueyama and Monger, 2005]. The analysis at BATS by Lozier *et al.* [2010] in particular, shows that mixing energy inputs from winds have consistently exceeded stratification-imposed energy requirements for overturning during bloom months over the past two decades. Local vertical mixing, in turn, is only one of many factors that impact nutrient supply to surface photosynthesizers. Horizontal surface Ekman transports from bordering subpolar regions have been shown to produce a significant influx of nutrients into the subtropics [Williams *et al.*, 1998; Ayers *et al.*, 2010]. In addition, interannual variability in the formation and subsequent advection of subtropical mode waters around the gyre has been shown to exert a strong control on the basin-wide subsurface nutrient reservoir and, consequently, the surface productivity that is fueled by upward fluxes of deep nutrients [Palter *et al.*, 2005].

In a sufficiently stratified region, however, mixing energy provided by surface winds or buoyancy changes may not be sufficient to induce vigorous seasonal overturning, resulting in a euphotic zone that is essentially permanently divided into upper and lower layers. Station ALOHA in the eastern subtropical North Pacific provides an example of such a system (Figure 1-1). Over the past two decades mixed layer depths at this location have rarely exceeded 100 m, with seasonal range of 36-96 m and a long term mean of 60 ± 24 m

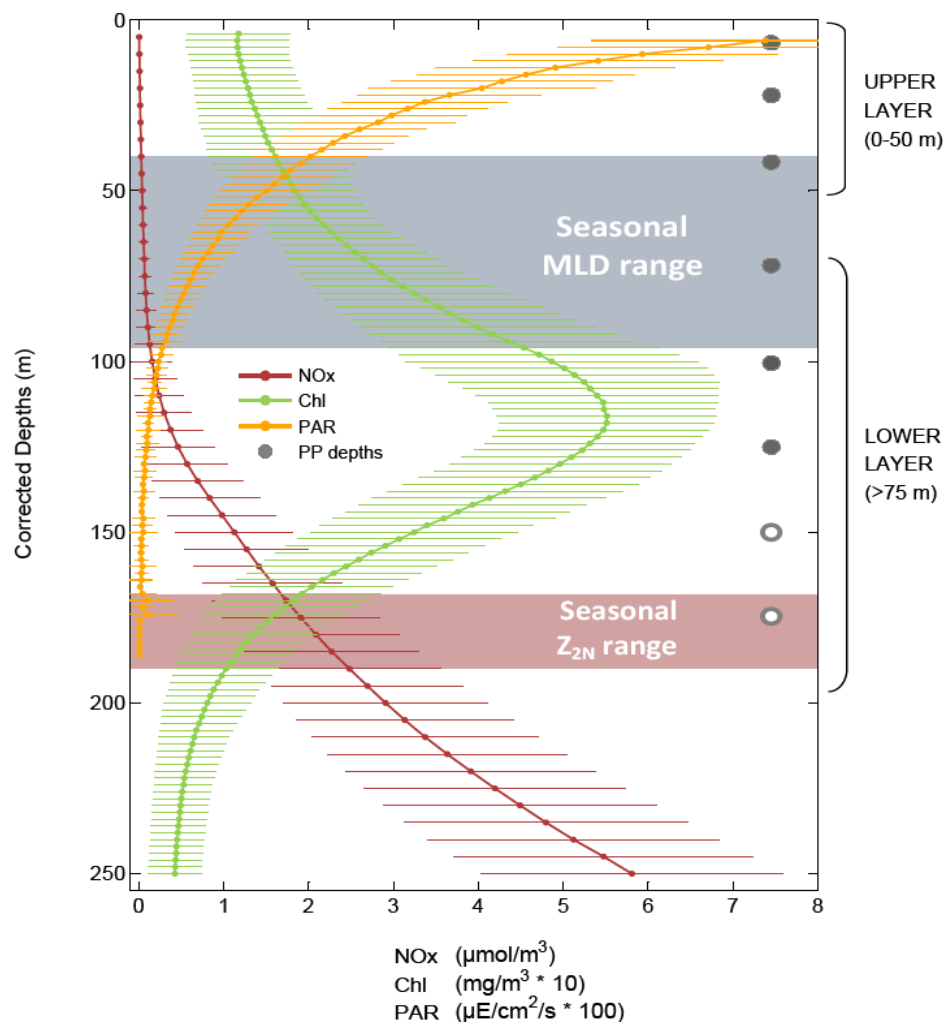


Figure 1-1: Long term average (1988–2008) vertical profiles of downwelling photosynthetically available radiation, PAR ($\mu\text{E m}^{-2} \text{s}^{-1}$, yellow line), CTD chloropigments (chl-*a* and phaeopigment, mg m^{-3} , green line) and nitrate plus nitrite ($\mu\text{mol kg}^{-1}$, red line) measured at HOT Station ALOHA. See Methods section for description of how ‘corrected depth’ profiles were generated. For each profile the bars indicate ± 1 standard deviation. Shaded regions showing the seasonal ranges of the surface mixed layer depth (blue) and the $2 \mu\text{mol kg}^{-1}$ NO_x (NO₃+NO₂) isoline (red) are plotted for comparison. Properties have been scaled to fit on the same horizontal axis. Grey circles indicate standard depths of primary productivity measurements; the open circles correspond to 150 m and 175 m measurements that were discontinued in 2000. The upper and lower layers of the euphotic zone are indicated with brackets.

(1σ). By comparison, the nutricline depth at this location (defined here as the $2 \mu\text{mol kg}^{-1}$ horizon of nitrate plus nitrite concentrations, $[\text{NO}_3 + \text{NO}_2]$ or 'NOx') has a seasonal range of 170-191 m (with a long term mean of 180 ± 25 m). As a consequence, nutrient supply from depth is perpetually restricted and nutrient levels in the surface mixed layer are almost completely depleted by biological uptake. Standing stocks of biomass in the upper 50 m are similarly low, with bulk chloropigment concentrations of $0.14 \pm 0.06 \text{ mg m}^{-3}$. Due to the lack of light-attenuating compounds at the surface, photosynthetically available radiation (PAR) is sufficiently intense at depth to support a persistent and pronounced DCM centered at ~ 125 m.

The vertical ecosystem structure illustrated in Figure 1 has historically been described by a two-layer ecological model for the subtropical North Pacific [Dugdale, 1967; Epply *et al.*, 1973; modified by Dore *et al.*, 2008]. In this model, the upper layer represents a light-replete, chronically nutrient-limited regime and the lower layer a light-limited and relatively nutrient-replete regime. In this context, it is difficult to imagine a single, unified response of productivity across the euphotic zone to interannual stratification variability. Recent research has focused on spatial and temporal changes in phytoplankton community structure and, in particular, on the contributions of nitrogen fixing organisms to the surface nutrient pool and to export production [Karl *et al.*, 2001; Dore *et al.*, 2002; White *et al.*, 2007; Church *et al.*, 2009]. In the lower euphotic zone, where deep nutrients are more readily available, vertical density gradients might be expected to play a significant role in controlling upward fluxes of nutrients from depth, but the interannual association between stratification and productivity in this layer has not yet been described. In the upper layer, where nutrient inputs are already severely restricted, the extent to which interannual

increases in the mean stratification state would impact nutrient supply also remains an open question.

1.2.2 Linkages to climate

Although the subtropical North Pacific gyre contains some of the lowest levels of biomass observed in the global ocean, the region also exhibits pronounced fluctuations in primary productivity, particulate export and phytoplankton community structure over a range of time scales [Karl, 1999]. It has been suggested that interannual and decadal ecosystem variability observed at Station ALOHA is driven by basin-wide climate processes (namely ENSO and PDO) which impact local stratification and, consequently, vertical nutrient transfers [Karl *et al.*, 1995; Karl *et al.*, 2001; Dore *et al.*, 2002; Corno *et al.*, 2007; Bidigare *et al.*, 2009]. Although no clear physical linkage between climate variability and stratification changes at this location has yet been detailed, suggested mechanisms include changes in local cloud cover, wind forcing, the hydrological cycle, as well as advection of anomalous T/S properties [Lukas, 2001; Dore *et al.*, 2002; Corno *et al.*, 2007; Bidigare *et al.*, 2009].

Whatever the mechanistic linkages involved, climate-driven changes in nutrient supply have been suggested to drive significant changes in export production and phytoplankton assemblages at ALOHA. Within the autotroph community in particular, decreases in nutrient supply from depth are thought to be responsible for an observed domain-shift from larger to smaller phytoplankton (which are better able to absorb nutrients from solution) as well as increases in diazotrophs (which are able to fix their own nitrogen) [Karl *et al.* 2001]. The response of primary productivity or particulate export at

ALOHA to a given ENSO or PDO state, however, has not been uniform. Explanations for this lack of consistency have tended to focus on the complex and nonlinear dynamics internal to the local biology, time delays associated with transmission of the climate forcing, as well as interactions and interferences between ENSO and PDO signals [Dore *et al.*, 2002; Corno *et al.*, 2007; Bidigare *et al.*, 2009]. One additional mode of climate variability that could explain ecosystem variability at Station ALOHA and that has not yet been compared to the HOT dataset, is the recently identified North Pacific Gyre Oscillation (NPGO). The NPGO has been suggested to drive fluctuations in biogeochemically relevant properties (salinity, nutrients, chlorophyll) within ecosystems of the Northeastern Pacific that do not appear to be strongly forced by PDO or ENSO [Di Lorenzo *et al.*, 2008]. NPGO variations reflect changes in regional and basin-scale wind-driven upwelling/ downwelling and advection, processes that are fundamental to controlling productivity in the subtropical gyres. A natural inquiry to make, therefore, is how NPGO variability is correlated (if at all) to ecosystem changes at ALOHA.

The impact that climate processes have on physical and biological properties at ALOHA must also be considered in the context of the two-layer ecosystem model described earlier. For example, interannual changes in the density field that are associated with surface heat and freshwater fluxes may affect productivity differently than changes caused by subsurface advection of T/S properties. Similarly, the nutrient-limited upper layer might respond differently to interannual changes in cloud cover than the light-limited lower layer. An interesting question to consider, then, is whether there might also be vertical structure in the response of the local ecosystem to climate forcing, with stronger correlations observed at some depths than at others.

The task of determining correlations between climate processes and ecosystem changes at ALOHA is made more arduous by the issue of time delays in local ecosystem response to climate perturbations that originate in the far-field. No clear picture has yet emerged as to how long it takes for the effect of these perturbations to be expressed in either stratification or productivity variability at this location. Estimates in the literature range from 10 months [Dore *et al.*, 2002] to 2-3 years [Corno *et al.*, 2007], the former based on a lag correlation analysis, the latter being based on theoretical considerations. To date, no comprehensive analysis has been made of the temporal structure (ie. time lags) of correlations between climate processes and stratification and productivity at ALOHA.

1.3 Study objectives

Determination of the relationship between stratification and productivity variability is crucial to understanding the long-term physical drivers of productivity in the subtropical oceans. The North Pacific subtropical gyre is of particular importance since it is the largest of the major oligotrophic regions and accounts for a significant portion of global productivity and export. In this study, we use the HOT dataset to address two sets of questions:

- 1) How is interannual variability in primary productivity in the subtropical North Pacific related to variability in the density stratification of the local water column? How can this relationship be interpreted within the context of a two layer model (ie. in the upper and lower euphotic zone)?

- 2) How is interannual variability in stratification and productivity in this region impacted by basin-wide climate variability? What is the spatial (ie. vertical) and temporal structure of any correlations that do exist?

1.4 Methods

1.4.1 Hydrographic and Biogeochemical Data

For this analysis we examine data from the HOT program's deep-water hydrostation ALOHA (nominally located at 22° 45'N, 158°W, 4750 m depth), at which extensive hydrographic and biogeochemical measurements have been made at approximately monthly intervals since 1988. This dataset provides detailed assessments of the local ecology and its physical environment over seasonal to decadal time scales [Karl and Lukas, 1996]; the core HOT data include continuous vertical temperature and salinity profiles, as well as discrete measurements of inorganic nutrients, phytopigment concentrations, primary production rates, particulate fluxes and plankton assemblages. Quality-controlled data are available online, along with detailed information about the program's analytical methods, at: <http://hahana.soest.hawaii.edu/hot/hot_jgofs.html>. In addition, solar irradiance data, including surface-incident photosynthetically available radiation (PAR) fluxes and vertical profiles of downwelling PAR fluxes, have been measured at Station ALOHA concurrently with the core observations since 1998. These data are managed by the Oregon State University Remote Sensing Ocean Optics (ORSOO) group and are available in their raw form online at: <<http://picasso.oce.orst.edu/ORSOO/data.html>>. We have employed quality control procedures outlined by Letelier *et al.* [2002] to prepare these data for analysis. Briefly, for the vertical PAR profiles, we have discarded values measured

during the downcasts of the profiling sensor (due to stability issues) and at all other intervals when the sensor was tilted greater than 5° with respect to the vertical, as well as all measurements shallower than 10 m (due to optical effects associated with surface turbulence). The remaining data were depth-averaged into 2 m bins, to match the sampling resolution of the CTD data.

In addition to the *in situ* chlorophyll data, we also examine gridded 8-day mean fields of satellite-derived surface chlorophyll concentrations from the SeaWiFS dataset (provided by NASA GSFC and available online at: <<http://oceancolor.gsfc.nasa.gov>>). The data are mapped on a 1/12° grid and span the second half of the HOT time span, 1997–2008. We obtain local values of chl-*a* using two methods: 1) linearly interpolating values to the spatial location and date of each cruise at Station ALOHA, and 2) spatially averaging chl-*a* concentrations within a 5° box (22°N, 160°W to 27°N, 155°W) that contains Station ALOHA.

1.4.2 Isotopic composition of particulate nitrogen export flux

We employ an isotopic mass balance calculation described by *Dore et al.* [2002] to deconvolve the export flux of particulate nitrogen (F_{PN}) out of the euphotic zone (measured by sediment traps at 150 m depth) into components that are supported by nitrogen fixation (F_{PN-N_2}) and by the supply of nitrate (NO_3^-) from depth (F_{PN-NO_3}):

$$\delta^{15}N_{F_{PN}} = (\delta^{15}N_{N_2}) * f_{N_2} + (\delta^{15}N_{NO_3}) * f_{NO_3} \quad (1)$$

$$F_{PN-NO_3} = F_{PN} * f_{NO_3}$$

$$F_{PN-N_2} = F_{PN} * f_{N_2}$$

where $\delta^{15}\text{N}$ represents nitrogen isotopic composition and $f_{\text{NO}_3^-}$ and f_{N_2} are the NO_3^- and N_2 -supported fractions of the PN flux, respectively. Implicit in this calculation are four basic assumptions [Dore *et al.*, 2002]: that F_{PN} is in balance with inputs into the euphotic zone of allochthonous nitrogen; that upward fluxes of NO_3^- , nitrogen fixation and F_{PN} are the only significant fluxes of nitrogen into or out of the euphotic zone; that the isotopic compositions of the two end-members of our mass balance calculation, $\delta^{15}\text{N}_{\text{N}_2}$ and $\delta^{15}\text{N}_{\text{NO}_3}$, are 0‰ and 6.5‰, respectively; and that the sediment trap data for particulate fluxes are not affected by fractionation or another isotopic bias.

1.4.3 Climate and wind data

The Multivariate ENSO Index (MEI) is used to assess variability in ENSO forcing. The MEI is calculated as the first principal component of a composite time-series of six properties monitored in the tropical Pacific: sea-level pressure, zonal and meridional components of surface wind, sea surface temperatures, surface air temperatures and cloud cover. The index is available online from the NOAA Climate Diagnostics Center at: <http://www.cdc.noaa.gov/people/klaus.wolter/MEI/table.html>. Positive and negative MEI values refer to El Niño and La Niña conditions, respectively. To assess variability in PDO forcing, we use the PDO index (PDOI). The index is obtained from the Joint Institute for the Study of the Atmosphere and Ocean and is available online at: <http://jisao.washington.edu/pdo/PDO.latest>. The index is determined from the leading principal component of monthly SST anomalies in the North Pacific, poleward of 20°N [Mantua *et al.*, 1997], and is strongly correlated with variability in atmospheric circulation

around the Aleutian low pressure system. Positive and negative index values refer to warm and cool PDO phases, respectively. To assess variability in NPGO forcing, we use the NPGO index, which is determined from the second principal component of sea surface height variability in the Northeast Pacific and, as such, is strongly correlated with fluctuations in the intensity of the geostrophic circulation in this region. The index is available online at: <<http://ocean.eas.gatech.edu/npgo/>>. Positive and negative index values refer to more and less intense gyre circulations, respectively.

To assess variability in the local wind field, we use gridded monthly mean surface wind fields from the QuikSCAT dataset (provided by CERSAT and available online at: <<http://www.ifremer.fr/cersat/en/>>). The data are mapped on a 0.5° grid and span the second half of the HOT time span, 1999–2008; they include wind stress and wind stress curl values. We obtain local values of zonal wind speed and the wind stress curl using two methods: 1) linearly interpolating values to the nominal location of Station ALOHA, and 2) spatially averaging monthly signals over a 5° box (22°N, 160°W to 27°N, 155°W) that contains Station ALOHA. Analyses of the QuikSCAT dataset are hampered by its relatively short duration; in this respect, a longer record such as the NCEP/NCAR reanalysis (1948-present) might be preferable. However, the topography of the Hawaiian Islands has long been known to influence local atmospheric circulation [*Smith and Grubisic, 1993; Xie et al., 2001; Chelton et al., 2004*], and, in this regard, the relatively coarse resolution NCEP data (mapped to a 2.5° grid) are probably less descriptive of the wind field around Station ALOHA than the QuikSCAT data.

1.4.4 Data analysis

Ecosystem assessments at Station ALOHA are made using a ‘burst-sampling’ strategy, in which a series of 12-18 hydrocasts approximately 3 hours apart span a complete inertial period (~31 hours at 20°N) as well as multiple semi-diurnal tidal periods. The resulting depth-averaged density profile effectively smoothes out variability in the density field that occurs at frequencies below the biological response time. Using a methodology similar to that of *Letelier et al.* [2002], we have calculated ‘corrected’ depths for individual bottle samples by mapping their density values onto the average density profiles for their cruise. Solar irradiance data are similarly affected by high-frequency variability in cloud cover, which can dramatically change PAR on time scales that are too short to engender a productivity response. We have again adopted the methodology of *Letelier et al.* and obtained ‘corrected’ downwelling PAR profiles using climatological surface PAR values to scale the values of PAR in the water column:

$$\text{PAR}_{z \text{ corrected}} = \text{PAR}_z \times \left[\frac{\overline{\text{PAR}_0}}{\text{PAR}_0} \right] \quad (2)$$

where PAR_z is an instantaneous downwelling PAR flux measured at depth z , PAR_0 is the concurrent measurement of PAR flux at the sea surface and $\overline{\text{PAR}_0}$ is the corresponding long-term monthly mean surface PAR flux. We have calculated this long-term monthly mean in two ways: 1) as the mean of all surface PAR measurements made at ALOHA during a given month for the period 1998–present, and 2) as the mean of all satellite-derived

(SeaWiFS, 1997–present) PAR values for that month, interpolated to the nominal position of Station ALOHA.

For our analysis of seasonal variability at Station ALOHA, we first average all observations of the relevant physical and biological parameters for a single cruise (i.e. the ‘cruise mean’) and then prepare time series of their long-term monthly means. Plots comparing seasonal time series of different properties present the dynamic range of each property, calculated by normalizing the long-term monthly mean values to a scale of 0 to 1. For our analysis of interannual variability, we calculate monthly anomalies of each property by subtracting the corresponding long-term monthly mean from each short-term (i.e. cruise) mean. To investigate linkages to basin-wide climate processes, we perform a lag correlation analysis between the MEI, PDOI and NPGO indices and a suite of time series describing upper and lower layer stability, surface physics (e.g. wind forcing, solar irradiance), primary productivity, particulate export and the nutrient field at Station ALOHA. All time series are smoothed using 3-month running means, and highly statistically significant linear correlation coefficients ($p < 0.01$) are calculated for a series of lag times, ranging from 0–96 months.

1.5 Results and discussion

1.5.1 Seasonal variability

Based on the vertical ecosystem structure described in the Figure 1-1, we delineate the upper and lower euphotic zone as the 0-50 m and >75 m depth ranges, respectively. Average monthly time series of ecosystem properties in these layers at Station ALOHA are presented in Figure 1-2. The plot updates important historical findings regarding seasonal

variability in the upper and lower euphotic zone at this location with data extending through 2008, incorporating more than a decade of additional measurements in some cases.

1.5.1.1 Upper layer

In the upper euphotic zone at Station ALOHA, chl-*a* is elevated during winter months when mixed layers are deeper and stratification is weaker (Figure 1-2a). This signal, however, is unlikely to result from productivity driven by entrainment of deep nutrients, since the nutricline here lies below the wintertime mixed layer. In fact, seasonal primary productivity is almost completely out of phase with chl-*a*, in that it is elevated during the spring and summer months when stratification is increasing. In the absence of large seasonal inputs of allochthonous nutrients, the wintertime chl-*a* increase has been attributed to phytoplankton photoadaptation and changing photosynthetic efficiency with deeper mixing rather than to an actual increase in biomass [Venrick, 1993; Letelier *et al.*, 1993; Winn *et al.*, 1995]. This dynamic highlights the potential difficulties in using satellite-based estimates of chlorophyll concentrations from this region as a proxy for phytoplankton biomass.

|



Figure 1-2: Seasonal time series of average monthly upper (a-c) and lower (d-f) euphotic zone properties at HOT Station ALOHA: (a) upper layer (0-50 m) stratification, average chlorophyll-a and integrated productivity; (b) upper layer integrated productivity with the N₂-supported PN flux out of the euphotic zone (measured at 150 m); (c) upper layer integrated productivity with the square of the average monthly QuikSCAT wind speed; (d) lower euphotic zone (75-150 m) stratification and nitrate-supported PN flux; (e) depth of the DCM and the 0.001 μE cm⁻² s⁻¹ PAR downwelling flux horizon; (f) PAR downwelling flux measured near the top of the lower layer (~100 m) with lower layer integrated primary productivity, chl-a concentrations, NO_x and soluble reactive phosphate (SRP) concentrations on the 24.5 sigma isopycnal surface. For all panels, bars indicate standard errors. Dynamic ranges of properties (0-1) have been plotted for each panel, except for (e) which shows absolute depths in meters.

The observed summer productivity maximum is thought to reflect phytoplankton blooms that result from enhanced nitrogen fixation, which increases in response to a synchrony of several conditions which favor the growth of key diazotrophic species: increased light intensity, stronger thermal stratification that further restricts nitrogen supply from depth and a calm, less turbulent air-sea interface [Karl *et al.*, 1995; Dore *et al.*, 2002; Grabowski *et al.*, 2008; White *et al.*, 2007; Church *et al.*, 2009]. The strong, positive seasonal correlation ($r=0.92$, $p<0.05$) of upper euphotic zone primary production with the fraction of particulate nitrogen flux out of the euphotic zone that contains recently fixed nitrogen (F_{PN-N_2}) is indicative of the importance of diazotroph activity (Figure 1-2b). Upper layer primary production is also negatively correlated with the square of the QuikSCAT wind speed (Figure 1-2c), but this statistical association is weak ($r = -0.35$, $p=0.24$). The available wind data therefore do not appear to offer a clear answer to the question of whether upper layer productivity is enhanced during periods of relative surface calmness. Approximately 80% of all nitrogen fixation at Station ALOHA occurs within 60 m of the surface, and evidence suggest that diazotrophs account for up to half of vertically-integrated new production in this region [Karl *et al.*, 1997; Dore *et al.*, 2002; Dore *et al.*, 2008]. Collectively, these findings challenge traditional conceptions of local stratification control, since they suggest that significant seasonal inputs of new nitrogen into the euphotic zone of the subtropical North Pacific result from increased stability in the upper layer.

1.5.1.2 Lower layer

As described in the 2-layer model, phytoplankton in the lower euphotic zone enjoy higher nutrient availability from the nutricline, but are also light-limited. An important

driver of annual cycles in productivity and nutrient uptake in this layer therefore is the seasonal evolution of the light field, which is shaped by the variations in solar radiation at the surface as well as changing concentrations of chlorophyll and other light-absorbing substances in the water column. *Letelier et al.* [2004] have shown that productivity levels and nutrient inventories in the lower euphotic zone track the seasonal penetration of isolumens. Our analysis confirms that the depth of the DCM closely follows the $0.001 \mu\text{E cm}^{-2} \text{ day}^{-1}$ PAR flux horizon throughout the year (Figure 1-2e). Moreover, summertime nitrate and phosphate concentrations along isopycnals in the lower layer are depleted relative to wintertime concentrations, as a result of increased uptake by phytoplankton during months with greater light intensity (Figure 1-2f). Productivity and phytoplankton biomass are greater during these months and exhibit a strong springtime increase that is analogous to the surface bloom events observed in light-limited waters at higher latitudes [*Letelier et al.*, 2004].

Productivity in the lower layer may also be impacted by annual cycles of stratification at the base of the euphotic zone. Since significant nitrogen fixation does not occur at these depths, upward fluxes from the deep nutrient pool are critically important for the maintenance of new production and the replenishment of depleted nitrogen and phosphorous in this layer. The data at Station ALOHA suggest that vertical density gradients may regulate these fluxes over seasonal time scales (Figure 1-2d). Lower layer stratification in the spring and early summer months is weaker than in the fall and winter and is negatively correlated with $F_{\text{PN-NO}_3}$, ostensibly a measure of lower-layer new production driven by deep nitrate, ($r = -0.82$, $p < 0.05$). The correlation is consistent with the expectation that increased diffusivity due to weaker vertical density gradients would

produce a greater upward flux of deep nutrients. In the lower layer, therefore, stratification appears to be related to seasonal productivity variability in a more conventional sense.

1.5.2 Interannual variability at Station ALOHA

The impact of stratification variability on productivity at Station ALOHA on interannual time scales is assessed by examining monthly anomalies for the period 1988-2008. A comparison of anomalies in depth-averaged chl-*a* and vertically integrated primary productivity with stratification, all assessed over the euphotic zone, shows no evidence of a correlative relationship (Figure 1-3a). Additional comparisons using satellite-derived surface chl-*a* concentrations from the SeaWiFS dataset in place of *in situ* values or mixed layer depths in place of stratification all yield similar results (not shown). Given the vertical ecosystem structure at this location, however, a single comparison over the entire euphotic zone may be overlooking dynamics occurring separately in the upper and lower euphotic zone. We extend our analysis to the upper and lower layers at Station ALOHA.

1.5.2.1 Stratification and productivity in the upper and lower layers

A visual comparison of monthly anomalies in upper layer stratification (assessed as $\rho_{50} - \rho_0$) with chl-*a* concentrations and integrated primary productivity in the upper 50 m

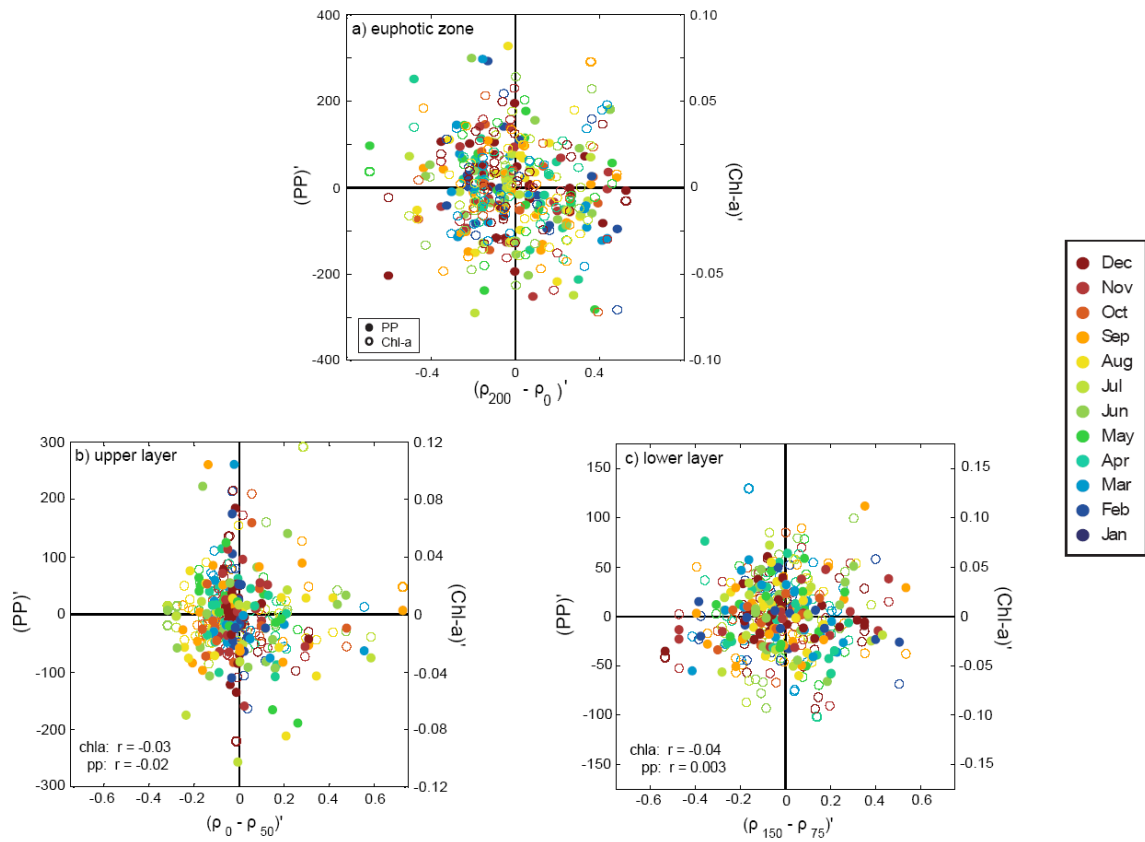


Figure 1-3: Monthly mean-subtracted anomalies of chlorophyll-*a*/ productivity versus stratification at Station ALOHA, 1988-2008: (a) average chl-*a* concentrations (0-150 m, mg/m³, open circles) and vertically-integrated primary production (0-125 m, mg C m⁻² day⁻¹, closed circles) versus stratification (assessed as $\rho_{200} - \rho_0$ for consistency with Behrenfeld *et al.* [2006]); (b) for the upper layer, chl-*a* (primary productivity) is averaged (integrated) over 0-50 m and stratification is assessed as $\rho_{50} - \rho_0$; (c) for the lower layer chl-*a* (primary productivity) is averaged (integrated) over 75-150 m (75-125 m) and stratification is assessed as $\rho_{150} - \rho_{75}$. The colors indicate the month of each observation.

reveals no statistically significant correlations on interannual scales over the previous two decades (Figure 1-3b). When the comparison is repeated using mixed layer depth and other metrics that have previously been used to assess stratification in the euphotic zone, similar results are obtained (Table 1). No statistically significant correlations are found between stratification and primary productivity. Statistically significant ($p < 0.05$) correlations do exist between surface chl-*a* and some of the stratification metrics, but, at most, only 13% of the observed chlorophyll variability can be explained by varying stratification. In any case, correlations between stratification and chl-*a* variability in the absence of correlations with productivity probably reflect physiological (photoadaptive) changes in phytoplankton rather than variability in biomass.

One additional property related to upper layer productivity is the export of particulate organic matter out of the euphotic zone. If a steady state is assumed to exist between new production and particulate export (this entails assuming that export due to DOM transport or zooplankton migration is less important) then variability in the total particulate carbon flux (F_{PC}) and the N_2 -supported fraction of the particulate nitrogen flux (F_{PN-N_2}) will reflect variability in net community production (NCP) across the euphotic zone and variability in the portion of new production in the upper layer driven by nitrogen fixation, respectively [Dore *et al.*, 2002; Brix *et al.*, 2006]. The correlation between F_{PC} and stratification (not shown) is not statistically significant for any measure of stratification. For F_{PN-N_2} we observe only a very weak association with some of the stratification metrics; these correlations are at most able to explain less than 4% of observed F_{PN-N_2} variability (Table 1).

Table 1-1: Correlations between stratification and productivity on interannual time scales at Station ALOHA. Statistically significant correlations ($p < 0.05$) between interannual variability in local stratification metrics at Station ALOHA and interannual variability in upper and lower euphotic zone integrated primary production, upper and lower euphotic zone chlorophyll-a concentrations and particulate nitrogen (PN) fluxes measured at the base of the euphotic zone (150 m). The correlation analysis is performed for monthly mean-subtracted anomalies in each property over the period 1988-2008. Stratification metrics 7-9 are adopted from Corno et al., [2007] (see Figure 1 in that reference). Non-significant correlations are presented as dashes.

Stratification Metric	Integrated PP				Average Chl- <i>a</i>				PN Flux @ 150m	
	0-50	40-110	75-125	100-125	0-50	50-100	75-125	100-150	PN-NO3	PN-N2
1. MLD	-	0.31	0.27	0.24	0.28	-0.19	-	-	-	0.19
2. $\Delta\rho$: 0-50m	-	-0.19	-0.17	-	-	0.19	-	-	-	-
3. $\Delta\rho$: 50-100m	-	-0.19	-0.23	0.18	0.20	-	-	-	-	0.15
4. $\Delta\rho$: 75-125m	-	-	-	-	0.15	-	-	-	-	-
5. $\Delta\rho$: 100-150m	-	-	-	-	-	-	-	-	0.19	-
6. $\Delta\rho$: 150-200m	-	-	-	-	-	-	-	-	-	-
7. $\Delta\rho$: 0 - (MLD+20m)	-	-	0.16	-	0.24	-	-	-	-	-
8. $\Delta\rho$: (MLD+20) - 100m	-	-0.22	0.20	0.17	0.35	0.15	-	0.15	-	0.15
9. $\Delta\rho$: (MLD+20) - 150m	-	-0.21	0.17	-	0.36	-	-	0.16	-	0.19
10. $\Delta\rho/\Delta z$: DCM - Z_{2N}	-	-	-	-	-	-	-	-	0.23	-

In the lower euphotic zone, a comparison of monthly anomalies in stratification (assessed as $\rho_{150} - \rho_{75}$) with chl-*a* concentrations and integrated primary productivity reveals no statistically significant correlations on interannual scales over the previous two decades (Figure 1-3c). As with the upper layer data, repetition of the comparison with an array of stratification metrics as well as a range of assessments of sub-surface productivity and chlorophyll, yields similar results (Table 1). Less than 10% of the variance in any measure of depth-integrated productivity and 13% of the variance in any measure of depth-averaged chl-*a* can be explained by any of the measures of stratification variability. A comparison using F_{PN-NO_3} as an indicator of new lower-layer production driven by deep nitrate also shows no clear association with stratification variability. At best, only 5% of the observed F_{PN-NO_3} variability is attributable to interannual stratification changes.

1.5.2.2 Alternate processes and time scales

An array of alternate local processes can be considered in place of stratification change as possible drivers of the observed biological variability on interannual time scales at Station ALOHA (Table 2). We compare productivity, chl-*a* and particulate export to changes in solar irradiance at the surface and at depth, local wind stirring and wind stress curl (which is directly related to Ekman pumping velocities), density values at the base of the euphotic zone (which would be sensitive to the heaving of deep isopycnals on seasonal and longer scales) and nutrient concentrations along isopycnals below the euphotic zone (which would indicate variability in the deep nutrient reservoir). Our analysis, however,

Table 1-2: Correlations between productivity and other properties on interannual time scales at Station ALOHA. As with Table 1-1, statistically significant correlations ($p < 0.05$) between variability in upper and lower euphotic zone integrated primary production, upper and lower euphotic zone chlorophyll-a concentrations and particulate nitrogen (PN) fluxes with a suite of physical properties measured or evaluated at ALOHA: QuikSCAT winds, photosynthetically available radiation (PAR), potential density at 150 m and 200 m and nutrient concentrations at and below the base of the euphotic zone.

	Integrated PP				Average Chl- <i>a</i>				PN Flux @ 150m	
	0-50	40-110	75-125	100-125	0-50	50-100	75-125	100-150	PN-N ₀₃	PN-N ₂
Windspeed ²	-	-	-	-	0.33	-	-	-	-	-
Wind stress curl	-	-	-	-	-	-	-	-	-	-
PAR @ 0m	-	0.25	0.30	0.29	-	-	-	-	-	-
PAR @ 50m	N/A	-	-	-	N/A	- 0.20	-	0.23	-	-
PAR @ 100m	N/A	-	0.23	0.21	N/A	- 0.37	-	0.27	0.26	-
σ_θ @ 150m	-	-	-	-	-	-	-	-	-	-
σ_θ @ 200m	-	-	-	-	-	-	-	-	-	-
[NO _x] @ 150m	-	-	-	-	-	0.20	-	-	-	-
[NO _x] @ 200-500m	-	0.18	0.18	-	-	0.22	0.22	-	-	-
[SRP] @ 150m	-	- 0.21	- 0.20	- 0.20	-	0.17	-	-	-	-
[SRP] @ 200-500m	-	0.15	0.16	-	-	0.20	0.20	-	-	-

finds no clear evidence of a correlative relationship between productivity and any of these properties.

The choice of monthly time intervals is potentially significant for this temporal correlation for several reasons. First, the weak month-to-month correlations between particulate fluxes and stratification variability observed here may also simply reflect a temporal lag between the production of new biomass and its eventual export. In addition, the use of particulate flux data to infer productivity variability relies on an assumption of steady state between new production and export that becomes less robust on shorter time scales. Furthermore, the response of nitrogen fixing phytoplankton to strengthening of vertical density gradients may ultimately be dependent on the duration of the enhanced stratification state [Dore *et al.*, 2002]. The onset of greater stratification and a decrease in nutrient supply from depth would initially confer a competitive advantage to diazotrophs. This advantage could eventually disappear under conditions of prolonged, intense stratification, due to the depletion of other limiting nutrients such as phosphorous, leading to diazotroph population crashes. All of these issues could be at least partially addressed by averaging data over each season and each year of the HOT dataset. Comparisons of data averaged over these intervals, however, again reveal no statistically significant correlations between any of our measures of upper and lower layer productivity and stratification.

The results at Station ALOHA suggest that productivity does not respond linearly or even monotonically to changes in the mean stratification state. Comparisons focusing on intervals when the strongest stratification anomalies occur also yield the same result. Intriguingly, the strong biological and physical coupling observed here on seasonal time scales does not extend to interannual scales. The correlations that are observed on

interannual time scales are extremely weak; when the test for significance is made more stringent ($p < 0.01$), more than half of them disappear. The lack of a consistent biological response to even the strongest observed anomalies in any of the physical parameters suggests that a minimum forcing threshold may not yet have been reached.

1.5.3 Linkages to climate variability

Forcing from ENSO and PDO has consistently been invoked to explain interannual and decadal scale ecosystem variability at Station ALOHA [*Karl et al.*, 1995; *Karl et al.*, 2001; *Dore et al.*, 2002; *Corno et al.*, 2007; *Bidigare et al.*, 2009]. In the absence of a strong interannual association between stratification and productivity at this location, however, the linkage between local biological variability and climate variability (thought to be mediated by local stratification changes) appears tenuous. Direct comparisons of variability in HOT properties with either of the PDO or ENSO indices do little to strengthen the case for climate linkages. Given the time scales (20-30 years) associated with PDO cycles, the HOT record is probably too short for a robust correlation analysis. Comparisons with the higher frequency ENSO signal can be made with greater statistical confidence, but the response of biology at Station ALOHA to a given ENSO state has been demonstrably inconsistent [*Dore et al.*, 2002; *Corno et al.*, 2007]. It may be that the forcing effects from these climate signals are not transmitted strongly to this position, or that, even if these effects are transmitted, complex interactions between the signals originating from the tropics (ENSO) and higher latitudes (PDO) produce an incoherent local expression at this intermediate ($\sim 20^\circ\text{N}$) location.

In the absence of a direct correlation of local stratification and productivity with ENSO or PDO, recent studies have instead treated ecosystem variability at Station ALOHA as a function of the combined variability of the two climate processes. *Corno et al.* [2007], for example, argue that the records of local stratification, vertical nutrient delivery, productivity and community structure at Station ALOHA from 1988–2004 can be separated into intervals that are each characterized by a distinct pattern of phasing and relative intensity between ENSO and PDO. Similarly, *Bidigare et al.* [2009] assert that a strong, concurrent transition in both ENSO and PDO during the summer of 1998 forced a transition to a weaker stratification state leading to stronger vertical mixing, greater nutrient fluxes from depth and subsequent changes in plankton assemblages and particulate export at ALOHA. However, while a comparison of productivity rates before and after this 1998 ENSO/PDO shift does suggest a shift to higher productivity (most pronounced at ‘middle depths’ within the euphotic zone), there is no clearly observable change in stratification before and after this transition, either in the surface layer or at the base of the euphotic zone (Figure 1-4).

While much attention has been paid to the influence of ENSO and PDO fluctuations in driving ecosystem variability at Station ALOHA, the role of the recently identified North Pacific Gyre Oscillation has yet to be considered. Since NPGO variability reflects basin-wide changes in wind-driven circulation and has been correlated with nutrient and productivity variations elsewhere in the North Pacific [*Di Lorenzo, 2008*], this climate process is a natural

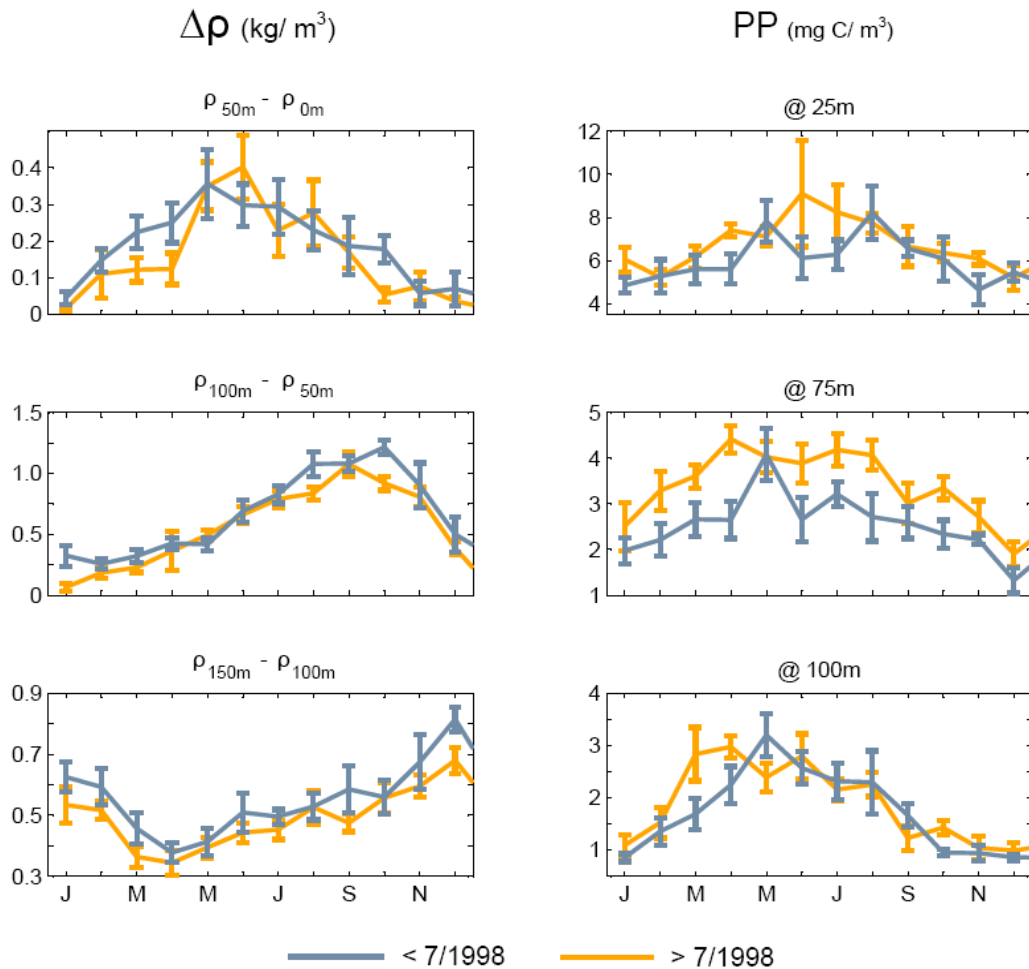


Figure 1-4: Comparison of stratification and primary productivity at Station ALOHA before and after the strong ENSO/PDO transition in July 1998. The left-hand column presents average monthly values of stratification, assessed as the change in potential density (a) in the upper layer 0-50 m; (b) over 50-100 m; and (c) near the base of the euphotic zone 150-200 m. The right-hand column presents average monthly values of primary productivity measurements (d) within the upper layer, 25 m; (e) at the transition between the upper and lower layers, 75 m; and (f) near the base of the euphotic zone, 100 m. For all panels, the blue line corresponds to the time period before the transition and the yellow line corresponds to the period following the transition. Bars indicate the standard errors.

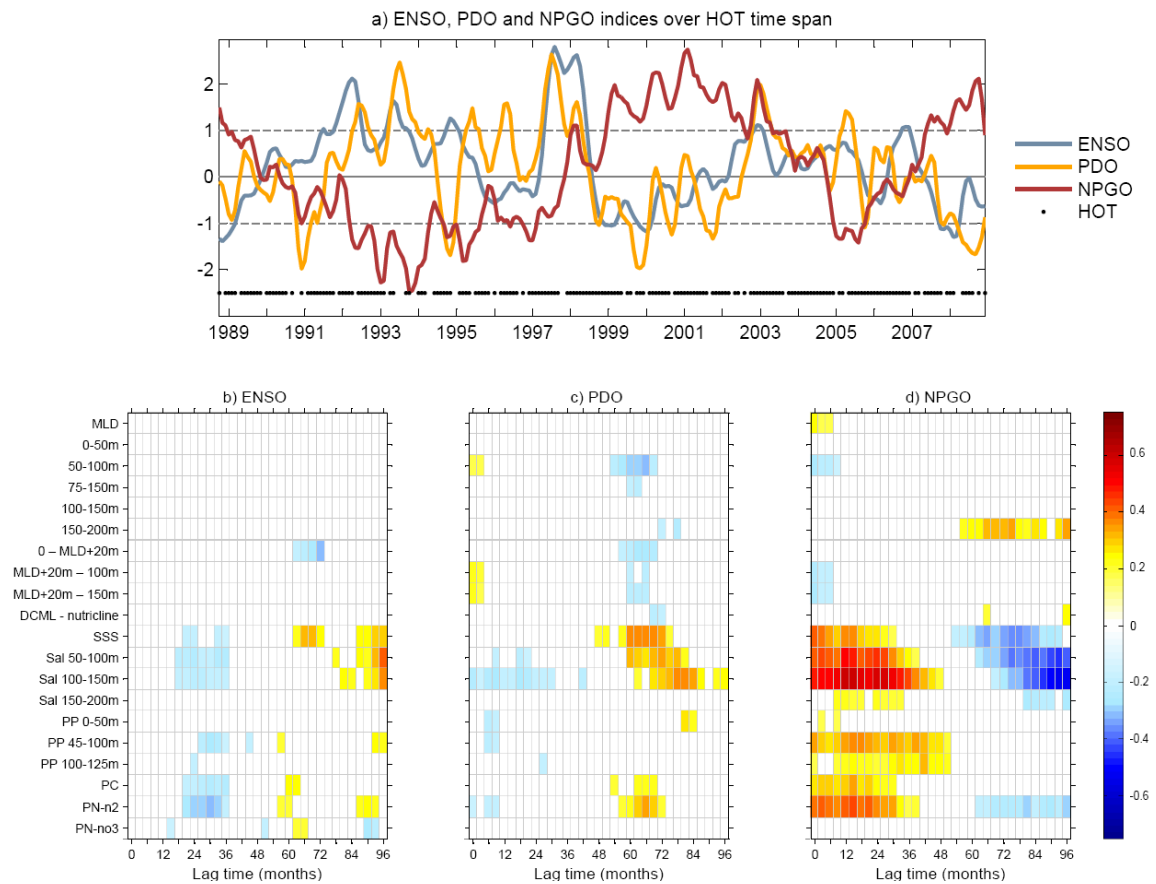


Figure 1-5: Comparison of basin-scale climate variability to HOTS Station ALOHA: (a) 3-month running means of the Multivariate ENSO Index (MEI, yellow), PDO Index (PDOI, blue) and NPGO index (red) over the HOTS record. Black dots indicate months when HOTS data were collected. Dotted lines delineate strongly positive and negative index values; (b-d) statistically significant ($p < 0.01$) linear correlations between the MEI/ PDOI/ NPGO indices and stratification and productivity time series at Station ALOHA. For each panel, the color indicates the strength and sign of the correlation. The horizontal axis corresponds to monthly lags ranging from 0 -96 months in increments of 3 months. The vertical axis corresponds to specific properties measured at Station ALOHA.

candidate for comparison with the HOT dataset. A temporal lag-correlation analysis between the NPGO index and time series of stratification and productivity at ALOHA is shown in Figure 1-5. For visual comparison, we include correlations of these HOT properties with the Multivariate ENSO Index (MEI) and PDO Index (PDOI). The lower panels show statistically significant ($p < 0.01$) correlations of ENSO, PDO and NPGO variability with a range of metrics used to describe variability in local hydrography and primary productivity over the observational record at Station ALOHA. As discussed earlier, the comparison reveals no evidence of a strong or consistent interannual association between ENSO and PDO variations and variability in local stratification or productivity. A comparison with the NPGO, however, reveals an interesting pattern of relatively stronger correlations between this climate process and primary production as well as with specific features of the local hydrography. In each case the correlations persist over a large range of time lags, and this persistence probably reflects the strong low-frequency component of the NPGO signal. The correlations are discussed in detail below.

Subsurface primary productivity at ALOHA is weakly positively correlated with NPGO variability for time lags of 0-50 months. The correlations are maximized for 'middle' and lower depths within the euphotic zone (45-100 m) and for time lags between 12-18 months, but are able to explain at most 12.5% of the observed variability ($r = 0.35$ at 18 months). The F_{PC} (related to total net community production) and F_{PN-N_2} fluxes (related to new production driven by nitrogen fixation) are also positively correlated with NPGO variability over a similar range of time lags, 0-33 months for F_{PC} and 0-44 months for F_{PN-N_2} . The correlations are both maximized at 15 months, similar to primary productivity, and are able to explain up to 11% of the observed variability in F_{PC} ($r = 0.33$) and 18% of the

variability in F_{PN-N_2} ($r = 0.43$). It is interesting to note that no correlation is observed between NPGO variability and the NO_3 -supported fraction of the particulate flux, suggesting that the correlation between the NPGO and local productivity somehow involves diazotroph activity. Since most nitrogen fixation is confined to the upper 60 m at ALOHA, it is uncertain why we do not therefore observe a stronger correlation involving primary productivity nearer the surface.

In contrast to the correlation observed between the NPGO index and local productivity variability, there is no equivalent association between NPGO variations and any of the metrics for stratification used in this study. Whatever the mechanisms that underlie the NPGO-productivity correlation, it appears that this linkage is not mediated by local stratification changes. Interestingly, however, a strong, positive correlation is observed between the NPGO index and local subsurface salinity over a similar range of time lags and depths as the NPGO-productivity correlations. These correlations extend to the surface but are maximized for 'middle-lower' euphotic zone (50-100 m and 100-150 m, abruptly weakening in waters >150 m) and for time lags between 12-18 months (again similar to the depths and time lags observed for the maximum NPGO-productivity correlations). The correlations are able to explain up to 37% of the observed variability at 100-150 m ($r = 0.61$ at 12 months). Salinity variability at these depths may be linked to the variability in North Pacific Tropical Water (NPTW), which is formed in frontal regions to the north and east of Hawaii characterized by high surface salinity. The subduction and subsequent advection of NPTW to Station ALOHA creates a persistent subsurface salinity maximum between the 24.3 and 24.7 σ_θ isopycnals, which lie on average between 100-140 m in depth [Suga, 2000; Lukas, 2001; Lukas and Santiago-Mandujano, 2008; Stammer et al.,

2008]. Variations in the intensity of the salinity maximum have been suggested to arise from changes in the surface heat and freshwater fluxes and dynamical convergences that produce the high salinity signature of the NPTW source regions [Lukas, 2001]. The observed correlation between the NPGO and subsurface salinity at ALOHA, therefore, probably reflects the strong role of this climate process in driving the formation of NPTW and possibly other water masses in the central subtropical gyre. The lag times for which the correlation between NPGO forcing and salinity variability is maximized, 12-18 months, are roughly consistent with time scales required for advection of NPTW from its source region to ALOHA [Lukas and Santiago-Mandujano, 2008]. Despite the similar spatial and temporal structure of the NPGO-salinity and NPGO-productivity correlations, it is unclear how subsurface salinity variability or NPTW variability can be mechanistically linked to changes in productivity and specifically to nitrogen fixation. One possible linkage may be that the nutrient content of NPTW varies concurrently with observed salinity changes, and that NPTW variability also produces variability in the local advective flux of nutrients transported by this water mass. An interesting future analysis would be to examine how 'upstream' property changes in the source regions of the NPTW are related to both the NPGO and local productivity variability at ALOHA.

Although the NPGO-productivity correlations described above are weak, the overall pattern stands in sharp contrast to the absence of associations between the HOT data and ENSO/ PDO variability. Even when we focus on the intervals within the record that are characterized by any combination of strong ENSO and PDO index values (i.e. $|index| > 1$, see Figure 1-5a), no consistent pattern of correlation is observed between these climate processes and either stratification or productivity at ALOHA. In contrast, the NPGO

variations correlate with local productivity and salinity variability over similar spatial (depth) and temporal scales patterns. Moreover, these correlations are observed in spite of the low degree of temporal smoothing (3-month moving averages) and a stringent significance threshold for reporting correlations ($p < 0.01$). Although the mechanisms produce the linkage between the NPGO and productivity at ALOHA are not clearly understood, the observational data suggest that the role of stratification is not dominant.

1.5.4 Why no interannual linkages to stratification?

Why is there no clear long-term correlation between the observed stratification variability at Station ALOHA and concurrent productivity variability? Inputs of allochthonous nutrients are required for the maintenance of new production, yet the mechanisms that supply these nutrients to surface photosynthesizers in the subtropical North Pacific are still not well understood. Episodic variability in new production at ALOHA has previously been suggested to result from nutrient injections caused by meteorological upwelling events, eddies and planetary waves [Letelier *et al.*, 2000; Sakamoto *et al.*, 2004; Fong *et al.*, 2008; Mahaffey *et al.*, 2008; Nicholson *et al.*, 2008; Rii *et al.*, 2008]. Consideration of this type of stochastic nutrient loading may be essential, since the continuous upward nutrient fluxes derived from observed and modeled open-ocean turbulent diffusivities have historically been considered insufficient to support observed rates of new production in the subtropical gyres [Lewis *et al.*, 1986; Ledwell *et al.*, 1993; McGillicuddy *et al.*, 1998]. However, the regular, monthly HOT sampling program is not ideally suited for detecting episodic variability in stratification, nutrient fluxes and productivity [Karl *et al.*, 2003]. Higher frequency observation programs using moored sensors have been implemented at

the HALE ALOHA site, but these have not been long enough to support robust interannual and decadal assessments.

The observational record at Station ALOHA does offer another potential explanation for the lack of a correlative relationship between productivity and stratification over interannual time scales. Figure 1-6 presents a comparison of the magnitudes of seasonal and interannual variability in stratification and productivity measured throughout the euphotic zone at this location. For each property, the histogram shows that the majority of monthly anomalies observed over the past two decades are smaller in magnitude than the average seasonal range (indicated by a solid line). The strength of the seasonal signal relative to interannual variability could potentially explain the correlations (or lack thereof) between stratification and productivity on seasonal and interannual time scales. In the upper euphotic zone, for example, while summertime stratification increases are apparently great enough to significantly decrease nutrient supply, enhance nitrogen fixation and produce summer blooms [White *et al.*, 2007; Dore *et al.*, 2008], stratification variations on interannual time scales may not be great enough to alter nutrient supply to a comparable degree. Dividing the dataset by time into pentads (indicated by different colors in Figure 1-6) does not reveal a clear temporal bias in the magnitude of the anomalies, including before and after the afore-mentioned 1998 ENSO/PDO transition. Similarly, no temporal bias is

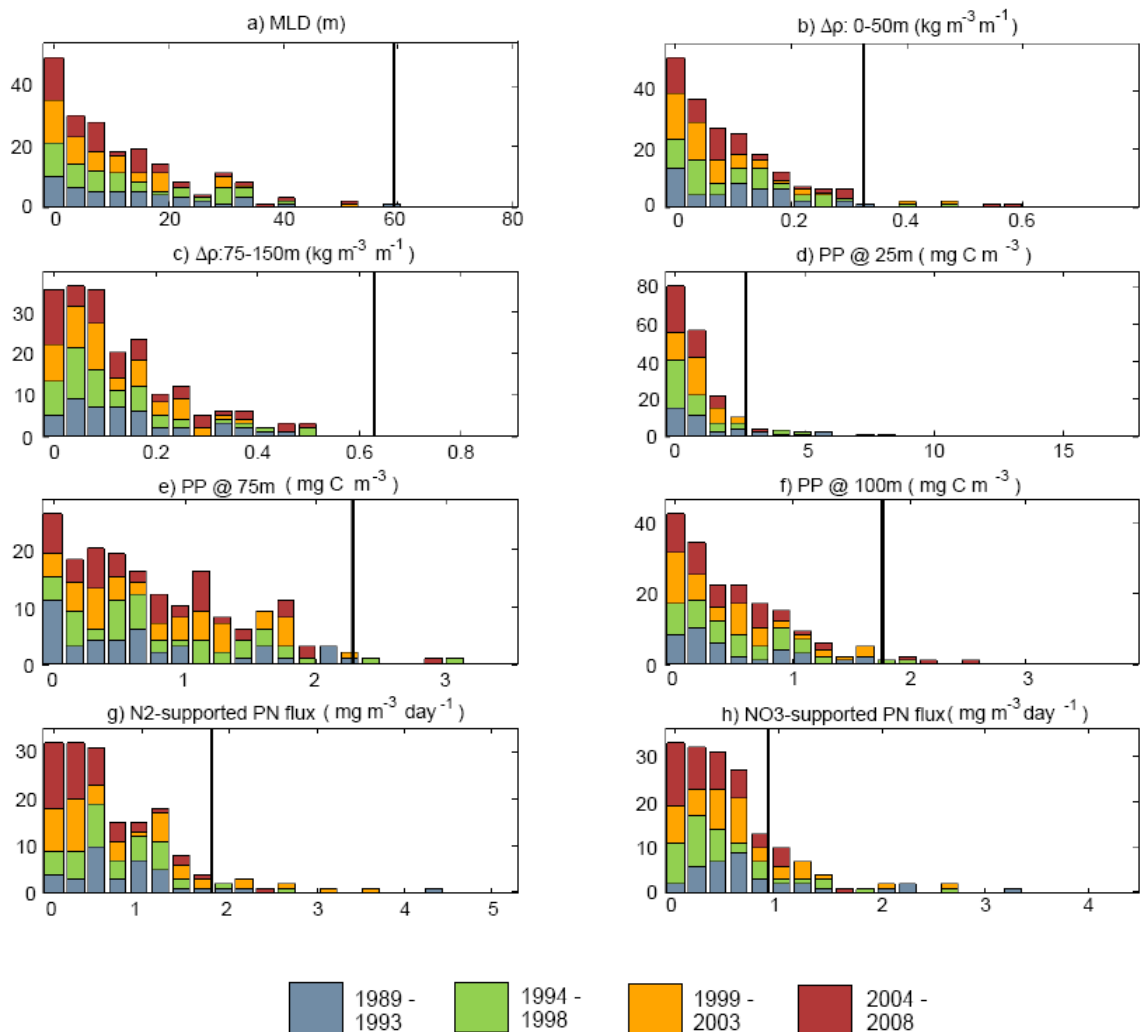


Figure 1-6: A stacked histogram of anomalies in stratification and productivity from 1988-2008 at Station ALOHA. The x-axis in each panel shows the absolute magnitude of anomalies of each property (calculated by subtracting the long-term monthly mean) as well as the magnitude of the seasonal range (indicated by a solid black line). Colors are used to separate the anomalies within each bin into distinct 5-year periods (pentads) within the HOT record: 1989-1993 (blue), 1994-1998 (green), 1999-2003 (yellow), 2004-2008 (red). The panels show: (a) mixed layer depth; (b) upper layer stratification, assessed as $\rho_{50} - \rho_0$; (c) lower layer stratification, assessed as $\rho_{150} - \rho_{75}$; (d-f) primary productivity rates measured in the upper (25 m), middle (75 m) and lower (100 m) euphotic zone; (g-h) the N_2 - and NO_3 -supported fractions of the particulate nitrogen flux, measured at 150 m.

observed when the data are divided by season (not shown). It appears that forcing from stratification changes at this location has consistently not been strong enough over the observational record to produce a consistent or coherent productivity response.

1.6 Conclusions

Over the time span of the HOT dataset (1988–2008) we conclude that there has been no consistent correlation between interannual variability in productivity and stratification at any depths within the euphotic zone. Indeed, the general biological and physical coupling that is strongly evident at seasonal time scales appears to vanish over longer time scales. Additionally, there is no clear or consistent pattern of correlation between local stratification or productivity at Station ALOHA and ENSO or PDO variability. The absence of evidence for a linkage to these climate processes may reflect the lack of a strong or consistent expression of ENSO or PDO signals at this location. A comparison of local ecosystem variability with the NPGO, however, reveals an intriguing correlation that has distinct structure in depth-space and in time. While local stratification variability at Station ALOHA is uncorrelated with the NPGO index, a similar pattern of correlation does emerge between the NPGO and both productivity and salinity in the ‘middle’ euphotic zone at this location. While the salinity correlation can be interpreted as evidence of a direct NPGO control on local hydrography, probably via NPTW variability, the question of how exactly NPGO variability could impact productivity and, specifically, nitrogen fixation at ALOHA remains unanswered.

Whatever the mechanisms are that create the observed linkages between local productivity and basin-wide climate variability, the observational evidence shows that local

stratification does not play a primary role. Stratification variability is not correlated with climate forcing and has simply not engendered a strong or consistent productivity response at this location over the last two decades. This result must be considered in the context of the complexity and non-linearity of the biological systems being observed, as well as the limitations of a regular, monthly observation program in a setting of potentially significant stochastic processes. However, another explanation for the general absence of strong correlative relationships on interannual time scales, is that the observations at ALOHA simply document a very strongly seasonally forced ecosystem.

The HOT and BATS records both provide evidence of a non-consistent response of subtropical productivity to forcing from interannual stratification variability, but apparently for different reasons. Primary productivity at BATS, which is driven by seasonal destratification, seems primed to respond negatively to future increases in upper ocean stability. The absence of correlation here reflects the complicating influence of other dynamics that affect vertical mixing and nutrient supply. The results at Station ALOHA, where seasonal destratification is not as strong or important, probably reflect instead the internal dynamics of a permanent 2-layer ecosystem model in a setting of weak interannual physical forcing. The degree to which these differences indicate fundamental dissimilarities between the Atlantic and Pacific hinges on the extent to which the HOT and BATS records are representative of their respective basins. An important consideration, then, is the relative location of each time series station within its gyre. BATS is located in the northwestern portion of the North Atlantic Subtropical gyre, a region characterized by vigorous circulation and strong seasonal wind and buoyancy forcing. The HOT program samples the relatively quiescent environment of the southern and eastern recirculation

zone of the North Pacific Subtropical gyre. It is interesting to consider whether observations at ALOHA might resemble more closely those at BATS, if Station ALOHA had been positioned farther enough to the north and west. In this respect it may be that, collectively, the HOT and BATS datasets might contribute to a single, comprehensive view of a generalized subtropical gyre.

2. The Role of Stratification and Advection in Driving Productivity in the Subtropical North Pacific and Equatorial Pacific

2.1 Introduction

Photosynthetically-driven primary production of organic matter by marine phytoplankton serves as the foundation for virtually all marine trophic networks [*Duarte and Cebrian, 1996*] and is a vital component of the biogeochemical cycles that are responsible for the large scale distributions of carbon, oxygen and nutrients in the global ocean [*Sarmiento and Gruber, 2006*]. The rate at which organic matter is generated is fundamentally modulated by variations in the amount of light energy and nutrients that are available to phytoplankton communities in the surface ocean. At the low and mid latitudes, where solar radiation is in generally abundant supply, the delivery of nutrients into the euphotic zone therefore becomes a critical determinant of new biomass production [*Falkowski et al., 1998*]. Understanding the physical factors that drive interannual and longer term variability in nutrient supply is thus crucial for understanding how marine productivity in the tropics and subtropics might respond to changes in the climate system.

Historically, the delivery of nutrients to surface photosynthesizers has been treated largely as a function of vertical exchanges between the nutrient-depleted surface layer and nutrient-replete waters directly below it, with an emphasis placed on the extent to which these exchanges are constrained by local vertical density gradients. This view reflects the expectation that variability in stratification will alter the water column's resistance to convective overturning or vertical mixing and, by extension, the entrainment of deep nutrients towards the surface. Thus, a strengthening of stratification (due, for example, to

warming or freshening at the sea surface) will depress vertical nutrient supply and, consequently, productivity, while a weakening of stratification (due to surface cooling or salinification) will enhance vertical nutrient supply and productivity [see *Doney, 2006*]. This model of local stratification control has long provided a first-order explanation for the observed seasonal cycles of marine productivity [as described by *Follows and Dutkiewicz, 2002*]. In recent years it has been extended to explain variability on interannual and longer time scales. A number of modeling studies, for example, have predicted that a warming climate will produce long-term reductions in new production at low and middle latitudes, through enhancement of upper ocean stratification, and a weakening of upward nutrient fluxes from depth [*Bopp et al., 2001; Boyd et al., 2002; Sarmiento et al., 2004; Schmittner, 2005; Cermeno et al., 2008; Riebesell et al., 2009*].

Numerous observational analyses have also attributed historical fluctuations in global records of surface chlorophyll (a proxy for phytoplankton biomass) to stratification changes produced by climate-driven changes in the upper ocean's heat content [including *Gregg et al., 2005; Behrenfeld et al., 2006; Polovina et al., 2008; Irwin and Oliver, 2009; Martinez et al., 2009; Vantrepotte and Melin, 2009; Boyce et al., 2010*]. Recent expansions of oligotrophic regions in the subtropics, for example, have been linked to interannual increases in sea surface temperature at mid-latitudes [*Polovina et al., 2008; Irwin and Oliver, 2009*]. One analysis in particular, by *Behrenfeld et al.* [2006], explicitly demonstrates a negative correlation (increasing stratification/ decreasing productivity, and vice versa) between anomalies in spatially-averaged, low- and mid-latitude productivity (estimated from satellite chlorophyll-*a*, or chl-*a*) and anomalies in spatially-averaged stratification (estimated from re-analyzed T, S fields). This result is observed for a period spanning the

aftermath of the very strongly positive phase of the El Niño-Southern Oscillation (ENSO) in 1997-1998, seemingly confirming the expectation that stratification control of nutrient supply is the primary mechanistic linkage between marine productivity and climate variability.

This view, however, is directly challenged by recent examinations of over two decades of *in situ* data from time series stations in the western subtropical North Atlantic (BATS program) and eastern subtropical North Pacific (HOT program). At both locations, interannual variability in local productivity has been shown to have essentially no correlative relationship with variability in local stratification over the observational record [Dave and Lozier, 2010; Lozier *et al.*, 2011]. These analyses of time series station data provide a rigorous test of the local stratification control model, since they make a direct comparison of stratification and productivity values measured at the same time and place. Yet the results can only provide definitive information for a single location in the ocean. Extending the analysis to the basin and global scales entails comparison of similarly contemporaneous stratification and productivity (or biomass) measures drawn from large spatial data sets, an undertaking that has until recently been hampered by a shortage of available data. The advent of satellite ocean color measurements and the proliferation of hydrographic profiles from autonomous floats and other observing platforms over the last decade, however, has greatly expanded the number of contemporaneous measurements of stratification and chlorophyll. Lozier *et al.* [2011] take full advantage of this development and match monthly SeaWiFS chl-*a* data from the subtropical North Atlantic with stratification values determined from over 35,000 profiles, demonstrating that variability in the two quantities is not strongly correlated on interannual time scales in this basin over

the period 1997-2009. Similar results are obtained for a range of different measures of stratification and productivity and also when the data are simply averaged over the spatial domain at each time step. Additionally, when the analysis of *Behrenfeld et al.* [2006] is repeated using the same re-analyzed hydrographic data and satellite-derived productivity estimates for the subtropical North Atlantic basin, no significant correlation between interannual changes in stratification and productivity is observed.

This last result underscores the likelihood that the global correlations between stratification and productivity reported previously do not apply everywhere and instead probably reflect strong associations in a particular region. An interesting question, therefore, is which region this might be. Two potential domains of interest are the subtropical North Pacific and the equatorial Pacific (Figure 2-1). In the subtropical North Pacific, the impact of stratification variability on productivity has previously been assessed at a single time series station [*Dave and Lozier, 2010*], with the observed lack of correlation there being suggested to reflect weakness in the interannual physical forcing at that location. It remains an open question, however, whether extending the analysis across the basin to incorporate regions where the interannual forcing is stronger would produce the same result. In the equatorial Pacific, no comparison of interannual stratification and productivity variability has yet been made. An investigation of this relationship here seems especially warranted since this region is the center of ENSO variability, which is a dominant component of variability in global records of ocean temperature and productivity [*Behrenfeld et al., 2006; Martinez et al., 2009*].

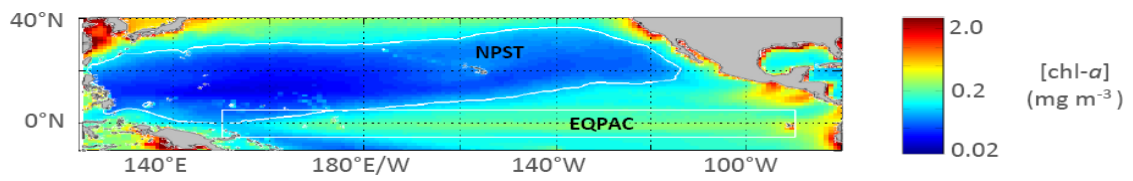


Figure 2-1: Annual mean SeaWiFS chlorophyll-*a* concentrations (chl-*a*, in units of mg m^{-3}) in the Pacific, with white contours delineating the spatial domains for this study: the North Pacific subtropical (NPST) region and the equatorial Pacific (EQPAC) region.

2.2 Background

2.2.1 Factors controlling local nutrient supply

Predictions of long-term changes in marine productivity in response to interannual and decadal variability in stratification of subtropical waters reflect an assumption that the strength of nutrient fluxes into the surface layer on these time scales is encoded in the local stratification variability. The absence of a strong historical interannual association between stratification and productivity, however, highlights two important considerations that undercut an argument for local stratification control of nutrient supply. The first is that stratification variability by itself does not predetermine the strength of vertical mixing; other processes that destroy the stratification and introduce mixing energy into the surface layer are also important. The dependence of nutrient supply on these factors is indicated by recent studies reporting correlations between subtropical productivity and variability in local buoyancy and wind forcing, both metrics from which the extent of vertical mixing can be inferred. In the North Atlantic, for example, the magnitude of seasonal phytoplankton blooms has been demonstrated to be sensitive to interannual variability in the intensity of local winds and/or buoyancy changes [Follows and Dutkiewicz, 2002; Ueyama and Monger, 2005; Henson *et al.*, 2009]. In addition, local interannual correlations are observed over much of the global ocean between chlorophyll variability and wind speed variability [Kahru *et al.*, 2010].

In all of these studies, however, the correlative relationships between subtropical productivity and metrics for vertical mixing are at best moderately strong and able to explain generally less than half of observed productivity variability. In addition, the reported positive correlations between North Atlantic bloom magnitude and interannual

wind/ buoyancy forcing [Follows and Dutkiewicz, 2002; Ueyama and Monger, 2005; Henson et al., 2009], are largely observed in waters in the southern portion of the subtropical gyre and also in the tropics. By contrast, an analysis of time series station data in the northern subtropical gyre (at BATS) by Lozier et al. [2011] demonstrates that metrics explicitly taking into account variability in vertical mixing, such as local mixed layer depth, are very weakly correlated with productivity variability. The same result is also obtained for time series station data from the subtropical North Pacific [Dave and Lozier, 2010].

Variability in vertical mixing (or the metrics from which it is inferred) thus cannot be assumed to be the sole predictor of variability in nutrient supply and productivity in the subtropics. A second point with regard to the physical controls on local nutrient supply, then, is that lateral inputs of nutrients from other locations may also be important. Previous studies have demonstrated the significant contributions of subsurface and surface horizontal advection to the climatological nutrient supply and biomass distributions in the subtropical North Atlantic [Williams and Follows, 1998; McClain et al., 2004; Palter et al., 2005] and to seasonal productivity variability in the subtropical North Pacific [Ayers and Lozier, 2010].

The local nutrient supply is thus impacted by a host of processes, including horizontal advection, that decouple stratification changes from productivity variability. However, the local stratification may itself also be impacted by horizontal advection, via lateral fluxes of heat. For example, horizontal convergence of cold, nutrient-rich waters would be expected to enhance biomass and also weaken local stratification by lowering temperatures at the surface. In other words, even in places where stratification and productivity are co-varying in a manner that is consistent with the local stratification

control model (weaker stratification/ higher productivity, and vice versa), the connection may not necessarily be causal.

2.2.2 Equatorial Pacific

Changes in local surface-layer nutrient and heat budgets in response to variable advection would be expected to be maximized in sectors of the ocean that exhibit large interannual changes in surface velocities or which have strong spatial gradients in heat and nutrients. One region in which both of these conditions apply is the equatorial Pacific. The large-scale distributions of temperature, nutrients and biomass here (Figure 2-2) are generally set by: 1) wind-driven thermocline shoaling and equatorial upwelling of cold nutrient-rich water in the eastern portion of the domain, and 2) the subsequent advection of these upwelled waters westward and away from the equator (see *Pennington et al.* [2006] and references therein). The importance of this advection has been indicated by a previous analysis of the annual nutrient budget in the warm, western regions of the tropical Pacific by *Pena et al.* [1994], who estimate that the advective supply of nutrients from the eastern equatorial Pacific is comparable to that provided by local vertical processes (mixing and upwelling). An interesting extension of this analysis, then, would be to examine how interannual variability in horizontal advection of nutrients may have impacted historical biomass distributions in the region.

2.3 Study objectives

Improvements in the spatial and temporal coverage of modern observational data sets provide an opportunity to test, at large spatial scales, a fundamental assumption about

environmental controls on marine primary productivity, namely that interannual variability in the delivery of nutrients to primary producers at low and mid latitudes is prescribed by changes in stratification. A previous study demonstrates that the assumption does not hold over the subtropical North Atlantic, yet the representativeness of this result for other subtropical basins or for the tropical ocean has not yet been established. It may be that strong associations are observed elsewhere that could account for previously reported global correlations between stratification and productivity. This study therefore addresses the question:

1. How has interannual variability in productivity in the subtropical North Pacific and the equatorial Pacific been impacted by variability in local stratification?

The equatorial Pacific, in particular, is a region that experiences substantial interannual changes in its velocity, nutrient and heat fields. To explore how these changes might impact productivity and also 'mask' a stratification signal, we explore the question:

2. How has interannual biomass variability in the equatorial Pacific been impacted by changes in horizontal advection?

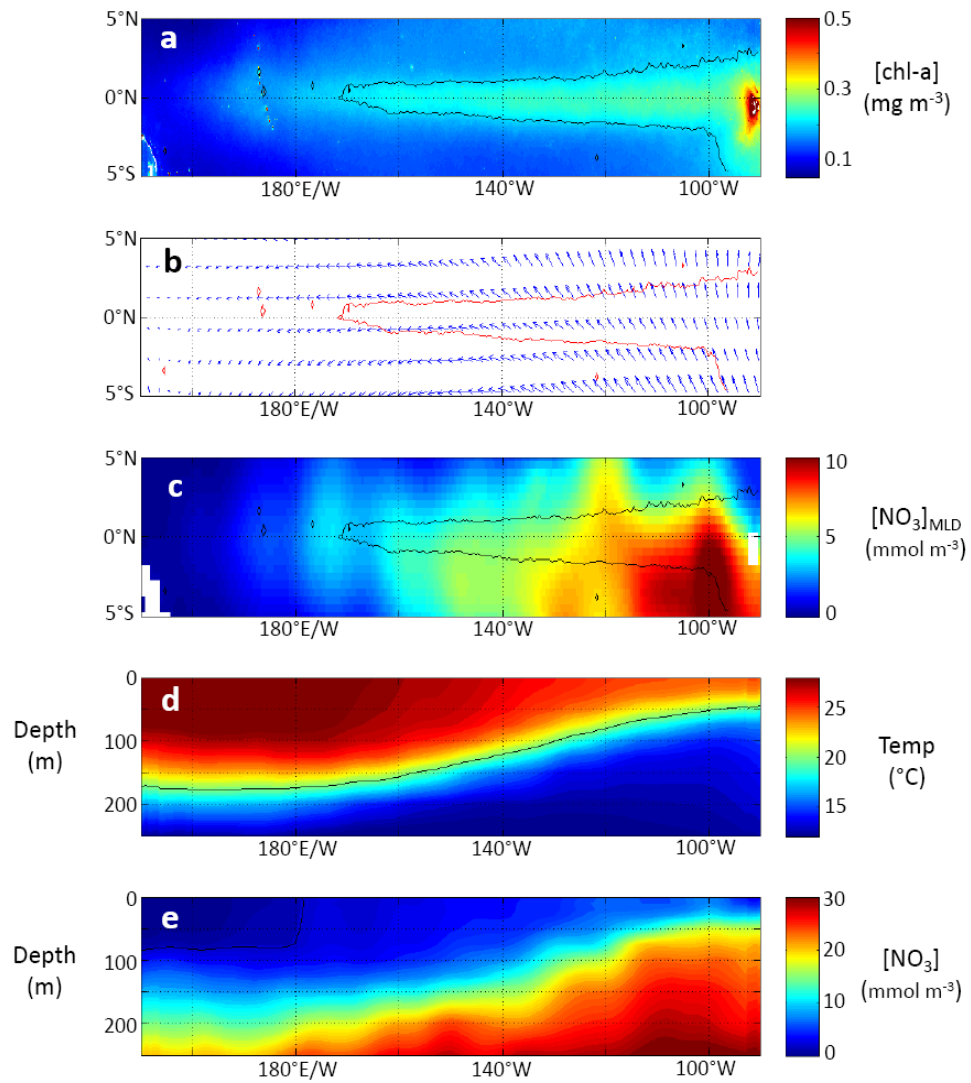


Figure 2-2: For the equatorial Pacific study region: maps of annual mean (a) SeaWiFS chlorophyll-*a* concentrations (mg m^{-3}), (b) ECMWF surface wind stresses (N m^{-2}), (c) WOA 2009 nitrate concentrations in the mixed layer (mmol m^{-3}), (d) WOA 2009 temperature cross section for 0-250 m, and (e) WOA 2009 nitrate cross section for 0-250 m. In panel (a), the black contour shows the 0.1 mg m^{-3} isoline of chlorophyll-*a*. This contour is also added to the nutrient and wind stress maps. Panels (a) and (c) show average values for the period September 1997-December 2010. Panels (b-e) show average values over the WOA timeline. The cross-sections in panels (d,e) are averaged over the range 5°S - 5°N .

2.4 Comparing basin-wide measures of in situ stratification and satellite productivity

2.4.1 Linking chl-*a* and stratification

In order to compare productivity and stratification over the subtropical North Pacific and equatorial Pacific domains, we assess phytoplankton biomass variability using the SeaWiFS chlorophyll-*a* dataset, which spans the period September 1997 - December 2010, and assess stratification using hydrographic profiles measured over the same time period. The subtropical North Pacific is well sampled, with over 200,000 available profiles, as is the equatorial Pacific, with over 188,000 profiles (Figure 2-3). In both domains we match each profile with values drawn from the corresponding monthly SeaWiFS chl-*a* field averaged within a 'capture-radius' defining a region over which the associated profile measurement is representative (see Appendix A2.1). Thus paired, the profile and satellite ocean color data provide over 13 years of contemporaneous measurements that adequately represent seasonal and interannual variability in both spatial domains (see Figures A-1 - A-6). To assess interannual variability, we subtract the local monthly mean from individual profiles and their associated chl-*a* values and then average the resulting anomalies for each month of each year within their spatial domains. The correlative relationships between these interannual time series are described in detail below.

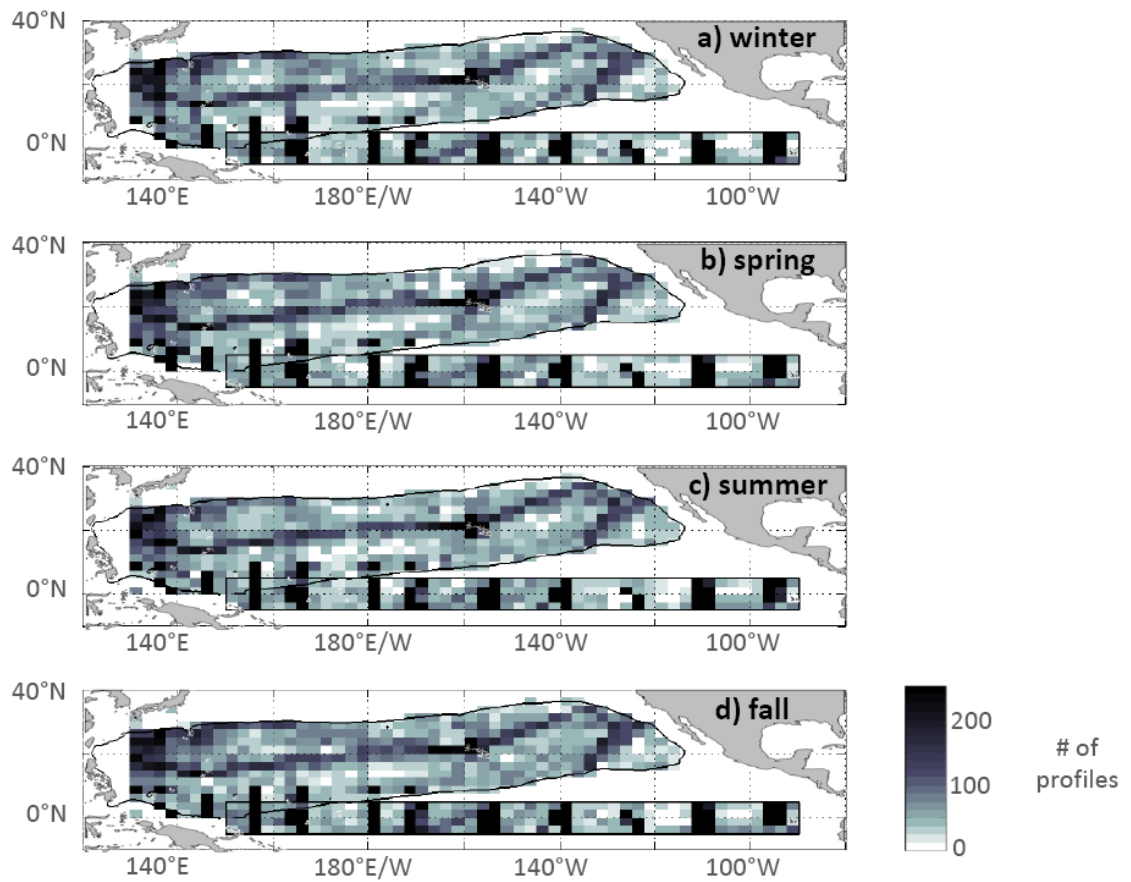


Figure 2-3: Hydrographic data coverage in the Pacific. Black contours delineate the spatial domains for this study. (a-d) Color map indicating number of individual hydrographic profiles available for analysis within these domains in the boreal winter (JFM, 49,051 profiles total), spring (AMJ, 50,442 profiles total), summer (JAS, 49,843 profiles total) and fall (OND, 52,238 profiles total).

2.4.2 Subtropical North Pacific

A comparison of interannual variability in chl-*a* and stratification (assessed as T_0 - T_{200} , for consistency with *Lozier et al.* [2011] and *Behrenfeld et al.* [2006]) within the subtropical North Pacific shows that the two properties are not strongly correlated on interannual scales (Figure 2-4a). This finding corroborates the results previously reported for the *in situ* time series comparisons at HOT and BATS and for the basin-wide comparison in the subtropical North Atlantic. A scatter comparison (Figure 2-4b) again shows that, while stratification and chl-*a* exhibit the expected negative association seasonally (as shown by the intergroup comparison), strong interannual correlations between the two properties are not observed within any given season (as shown by the intragroup comparison). In other words, chl-*a* variability does not appear to have been strongly impacted by stratification variability in this basin over the observational record.

One point of contrast between these basin-scale results and those from the North Atlantic is that the interannual correlations observed in the subtropical North Pacific are in fact statistically significant and weakly positive (for the overall time series, $r=0.30$, $p<0.05$), suggesting that biomass within this region has actually been (slightly) enhanced when stratification is stronger. A closer examination of the scatter comparison reveals that this positive correlation has been strengthened by outlier values (strongly positive biomass anomalies associated with very strongly positive stratification anomalies) from the period summer 1997 - spring 1998, which spans the peak intensity of the major 1997-1998 El Niño event. If values from this period are excluded, then the interannual correlations observed for each season as well as for the overall time series all weaken to the point of becoming non-significant ($p>0.05$).

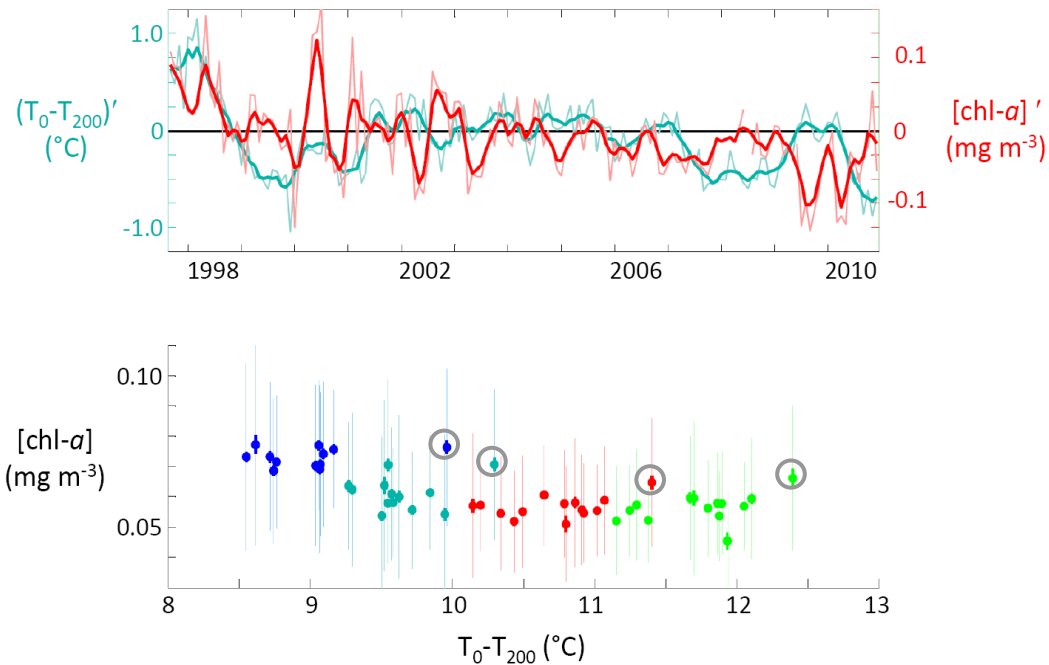


Figure 2-4: A comparison of stratification and surface chl-*a* variability over the entire subtropical North Pacific study domain from Sep 1997 to Dec 2010. (a) Time series comparison of $T_0 - T_{200}$ anomalies (blue), as measured by hydrographic profiles, and chl-*a* anomalies (red), as measured by the ‘profile-captured’ SeaWiFS data. Each time series consists of the average of all local anomalies in the subtropical North Atlantic domain for each month of each year (see Appendix A for details). Thin (bold) lines show monthly (5-month running) averages. Both the unsmoothed and smoothed time series exhibit a weak, but statistically significant, positive correlation ($p < 0.05$). (b) Scatter comparison showing the seasonally averaged anomalies in stratification and contemporaneous, profile-captured chl-*a* from winter of 1997 to winter of 2010. The shaded vertical bars indicate the standard deviations for chl-*a*, while the solid bars show ± 2 standard errors. Each seasonal value shown is produced by averaging the monthly anomalies shown in the upper panel and then adding the corresponding seasonal mean for the whole domain. The resulting points are colored to indicate the seasons, as defined in Figure 2-1. As with the time series comparison, the seasonal groupings reveal a weak but statistically significant positive interannual correlation ($p < 0.05$). These correlations are driven by outliers (labeled with grey circles) that are associated with the 1997-1998 El Niño event. When these outliers are disregarded, the observed correlative relationships disappear in both the time series and scatter comparisons.

An additional difference observed between the subtropical North Atlantic and North Pacific is that seasonal stratification values averaged over the subtropical North Pacific (~8.5-12.5°C, see Figure 2-4b) are generally stronger than those averaged from the North Atlantic (~3-9°C, see Figure 3b in *Lozier et al.*, [2011]), indicating that the same measure of stratification may not be appropriate for both basins. In the more strongly stratified North Pacific, shallower metrics may be more suitable. Repetition of our analysis using temperature differentials between the surface and 50, 100 and 150 m, however, produces essentially the same results- that is, no strong interannual association between chl-*a* variability and stratification.

A similar absence of evidence for a strong stratification control is observed when daily SeaWiFS chl-*a* fields are used in place of monthly fields, when the daily chl-*a* fields are lagged to account for phytoplankton response to stratification variability or when the chl-*a* tendency is calculated by differencing the contemporaneous and lagged chl-*a* values. Additionally, essentially the same results are obtained when the chl-*a* data are simply averaged over the spatial domain at each time step and when satellite-derived productivity fields are substituted for chl-*a* [Figure A-7a,b]. Finally, when the analysis of *Behrenfeld et al.* [2006] is reproduced for the subtropical North Pacific using the same re-analyzed hydrographic data and satellite-derived productivity estimates (in order to address concerns that methodological or dataset differences might be responsible for our contradictory results) the analysis shows no significant correlation between interannual changes in stratification and productivity (Figure A-7c).

A wide range of metrics from the subtropical North Pacific thus demonstrate that local, interannual stratification variability has not significantly impacted productivity in this region. These results, combined with those already obtained for the subtropical North Atlantic, strongly suggest that the previously reported global, climate-driven correlation between stratification and productivity at low- and mid-latitude is not driven by variability in the subtropical oceans. The next section examines the association between stratification and biomass at lower latitudes, in the equatorial Pacific region where ENSO variability is most pronounced.

2.3.3 Equatorial Pacific

A time series comparison of interannual variability in stratification (assessed as $T_0 - T_{200}$) and chl-*a* for the equatorial Pacific (Figure 2-5a) reveals that the two quantities are strongly negatively correlated over the observational record ($r = -0.60$, $p < 0.05$). This result is consistent with what would be predicted by the local stratification control model and is compelling evidence that the global correlations reported by *Behrenfeld et al.* [2006] are largely a reflection of variability in the equatorial Pacific. In this region, however, it is unlikely that changes in stratification over the upper 200 m would be directly important to productivity variability, since stratification here is generally strong and monthly climatological mixed layer depths rarely exceed 75 m (World Ocean Atlas 2009). A more appropriate measure for stratification, therefore, would be based on shallower depths. Such a comparison (Figure 2-5b,c) shows that the strong negative correlation between chl-*a*

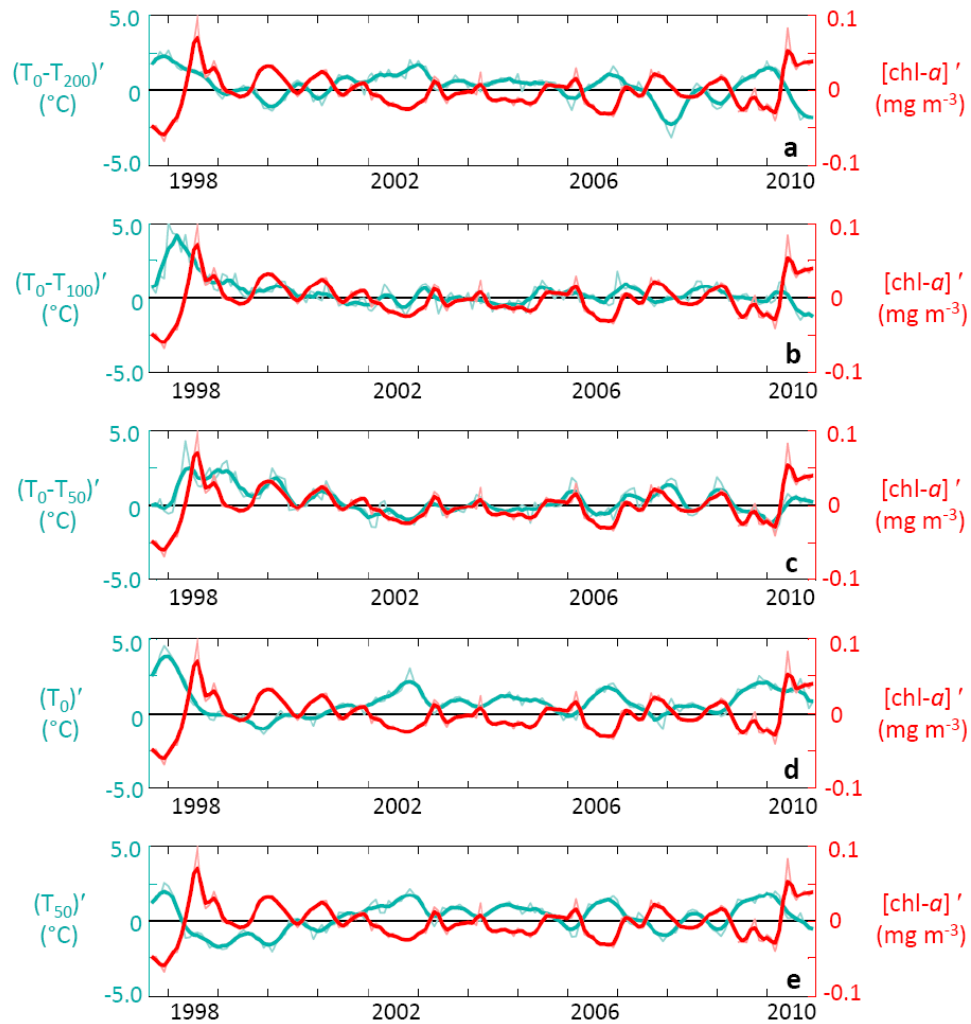


Figure 2-5: A comparison of stratification/ surface temperature anomalies (blue lines), as described by hydrographic profiles, and surface chl-*a* anomalies (red lines), as described by the 'profile-captured' SeaWiFS data, in the equatorial Pacific study domain from Sep 1997 to Dec 2010. Time series comparisons show the following correlations: chl-*a* vs. (a) T_0-T_{200} ($r = -0.60$, $p < 0.05$), (b) T_0-T_{100} ($r = -0.06$, $p > 0.05$), (c) T_0-T_{50} ($r = 0.53$, $p < 0.05$), (d) T_0 ($r = -0.61$, $p < 0.05$), and (e) T_{50} ($r = -0.71$, $p < 0.05$). Calculation of anomalies and temporal smoothing of time series are performed as described in Figure 2-4.

variability and stratification essentially disappears when stratification is assessed as T_0 - T_{100} ($r=-0.06$, $p>0.05$); the correlation actually reverses sign and becomes positive when stratification is assessed as T_0 - T_{50} , essentially within the surface layer ($r=0.53$, $p<0.05$).

The sharp change in the correlative relationship between chl-*a* variability and progressively shallower metrics for stratification is indicative of the strong role that surface temperature variability plays in setting local stratification. Indeed, when variability in chl-*a* is compared directly to temperatures at the surface (T_0) and at 50 m (T_{50}), the strong negative correlation is recovered ($r=-0.61$, $p<0.05$ and $r=-0.71$, $p<0.05$, respectively. Figure 2-5d,e). This association, as discussed earlier, may not be causal since some of the processes that can strongly impact surface layer temperatures in this region, such as wind-driven vertical (upwelling) and horizontal advection, will also directly impact the supply of nutrients. The next section considers in greater detail the interannual relationship between wind forcing, hydrographic variability and biomass in this region.

2.5 Considering the influence of wind-driven horizontal advection on biomass variability in the equatorial Pacific

A comparison of interannual variability in chl-*a* and wind fields in the equatorial Pacific reveals a striking difference in the biomass response to local wind forcing between the central and western equatorial Pacific (CWEPAC) region and the eastern equatorial Pacific (EEPAC) region (Figure 2-6). In this section we review how this spatial pattern is also observed in the relationships between chl-*a* and hydrographic variability, and attempt to place these observations in a context of a horizontal advective control of nutrient supply.

2.5.1 CWEPAC

In the central and western equatorial Pacific, chl-*a* is enhanced when wind speed increases (Figure 2-6a) and when the zonal winds are more strongly westward (Figure 2-6b). This relationship at first appears to plainly reflect the dynamics of the equatorial Pacific upwelling system: strengthened wind speed and westward winds (i.e. negative zonal anomalies) create stronger mixing and Ekman divergences at the equator, drawing up cold, nutrient-rich water and, consequently, enhancing productivity and phytoplankton biomass. This interpretation is apparently bolstered by observations that chl-*a* variability is strongly enhanced with cooler temperatures in the surface layer (Figure 2-7a,b) and that these cooler temperatures occur with greater wind speed (which enhances mixing) and stronger westward winds (which enhances upwelling) (Figure 2-7e,f).

This appealingly simple explanation, however, is complicated by another fundamental feature of the equatorial Pacific, namely that the nutricline in the central and western regions is quite deep (see Figure 2-2d), such that upwelling or wind mixing in these regions cannot automatically be assumed to draw up enough nutrients to support substantial levels of new production at the surface or enough cold water to explain the observed temperature decreases [Barber and Chavez, 1991; Pena et al., 1994; Le Borgne et al., 2002]. In such a setting, it is not clear that variability in upwelling alone would predetermine productivity and biomass variability. The problem is compounded by the observation that chl-*a* increases when temperatures at 150 and 200 m also increase (Figure 2-7c,d), a relationship that is difficult to imagine being directly causal or associated with upwelling.

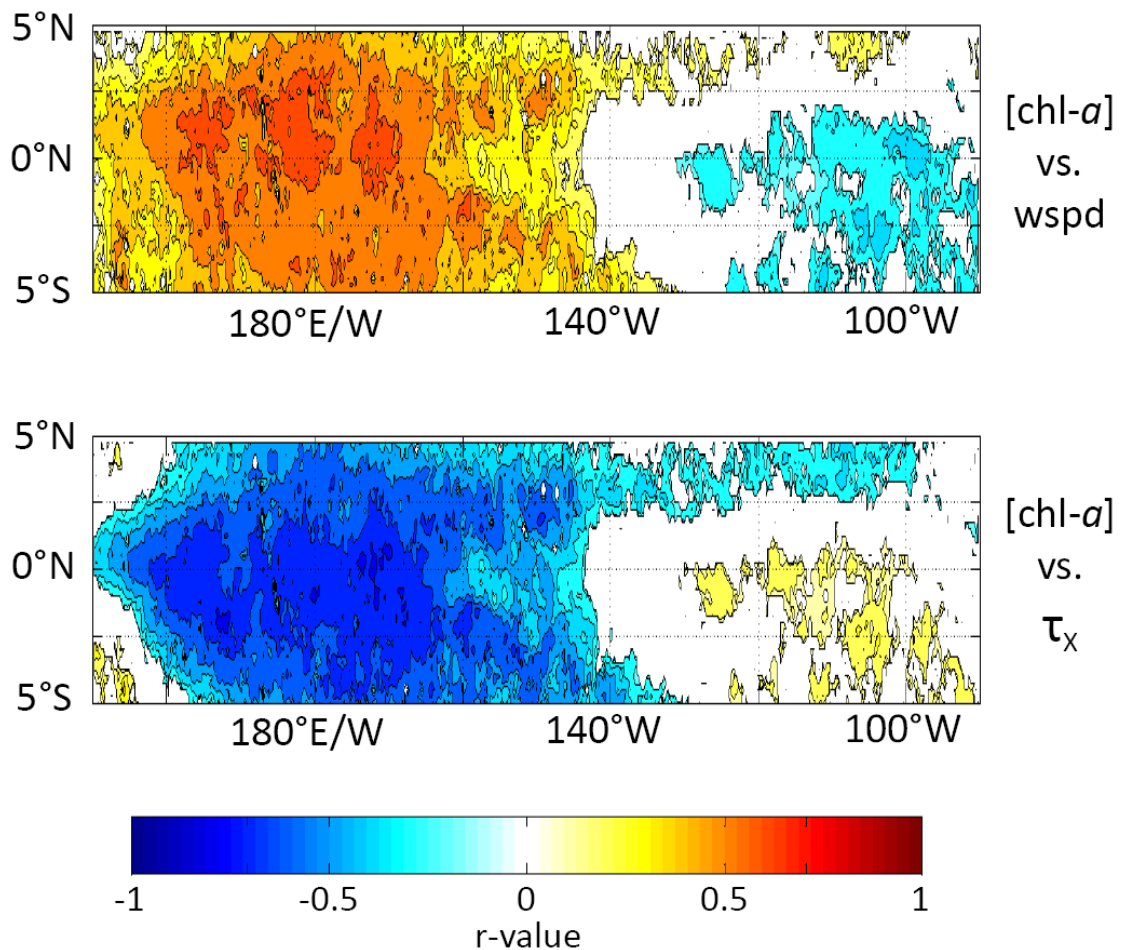


Figure 2-6: In the equatorial Pacific study region: maps of the local, temporal correlations between SeaWiFS chl-*a* anomalies and (a) ECMWF wind speed anomalies, (b) ECMWF zonal wind stress anomalies. Anomalies are calculated by subtracting the corresponding long-term monthly mean at every pixel for every time step. Colored areas of the maps indicate pixels where the correlation is statistically significant ($p < 0.05$) and there are greater than 50 data points to make the comparison. Warmer colors reflect a positive correlation, while cooler colors reflect a negative correlation. The spatial patterns of correlation are relatively unchanged even when the strongest ENSO forcing intervals (September 1997-September 1998, May-December 2010) are excluded from the comparison

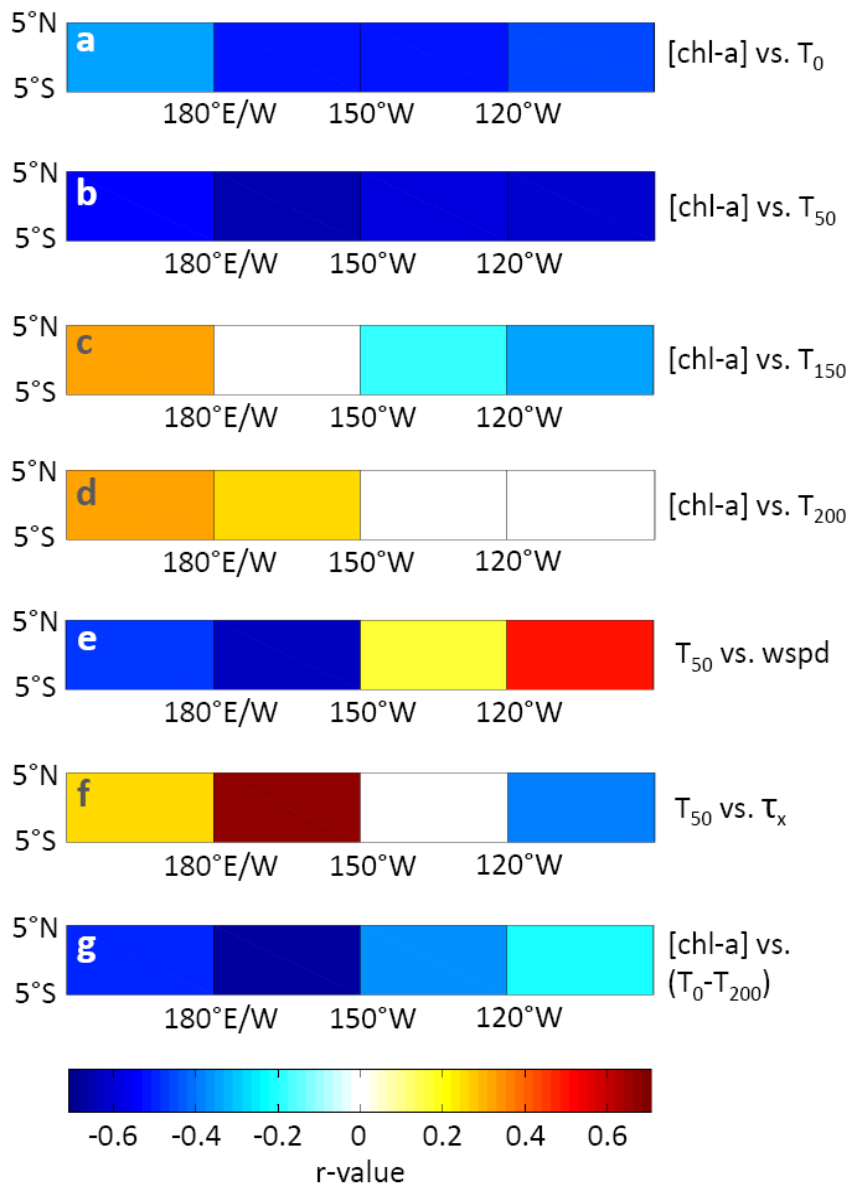


Figure 2-7: In the equatorial Pacific study region: maps of the local, temporal correlations between SeaWiFS chl-a anomalies and anomalies in (a) T_0 , (b) T_{50} , (c) T_{150} , (d) T_{200} , (e) ECMWF wind speed, (f) ECMWF zonal wind stress and (g) $T_0 - T_{200}$. All anomalies and correlations are calculated as described in Figure 2-5. The equatorial Pacific is divided into sub-domains to highlight the differences between patterns of correlation in its eastern and western regions.

How, then, can we explain the observed relationships? It may be that other nutrient sources make a substantial contribution. Maintenance of observed levels of productivity in the CWEPAC region has previously been suggested to require the supplemental delivery of nutrients via a number of other processes, including nitrogen fixation, vertical mixing and horizontal advection [Pena et al., 1994; Bonnet et al., 2009; Stanley et al., 2010]. We propose that variability in westward, wind-driven horizontal advection from the EEPAC can at least partially account for our observations. For example, a strengthening of zonal winds would increase transports of cold, nutrient-rich water from east to west and would be expected to increase biomass and decrease surface layer temperatures in the CWEPAC. This advective mechanism might also explain the observed positive correlations between chl-a at the surface and temperatures at 150 and 200 m: we suggest that westward anomalies in the zonal wind-driven advection into the CWEPAC would intensify the surface convergence, increase the dynamic sea surface height in this region, depress the thermocline and thus cause temperatures at depth to increase. Taken together, the negative association between chl-a and surface temperature (Figure 2-7a,b) and the positive association between chl-a and temperatures at depth (Figure 2-7c,d) can offer a robust explanation for the strong negative correlation between chl-a and the stratification measure T_0-T_{200} (Figure 2-7g) that does not require stratification control. In other words, changes in the temperatures at the surface and at depth occurring in response to the wind-driven advection alter stratification at the same time as they alter the transport of nutrients at the surface.

2.5.2 EEPAC

Interpreting the observed relationship between eastern equatorial Pacific wind variability and its chl-*a* response poses challenges. The prevailing winds in this region are consistently southeasterly (Figure 2-2b) and, because they are less strongly zonal than in the CWEPAC, the intensity of equatorial upwelling they induce is also less than what is observed to the west [Johnson *et al.*, 2001; Meinen *et al.*, 2001; Kessler, 2006]. The nutricline in the EEPAC, however, is sufficiently shallow that the upwelling of nutrients is able to support levels of biomass and productivity that are far greater than those observed in the CWEPAC [see Pennington *et al.*, 2006 and references therein]. It is somewhat confusing, therefore, why chl-*a* in this region is observed to generally increase (albeit quite weakly) with weaker and less strongly westward winds (Figure 2-6; a similar relationship is observed by Kahru *et al.*, 2010). As in the CWEPAC, chl-*a* is enhanced with cooler surface layer temperatures (Figure 2-7a,b); however, unlike the CWEPAC, these cooler temperatures are not associated with greater wind speed (which enhances mixing) or stronger westward winds (which enhances upwelling) (Figure 2-7e,f).

While productivity and biomass in the EEPAC are enhanced relative to the CWEPAC because of stronger upwelling of macronutrients (N,P), these nutrients are never fully drawn down due to the low availability of the micronutrient iron [Barber and Chavez, 1991] and, to a lesser degree, silicate [Dugdale *et al.*, 1995, 2002]. Previous explanations for productivity variability in this region have thus focused on processes delivering these micronutrients into the surface layer. In the case of iron, changes in the runoff from the Galapagos Islands [Pennington *et al.*, 2006], aeolian deposition of dust [Gao *et al.*, 2003; Meskhidze *et al.*, 2003] and subsurface advection from the west by the Equatorial

Undercurrent (EUC) [Wells *et al.*, 1999; Ryan *et al.*, 2006] have all been linked to observed phytoplankton blooms over the past decade. Kahru *et al.* [2010] explain the negative correlation between chl-*a* and wind speed in this region by noting that these blooms, and the enhanced iron supply that is suggested to produce them, generally occur during the boreal winter and spring, when southeasterly winds in the EEPAC are weaker (less northward, less westward).

The advective control proposed for the CWEPAC region in the previous section may also offer a complementary explanation for the observed negative correlation between chl-*a* and wind speed. We suggest that the increase of chl-*a* in response to decreases in surface temperature and the surface layer warming when winds are stronger and more westward (Figure 2-7c,d) may at least partly reflect the influence of the wind-driven advection on the export of surface layer waters out of the EEPAC and towards the west. Specifically, when the winds slacken (become less strongly south-easterly) the wind speed decreases, the zonal component of the wind stress becomes more positive (less strongly westward) and the advection of cold, relatively nutrient-rich water out of the region decreases.

The observed correlative relationships between chl-*a*, winds and hydrography in the equatorial Pacific suggest that interannual variability in the horizontal advection of nutrients may play an important role in driving biomass fluctuations on both the eastern and western sides of the domain. To quantify the interannual impact of variability in advection on nutrient supply we first perform a climatological scaling analysis to determine the importance of horizontal advection relative to other processes that could provide nutrients in this region.

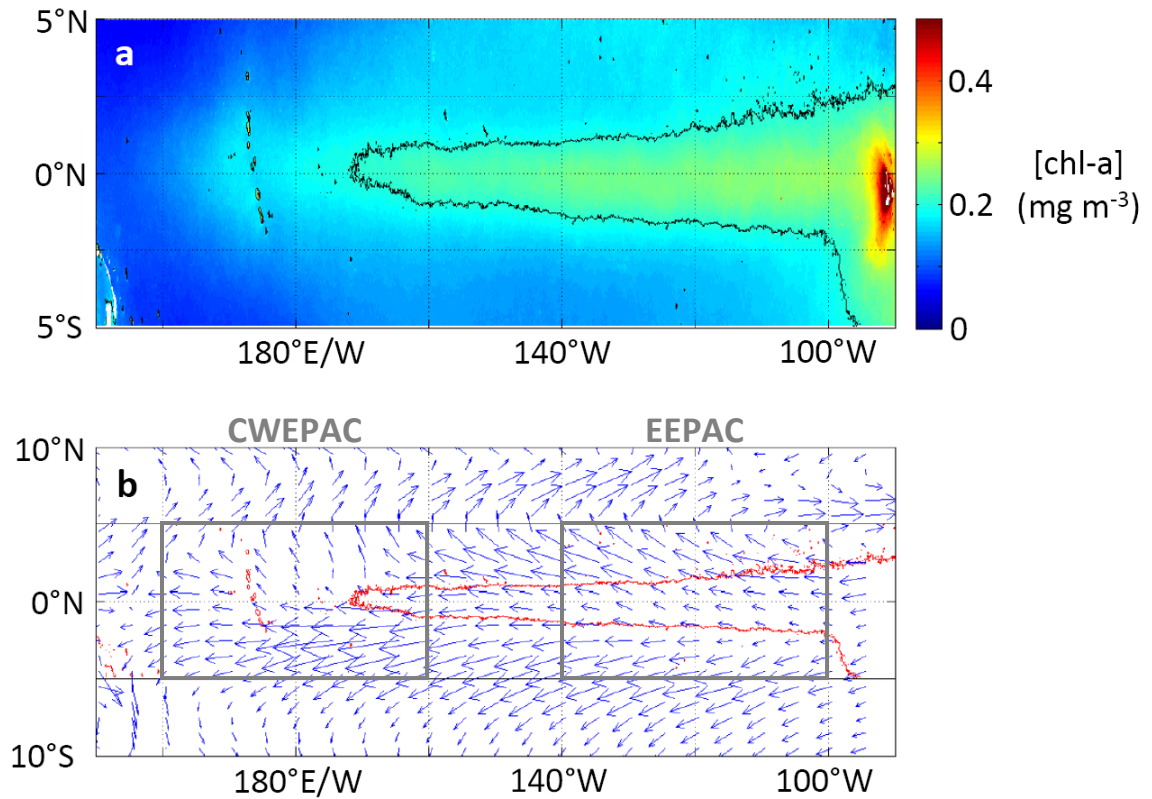


Figure 2-8 For the equatorial Pacific study region: maps of annual mean (a) SeaWiFS chlorophyll-*a* concentrations (mg m^{-3}) and (b) OSCAR total surface current vectors. In panel (a), the black contour shows the 0.1 mg m^{-3} isoline of chlorophyll-*a*. This contour is also added in red to the velocity vector map. Both fields represent average values over the period September 1997-December 2010.

2.5.3 Horizontal advection

2.5.3.1 Climatological

To determine the importance of advective fluxes relative to other processes, such as mixing, that contribute to the annual nutrient inventories of test regions in the CWEPAC and EEPAC, we perform a scaling analysis using a conservation equation for nitrate within the surface mixed layer:

In this expression, $[\text{NO}_3]$ is the nitrate concentration, averaged over the depth of the mixed layer (MLD), U_H is the total horizontal transport (Ekman + geostrophic, shown in Figure 2-8) in the mixed layer, w is the upwelling velocity and k_H and k_V are the horizontal and vertical turbulent diffusivity coefficients. The conservation equation states that the rate of change in local vertically integrated nitrate within the mixed layer in each test region, $\partial[\text{NO}_3]/\partial t$ (in units of $\text{mmol m}^{-2} \text{s}^{-1}$), reflects the sum of the contributions from processes on the right hand side of the equation, each vertically integrated over the depth of the mixed layer: (1) the convergence of vertical advective fluxes of nitrate, (2) the convergence of the horizontal advective fluxes of nitrate, (3) the horizontal mixing of nitrate, (4) the vertical turbulent mixing of nitrate and (5) changes in the strength of biological sources and sinks (SMS) of nitrate. The calculations are made for the deepest seasonal mixed layer, thus obviating the need to include a term for the vertical entrainment of nutrients that occurs with seasonal changes in depth of the mixed layer. For the scaling analysis we examine the annual average values of nutrient inputs arising from each of these processes in the EEPAC (5°N-5°S, 140°W-100°W) and CWEPAC (5°N-5°S, 160°E-160°W) domains. We delineate the zonal

(east-west) boundaries of these spatial domains to coincide with the regions identified by Kahru *et al.* [2010].

1. *Vertical advection* - As might be expected for this equatorial upwelling system, vertical advective fluxes into the mixed layer are the largest contributor of nutrients in the EEPAC region. Interestingly, our calculation also indicates that upwelling is the largest nutrient source in the CWEPAC region as well. Upward fluxes of $[\text{NO}_3]$ at the base of the mixed layer produce convergences of $2.1 \pm 0.31 \times 10^{-5} \text{ mmol N m}^{-2} \text{ s}^{-1}$ ($0.66 \pm 0.10 \text{ mol N m}^{-2} \text{ y}^{-1}$) in the CWEPAC and $9.5 \pm 0.24 \times 10^{-5} \text{ mmol N m}^{-2} \text{ s}^{-1}$ ($3.0 \pm 0.076 \text{ mol N m}^{-2} \text{ y}^{-1}$) in the EEPAC. For each region the upwelling velocities are calculated at the base of the mixed layer from the divergence of horizontal transports, using an assumption of continuity in the flow field. The uncertainties in the estimates of the vertical advective contribution are based on the temporal variance of the horizontal divergence field within each test region.

2. *Horizontal Advection* - The average annual convergence of nitrate in the CWEPAC due to horizontal advection within the mixed layer is approximately $7.5 \pm 1.1 \times 10^{-6} \text{ mmol N m}^{-2} \text{ s}^{-1}$ ($0.23 \pm 0.035 \text{ mol N m}^{-2} \text{ y}^{-1}$). The net convergence of nutrient fluxes occurs in spite of a net mass divergence observed for this region (and expected for an upwelling system), and is a result of the strong eastward gradient in $[\text{NO}_3]$ that is directed opposite to the prevailing westward flow (see Figures 2c and 8b). In the EEPAC, there is a net annual divergence of advective fluxes of both mass and nutrients in the mixed layer. The divergence of nutrient fluxes is approximately $-2.8 \pm 0.070 \times 10^{-5} \text{ mmol N m}^{-2} \text{ s}^{-1}$ ($-0.88 \pm 0.022 \text{ mol N m}^{-2} \text{ y}^{-1}$). The uncertainties here are based on the temporal variance in the horizontal velocities at the boundaries of each test region.

3 & 4. *Horizontal and Vertical Mixing* - In both the CWEPAC and EEPAC, the annual contributions made by horizontal and vertical mixing integrated over the mixed layer are significantly lower than the advective contributions. In the CWEPAC horizontal mixing produces a weak divergence of ranging from $-0.14 - 1.4 \times 10^{-7} \text{ mmol N m}^{-2} \text{ s}^{-1}$ ($-0.44 - 4.4 \times 10^{-4} \text{ mol N m}^{-2} \text{ y}^{-1}$), while vertical mixing produces a convergence of approximately $0.10 - 1.0 \times 10^{-5} \text{ mmol N m}^{-2} \text{ s}^{-1}$ ($0.032-0.32 \text{ mol N m}^{-2} \text{ y}^{-1}$). In the EEPAC horizontal mixing produces a convergence of approximately $0.90 - 9.0 \times 10^{-7} \text{ mmol N m}^{-2} \text{ s}^{-1}$ ($0.28-2.8 \times 10^{-2} \text{ mol N m}^{-2} \text{ y}^{-1}$), while vertical mixing produces a convergence of approximately $0.26 - 2.6 \times 10^{-5} \text{ mmol N m}^{-2} \text{ s}^{-1}$ ($0.082-0.82 \text{ mol N m}^{-2} \text{ y}^{-1}$). The ranges given for the mixing terms reflects our choices of values for the horizontal and vertical mixing coefficients (k_H and k_V , respectively). For k_H we have used values ranging from $500-5000 \text{ m}^2 \text{ s}^{-1}$, which have previously been observed for the equatorial Pacific [Bryden and Brady, 1989] and supported by recent modeling studies [Lengaigne et al., 2003; Cravatte et al., 2007], These values are generally higher than those traditionally used elsewhere in the North Pacific (for example, $500 \text{ m}^2 \text{ s}^{-1}$ Visbek et al., 1997) and reflect the enhanced lateral mixing arising from strong meridional shears associated with the mean equatorial currents, as well as with the tropical instability waves that have been documented to redistribute nutrient and biomass in the equatorial Pacific [Strutton, 2001; Richards and Edwards, 2003; Evans et al., 2009]. For k_V we have used values ranging from $1-10 \times 10^{-4} \text{ m}^2 \text{ s}^{-1}$, which have been previously measured for waters underlying the mixed layer in the equatorial Pacific [Peters et al., 1998; Lien et al., 1995; Carr et al., 1996; Moum and Nash, 2009]. The k_V values are greater than what has

Table 2-1: Climatological scaling analysis for processes providing nitrate in the equatorial Pacific

EEPAC: 5°S-5°N, 140-100°W

CWEPAC: 5°S-5°N, 160°E-160°W

Convergence of NO₃ in EEPAC due to:

Mechanism	(mmol N m ⁻² s ⁻¹)
1. Vertical advection	9.5±0.24 ×10 ⁻⁵
2. Horizontal advection	-2.8±0.070 ×10 ⁻⁵
3. Horizontal mixing	0.9 – 9 ×10 ⁻⁷
4. Vertical mixing	0.26 – 2.6 ×10 ⁻⁵

Convergence of NO₃ in CWEPAC due to:

Mechanism	(mmol N m ⁻² s ⁻¹)
1. Vertical advection	2.1± 0.31 ×10 ⁻⁵
2. Horizontal advection	7.5± 1.1 ×10 ⁻⁶
3. Horizontal mixing	-0.14 – -1.4 ×10 ⁻⁷
4. Vertical mixing	0.10 – 1.0 ×10 ⁻⁵

historically been used for the global thermocline ($1-10 \times 10^{-5} \text{ m}^2 \text{ s}^{-1}$ *Li et al.*, 1984; *Gregg*, 1991) and reflect the enhancement of mixing by vertical velocity shears created by the superposition of westward, wind-driven flows at the surface and eastward, subsurface flow of the Equatorial Undercurrent (EUC) [as described by *Pennington et al.*, 2006]. We note that, using our range of k_v values, the upper values calculated for the contribution of vertical mixing to mixed layer nutrients in the CWEPAC is actually higher than that attributed to horizontal advection. One reason for this may be that the majority of k_v values referenced here were measured at $\sim 140^\circ\text{W}$, closer to the eastern equatorial Pacific where the EUC shoals towards the surface and where the vertical velocity shears would thus be expected to be somewhat stronger. For this reason, the upper range of our vertical mixing calculation may overestimate its impact in the CWEPAC.

5. Sources and Sinks: Nitrogen Fixation - Non-dynamical sources of nutrients are also included in the conservation equation. One potentially important source of nitrogen into the mixed layer is nitrogen fixation by diazotrophic phytoplankton. Generally, rates of nitrogen fixation in the equatorial Pacific are relatively low due to the strong dynamical supply of nitrogen, as well as the iron limitation that characterizes these waters. Rates of nitrogen fixation for the equatorial Pacific have been inferred from numerical ecosystem simulations, with reported values ranging from $0.0082 \text{ mol N m}^{-2} \text{ y}^{-1}$ [*Moore et al.*, 2002] to $0.014-0.02 \text{ mol N m}^{-2} \text{ y}^{-1}$ [*Mills and Arrigo*, 2010]. Recent measurements of nitrogen fixation in situ made by *Bonnet et al.* [2009] also provide important clues on the relative importance of nitrogen fixation with respect to dynamical sources as the observer moves from east to west along the equator. Within the EEPAC, where the upwelling of macro-nutrients is strong but iron limitation places a strong constraint on productivity, measured rates of nitrogen

fixation are as low as $0.060\text{-}2.8 \times 10^{-9} \text{ mol N L}^{-2} \text{ d}^{-1}$ (approximately $0.0011\text{-}0.051 \text{ mol N m}^{-2} \text{ y}^{-1}$, assuming a mixed layer of 50m). The nitrogen supply from diazotrophs is estimated to be $\sim 2\%$ of the upwelled nitrogen supply, and is estimated to be able to meet only 0.8% of the productivity demand of nitrogen in this region. In the CWEPAC, by contrast, upwelling of nutrients is significantly lower, and measured rates of nitrogen fixation range from 0.11 to $18.2 \times 10^{-9} \text{ mol N L}^{-2} \text{ d}^{-1}$ (approximately $0.0020\text{-}0.33 \text{ mol N m}^{-2} \text{ y}^{-1}$). Nitrogen fixation in this region is estimated to meet up to 22% of the demand inferred from measured rates of net primary production, and up to 50% of the demand estimated for new production [Bonnet *et al.*, 2009].

In summary, this scaling analysis of the conservation equation for nitrate quantitatively demonstrates that the convergence of horizontal advective fluxes is an important dynamic process in setting mixed layer nitrate concentrations across the equatorial Pacific, with the possibility that nitrogen fixation could play an important role in the CWEPAC. The overall contribution of advection to nutrient inventories in the CWEPAC and EEPAC is roughly comparable to that made by upwelling and vertical mixing (consistent with the results of *Pena et al.* [1994]), but many times larger than the contribution made by horizontal mixing. In the CWEPAC, advection provides a net positive annual contribution of nutrients, while in the EEPAC advection removes nutrients on an annual basis. This spatial pattern is consistent with the hypothesis developed in the previous section that interannual biomass variability across the equatorial Pacific can be at least partially explained by variability in the westward advection of nutrients from the east to the west. In the next section, we attempt to quantify the interannual variability in the horizontal and vertical

advection of nutrients in the CWEPAC and EEPAC, and relate this variability to observed biomass variability in each region.

2.5.3.2 Interannual variability

The interannual variability of horizontal and vertical advective fluxes of mixed layer nutrients into the CWEPAC and EEPAC test regions is calculated by pairing interannually varying horizontal and vertical velocity fields with climatological nutrient fields. These fluxes are integrated across the appropriate spatial boundaries of the two test regions to determine the total amount of nutrients transported into the CWEPAC and EEPAC at each time step (Figure 2-9; see Appendix A4). A more accurate reconstruction of the variability in nutrient advection would undoubtedly be achieved through the use of interannually varying fields of nutrients and mixed layers, but historical observational records of these quantities are not available. The approach taken here, however, has the advantage of demonstrating whether or not interannual variability in advection by itself can account for observed variability in biomass distributions. A time series comparison reveals that convergences of horizontally advected nitrate in the CWEPAC region are associated with divergences of horizontally advected nitrate in the EEPAC ($r=-0.56$, $p<0.05$). This negative association is consistent with our expectation that an advective loss of nutrients in the east would be accompanied by an advective gain of nutrients in the west.

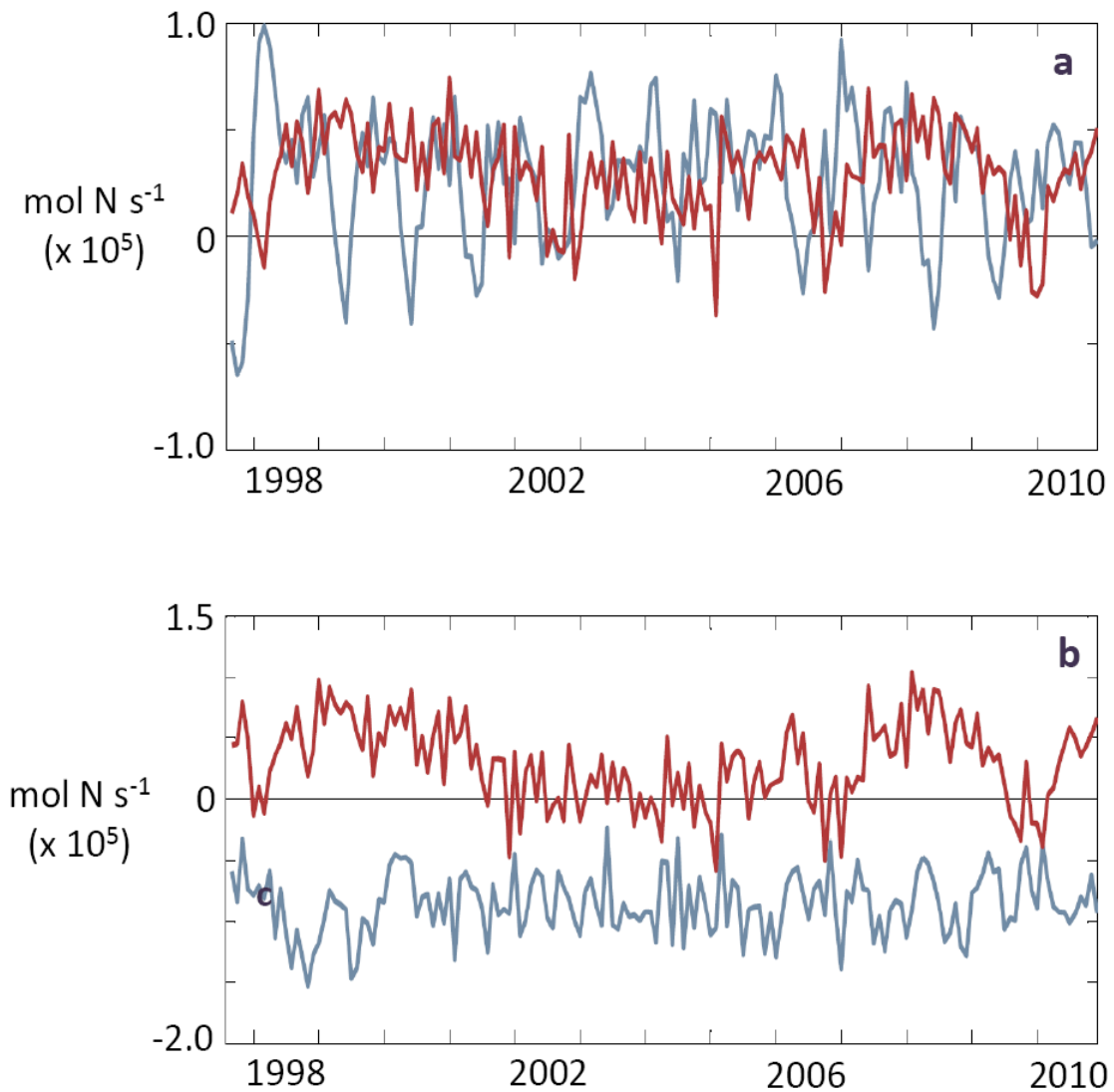


Figure 2-9: Horizontal (blue) and vertical (red) advection of mixed layer nitrate (in mmol s^{-1}) into the (a) CWEPAC and (b) EEPAC study regions. The time varying advective fluxes of nitrate are calculated by pairing interannually varying velocity data with climatological fields of mixed layer nitrate (see Appendix A4). Vertical advection is derived from horizontal divergences in the velocity field, using an assumption of continuity (see Appendix A4). The time rate of change in nitrate in each region is calculated by treating each study region as a control volume and integrating the fluxes across its N,E,S,W faces.

Within the CWEPAC region, the convergence of the horizontal advective flux of nitrate is positively correlated with chl-*a* variability when the advection leads chl-*a* by two months ($r=0.53$, $p<0.05$) (Figure 2-10a), meaning that biomass is generally enhanced when there is an advective gain of nutrients in this region. That this association is maximized when advective variability leads chl-*a* variability is consistent with the idea that the productivity across this region will take some time to respond to inputs from an external nutrient source. The lag of 2 months is consistent with the advective time scale for this region; average surface velocities of 0.2 m s^{-1} over 2 months (60 days) will transport nutrients over 1000 km, which is roughly the length scale of the CWEPAC region. The convergence of the upwelling flux of nitrate is also positively (and more strongly) correlated with chl-*a* variability in the CWEPAC ($r = 0.75$, $p<0.05$) (Figure 2-10b). The correlation is maximized with a 0-month lag, however, reflecting the fact that productivity is quick to respond to changes in this 'internal' supply of nutrients within this region.

Consistent with their mutual positive correlation with chl-*a* variability, when horizontal and vertical convergences of advected nitrate into this region are compared with each other, we observe a positive (albeit weak) correlation ($r=0.22$, $p<0.05$) that is maximized when vertical advection lags horizontal advection by 2 months. The reason for the weakness of the correlation is not immediately clear; we suggest that it may be partly due to the fact that both flux convergence time series do not represent the true interannual variability in these quantities, since the fluxes are approximated using climatological instead of interannually varying nutrient fields. We produce a composite time series that linearly combines the upwelling nutrient fluxes with 2-month forward-lagged horizontal advective fluxes and correlate with chl-*a* variability (Figure 2-10c); the resulting association

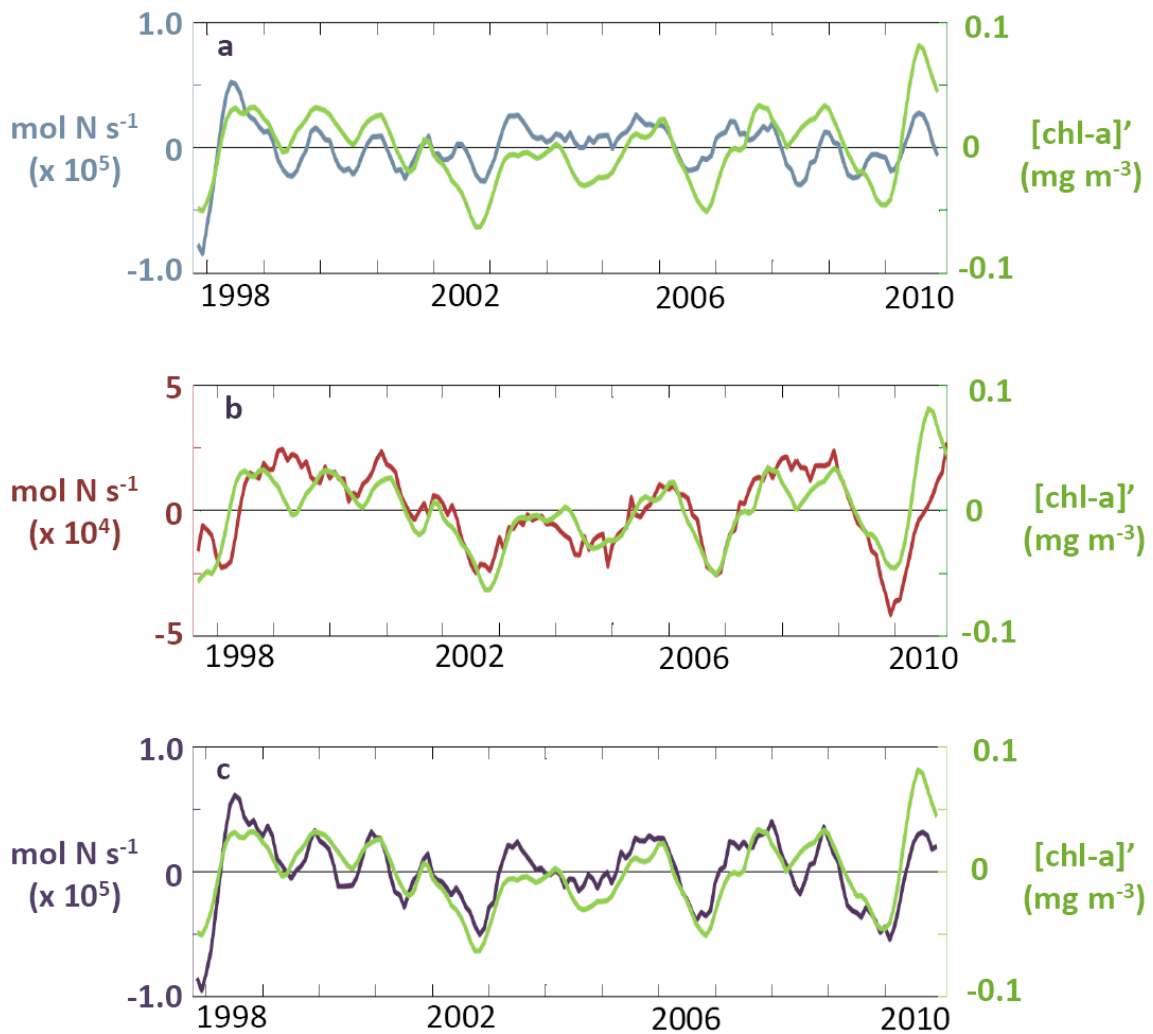


Figure 2-10: For the CWEPAC study region: Time series of average SeaWiFS chl-*a* concentrations (green) versus (a) the convergence of horizontal advective fluxes of mixed layer nitrate (blue), showing a strong positive correlation that is maximized with a 2-month lag ($r=0.53$, $p<0.05$), (b) vertically advected (upwelled) nitrate (red), showing a strong positive correlation that is maximized with zero lag ($r=0.75$, $p<0.05$) and (c) combined horizontally and vertically advected nitrate (purple, $r=0.83$, $p<0.05$). The time varying advective fluxes of nitrate are calculated as described in Figure 2-9.

is stronger than for either of the individual comparisons ($r=0.83$, $p<0.05$) and reinforces the notion that productivity is impacted by horizontal advection as well as upwelling of nutrients.

We note that the westward (negative zonal) wind stress over CWEPAC is positively associated with mass divergence ($r=0.57$, $p<0.05$) in the region and negatively associated with the divergence of both the upwelling ($r=-0.79$, $p<0.05$) and horizontal ($r=-0.25$, $p<0.05$) nutrient fluxes. These correlative relationships are consistent with the mechanistic relationship we have outlined in the previous section: when the westward winds strengthen (i.e. become more upwelling favorable), the Ekman divergence about the equator intensifies and draws more cold, nutrient-rich waters up from depth; at the same time, the stronger westward winds also increases the horizontal transport of nutrient-rich waters from the east. The end result is enhanced chl-*a* in the CWEPAC.

The same comparison repeated for the EEPAC region shows that the convergence of horizontal advective fluxes is negatively correlated with chl-*a* variability ($r=-0.46$, $p<0.05$), meaning that when there is a greater advective loss of nitrate, the biomass actually increases. The reason for this association is not clear. One interpretation might be that variability in the horizontal advection is tightly coupled with changes in the vertical, such that an intensified convergence of vertical nutrient fluxes (stronger upwelling) is able to compensate for the horizontal advective losses of nutrients. However, this argument is undermined by the earlier observation that the vertical and horizontal nutrient flux convergences are not strongly linked within the EEPAC (see Figure 2-9b). Moreover, chl-*a* variability in this region is also not strongly linked to upwelling nutrient fluxes ($r=0.18$, $p<0.05$) (Figure 2-11b). The relative insensitivity of biomass variability to changes in

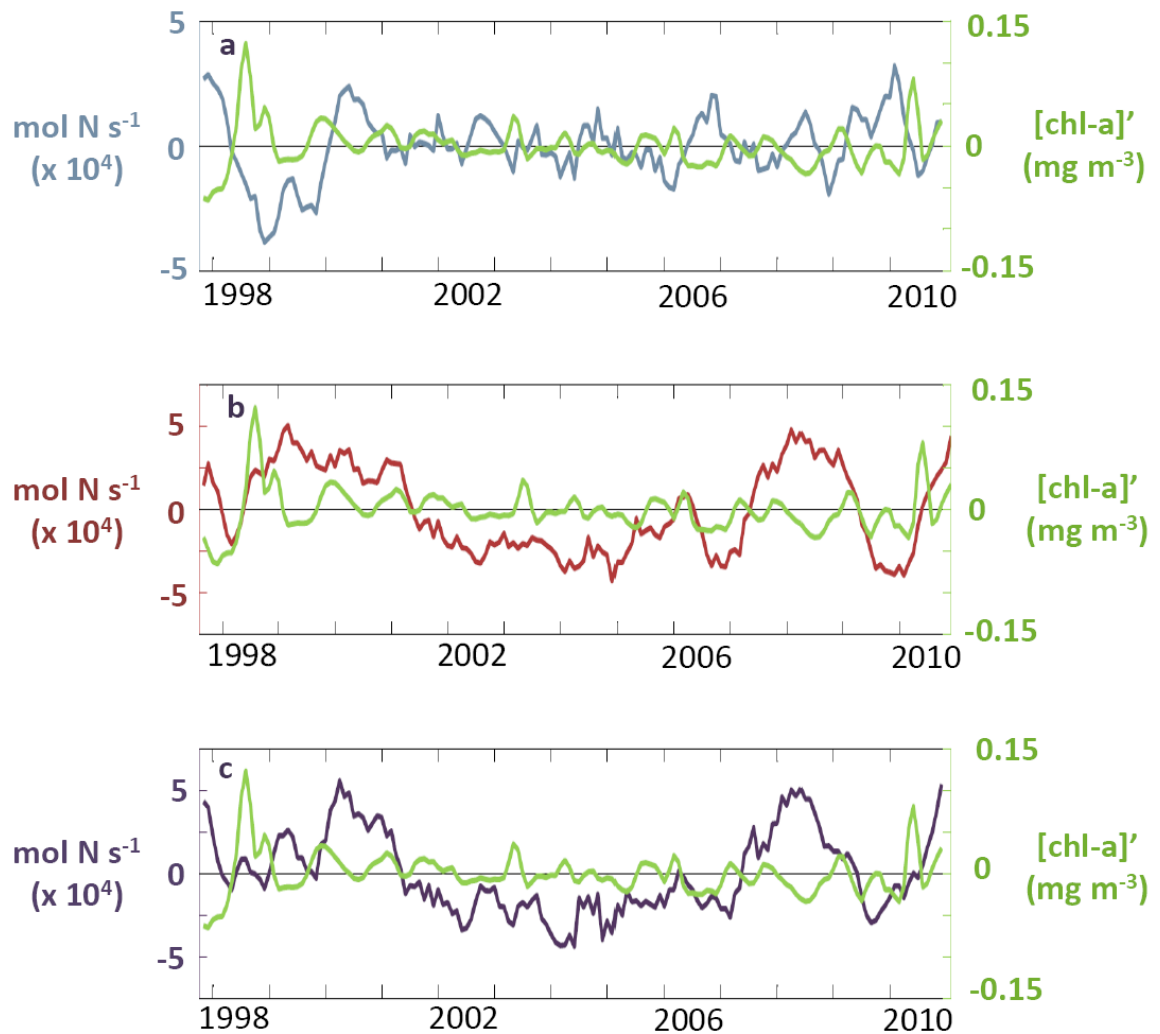


Figure 2-11 As with Figure 2-10, but for the EEPAC study region. Time series of average SeaWiFS chl-a concentrations (green) versus (a) the convergence of horizontal advective fluxes of mixed layer nitrate (blue), showing a negative correlation that is maximized with a 2-month lag ($r=-0.46$, $p<0.05$), (b) convergence of vertically advected (upwelled) nitrate (red), showing a weak positive correlation that is maximized with zero lag ($r=0.18$, $p<0.05$) and (c) combined horizontally and vertically advected nitrate (purple), showing no significant correlative relation ($r=0.07$, $p>0.05$).

upwelling perhaps reflects the fact that the EEPAC is a high nutrient-low chlorophyll (HNLC) region in which productivity is restricted more by the availability of micronutrients such as iron, rather than macronutrients [Barber and Chavez, 1991]. Indeed, it has been estimated that a cessation of upwelling here would not produce significant declines in productivity or biomass for 6 months [Pennington et al., 2006 and references therein]. It is difficult, however, to reconcile this view with the explanation offered for the correlation between biomass and horizontal advection. If productivity in the EEPAC is insensitive to changes in upwelled nutrients, why would it be sensitive to changes in horizontal advection? One potential explanation is that changes in the fluxes of nutrients in this region do not matter, rather it is the physical transport of actual biomass into and out of the region that is more important. The relative insensitivity of productivity to changes in nitrate supply seems to be underscored by the weakness of correlation between chl-a variability and a composite time series for nitrate advection (Figure 2-11c).

2.6 Conclusion

A comparison of the interannual variability in profile measurements of stratification and satellite measures of biomass and productivity in the subtropical North Pacific, demonstrates that stratification and productivity are not strongly correlated over the observational record. This finding stands for a wide range of different metrics describing stratification and productivity. These results are in agreement with those obtained from previous *in situ* comparisons of time series data from the eastern subtropical North Pacific and western subtropical North Atlantic, and with a similar comparison of satellite chl-a/ productivity data with *in situ* hydrographic data over the broader subtropical North Atlantic. Collectively these results, offer a strong challenge to a traditional mechanistic

explanation offered for interannual variability in marine primary productivity – namely that this variability is primarily driven by the local stratification control of nutrient supply.

An extension of this analysis to the equatorial Pacific, however, reveals that interannual biomass variability is strongly negatively correlated with deep measures of stratification in this region. This suggests that the previously reported global correlations between stratification and productivity have been biased by the strong associations in the tropical Pacific. A closer examination of the stratification signal here reveals that it is largely driven by changes in temperature near the surface, which are strongly impacted by the wind driven dynamics of this region. An analysis of the spatial patterns of correlation between chl-a with winds leads us to suggest that wind-driven surface currents may be responsible for fluxing nutrients (and possibly biomass) out of the eastern equatorial Pacific (EEPAC) and into the central and western equatorial Pacific (CWEPAC). We argue that that these transports also redistribute heat in a way that masks the local stratification signal and gives the appearance of a local stratification control.

A climatological scaling analysis indicates that surface advection makes a significant contribution to nutrient inventories in both the CWEPAC and EEPAC. Interannual variability in surface advective fluxes of nutrients appears strongly correlated to biomass variability in both the CWEPAC and EEPAC. In the CWEPAC, horizontal and vertical advective supply of nutrients can together account for a substantial portion of biomass variability in the region. In the EEPAC, relative insensitivity of biomass variability to changes in upwelling perhaps reflects the fact that the EEPAC is an HNLC region in which productivity variability may be relatively insensitive to changes in upwelled nutrients. It

may be that changes in the fluxes of nutrients in this region do not matter, rather it is the physical transport of actual biomass into and out of the region that is more important.

3. The impact of seasonal variability in horizontal advection on oligotrophic geometry in the subtropical North Atlantic

3.1 Introduction

The oligotrophic regions of the subtropical ocean are characterized by relatively small standing stocks of biomass and generally low rates of new production, yet their enormous size makes their total annual contribution to global marine productivity and export significant [McClain *et al.*, 2004]. Despite their oligotrophy, these regions still exhibit considerable biological variability on a range of spatial and temporal scales [Karl and Lukas, 1996] and are thus a key ecosystem of interest for studies examining the environmental factors controlling marine productivity. Because the subtropical setting of the oligotrophic regions is generally light-replete, the production of new biomass here on seasonal, interannual and longer time scales is critically dependent on the supply of nutrients from outside of the local euphotic zone (i.e. allochthonous or 'external' nutrients). Traditionally, this supply has been thought to be mainly provided by a range of vertical processes that draw deep, nutrient-rich waters upward into the surface layer, including convective overturning and mixing, eddy heaving, internal waves and meteorological upwelling events [McGillcuddy *et al.*, 1998; Sakamoto *et al.*, 2004; Mahaffey *et al.*, 2008; Nicholson *et al.*, 2008; Rii *et al.*, 2008]. Climate-driven fluctuations in vertical nutrient delivery have been widely suggested to be the principal factor in driving historical changes in subtropical marine productivity that have been observed at the basin- and global-scales [e.g. Gregg *et al.*, 2005; Behrenfeld *et al.*, 2006; Vantrepotte and Melin, 2009; Martinez *et al.*, 2009; Boyce *et al.*, 2010]. Of particular note are recent studies of satellite-derived fields of surface chlorophyll

(a proxy for phytoplankton biomass) that posit that a weakening of upward nutrient fluxes from depth is responsible for observed increases in the areal extent and/or intensity of the ocean's oligotrophic regions over the last decade [McClain *et al.*, 2004; Polovina *et al.*, 2008; Irwin and Oliver, 2009].

Interannual variability in the geometry (i.e. size and shape) and intensity of oligotrophic regions, however, is generally far smaller than that observed on seasonal scales [McClain *et al.*, 2004]. The precise environmental factors that control these seasonal changes are not fully understood. However, one process that may play an important role is the lateral advective input of nutrients originating from outside of the oligotrophic regions. Ekman advection from neighboring nutrient-rich areas has previously been shown to make a net positive annual contribution to nutrient supply in oligotrophic regions across the global ocean [Williams *et al.*, 1998; McClain *et al.*, 2004] and to explain seasonal variations in productivity in the subtropical North Pacific [Ayers and Lozier, 2010]. An understanding of the role of horizontal advection in driving seasonal variability in oligotrophic geometry is therefore crucial to understanding the mechanisms that underlie the longer term changes that have been previously reported. To this end, this analysis examines whether changes in the horizontal advection of nutrients have impacted the seasonal changes in the geometry and intensity of the oligotrophic region of the well-sampled subtropical basin in the North Atlantic.

3.2 Background

3.2.1 Climatological geometry of the oligotrophic region in the North Atlantic

A climatological map of surface chlorophyll-*a* (chl-*a*) in the North Atlantic shows substantial spatial asymmetry in the oligotrophic conditions and a characteristic ‘anvil’ shape for the region (Figure 3-1a). Chlorophyll concentrations are lowest in the central and western portions of the subtropical basin, reaching levels below 0.02 mg m⁻³ in the oligotrophic ‘core’, with values increasing radially outward. This broad spatial pattern can be generally treated as a function of nutricline depth in this region (Figure 3-1b); lower chlorophyll concentrations are observed in regions where the nutricline has been depressed, either as an adjustment in response to the wind-driven circulation or by the presence of relatively low-nutrient mode waters [McClain *et al.*, 2004; Palter *et al.*, 2005]. At the periphery of the oligotrophic region, a strongly zonal geometry is observed along its northern boundary with the more productive waters of the subpolar gyre, while the region’s southeastern and southwestern borders conform to the boundaries of the West African coastal upwelling zone and the Amazon/Orinoco outflow region, respectively. A lobe of the oligotrophic region extends southward towards the tropics.

An interesting feature of this geometry is in the Amazon/ Orinoco river outflow region, where various processes have been suggested to account for the elevated chl-*a* levels implied by the ocean color field. One such process may be the upwelling of nutrients, and subsequent enhancement of biomass at the surface, by cyclonic eddies that are shed off of the Brazil Current as it retroflects off the coast of South America [Longhurst, 1993; Longhurst, 1995]. Another explanation for the elevated satellite chl-*a* values is that the Orinoco/ Amazon discharge into the Caribbean and North Atlantic generates an extensive

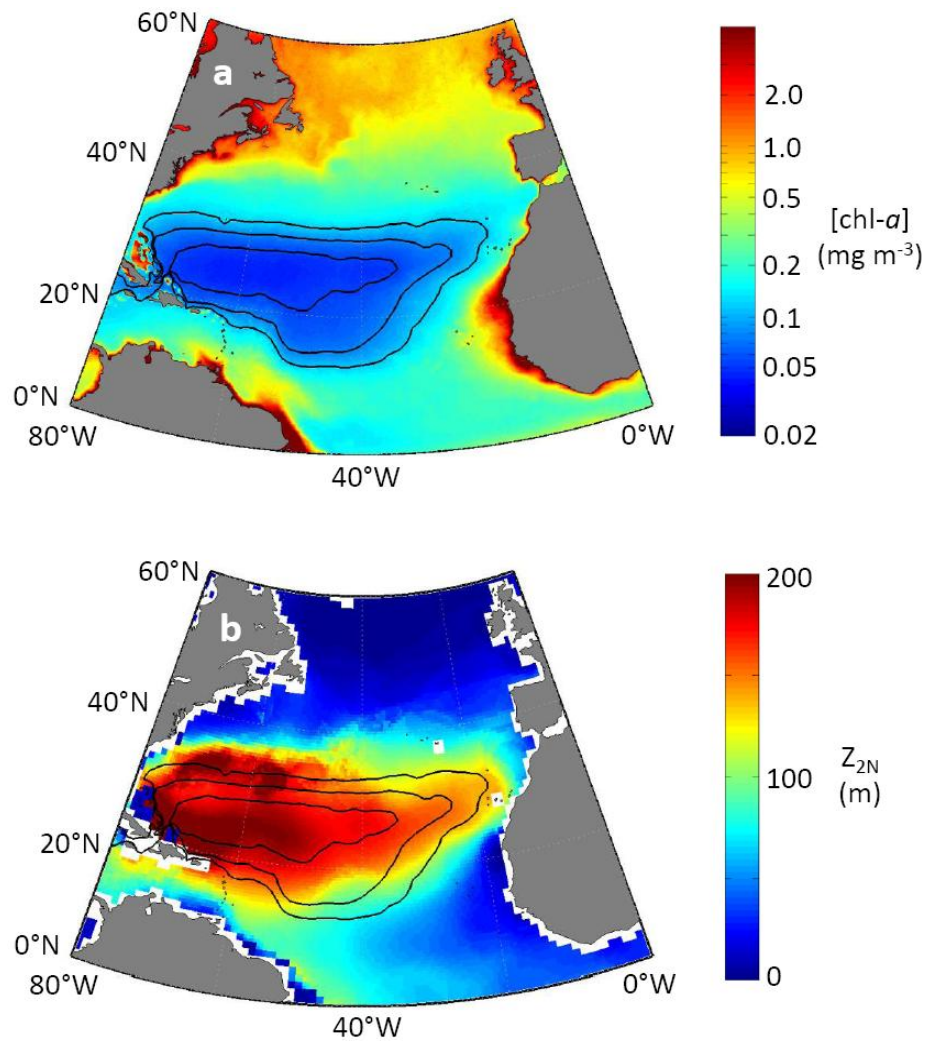


Figure 3-1: Annual mean fields of (a) surface chlorophyll-*a* (chl-*a*) and (b) nutricline depth in the North Atlantic (0°N-60°N, 0°W-80°W). The chl-*a* concentrations are plotted on a log scale, in units of mg m^{-3} . The climatological field represents the average of 153 individual 9-km resolution ($\sim 1/12^\circ$) monthly fields, derived from SeaWiFS ocean color measurements spanning the period September 1997 to December 2010. Nutricline depth is defined as the depth of the 2 mmol m^{-3} horizon and is displayed in units of meters below the sea surface. This climatological field is obtained as a 1° field from the World Ocean Atlas, 2009. In both panels, black contour lines indicate the climatological positions of the 0.05, 0.07, and 0.1 mg m^{-3} isolines of chl-*a*, which have historically been used to delineate oligotrophic regions.

plume enriched in nutrients as well as colored dissolved organic matter (CDOM) [Muller-Karger *et al.*, 1988; Muller-Karger *et al.*, 1995]. The presence of CDOM may cause satellite measurements to mischaracterize the chlorophyll concentration, since the satellite values are primarily calibrated against optically clear, open-ocean waters (“Case I” waters). More recent analyses have emphasized the relative importance of the CDOM contribution to the coloration of the Amazon/ Orinoco plume [Wilson & Adamec, 2002; Hu *et al.*, 2004]; these results suggest that an important spatial component of the oligotrophic geometry in the North Atlantic may reflect processes that do not significantly involve changes in nutrient supply or biomass.

3.2.2 Oligotrophy and nutrient supply

As discussed in the previous section, the oligotrophic regions are clearly defined by upper ocean nutrient and biomass distributions; their physical setting, however, is not as easy to delineate. Oligotrophic regions are generally thought to exist as a spatial subset of the dynamical regime of the subtropical gyres, which are characterized by a deep light field, relatively strong stratification and an anti-cyclonic wind stress curl. The wind field drives surface Ekman transport convergences and their associated downward Ekman pumping (downwelling). The observed low levels of biomass and new production in the oligotrophic regions thus primarily result from the restriction of upward nutrients fluxes from depth by the downward deflection of the nutricline in response to the wind-driven gyre circulation. A comparison of the wintertime and summertime chl-*a* fields in the North Atlantic, however, shows that dramatic changes in the geometry of the oligotrophic region in this basin are not accompanied by a comparable movement in the boundaries of the subtropical gyre or its

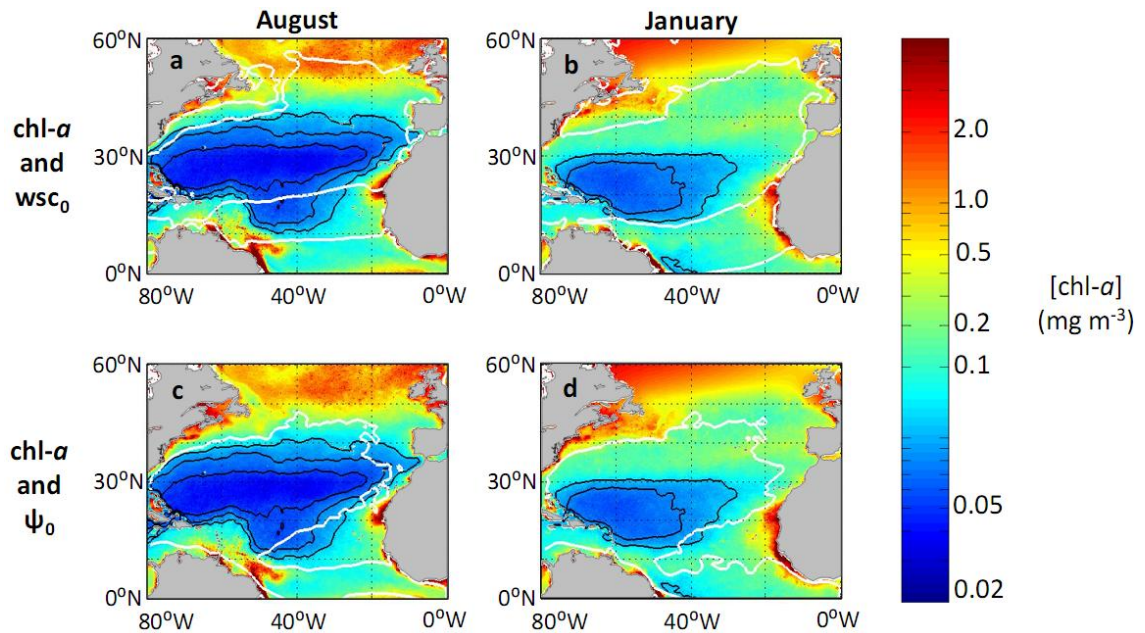


Figure 3-2: Maps showing the summer (August, left panels) and winter (January, right panels) geometries of the oligotrophic region and subtropical gyre in the North Atlantic. The oligotrophic region is indicated by the color field of SeaWiFS chl- a , along with black contours showing the position of the 0.05, 0.07 and 0.10 $mg\ m^{-3}$ isolines. The dynamical boundaries of the subtropical gyre are delineated using white contours for two metrics: the line of zero wind stress curl (top panels) and the separatrix of the geostrophic streamfunction (bottom panels). The wind stress curl data are obtained from 0.25° QuikSCAT fields, spanning the period July 1999 to November 2009. The geostrophic streamfunction is calculated from AVISO geostrophic velocity fields using an approach outlined by *Li et al.* [2006] (see Appendix B).

downwelling regime (Figure 3-2). In summer months, the oligotrophic region appears to fill out the full extent of the downwelling gyre, while in winter months its borders have retreated substantially, even though the gyre boundaries remain relatively stationary and the intensity of downwelling is actually observed to increase [McClain *et al.*, 2004; Palter *et al.*, 2005].

Why does the oligotrophic region not fill out this intensified downwelling regime during the winter months? The oceanic flow field is continuous, meaning that changes in Ekman pumping within the subtropical gyre must be accompanied by changes in horizontal advection across the gyre boundaries. Thus, the intensification of wind-driven downwelling during the winter would be expected to coincide with an increase in advection into the gyre from neighboring nutrient-rich regions, while relaxation of downwelling during the summer would coincide with decreased advection. The extent to which these lateral inputs would offset losses due to increased downwelling would depend on the spatial gradients over which they operate and the rapid biological drawdown of the nutrients as they are transported within the gyre. The spatial signature of the advective nutrient inputs would thus be expected to be limited to the periphery of the oligotrophic regions wherever they border eutrophic systems: the subpolar gyre, the tropics and also eastern boundary coastal upwelling systems. Previous studies have confirmed that horizontal Ekman advection from these regions makes a net positive annual contribution to nutrient budgets in oligotrophic regions across the global ocean [McClain *et al.*, 2004], including the North Atlantic subtropical gyre [Williams and Follows, 1998], and can explain the seasonal migration of the transition zone chlorophyll front in the North Pacific [Ayers and Lozier, 2010]. The focus of this study is to examine whether seasonal variability in horizontal advective fluxes of

nutrients in the North Atlantic can explain seasonal variability in the geometry of the entire oligotrophic region in this basin.

3.3 Seasonal cycle in oligotrophic geometry and intensity

An examination of the seasonal cycle in oligotrophic size (Figure 3-3 a,c,e) reveals that the oligotrophic core undergoes a 6-fold expansion from its minimum areal extent of $8.6 \pm 4 \times 10^5 \text{ km}^2$ during winter to its maximum extent of $5.5 \pm 0.8 \times 10^6 \text{ km}^2$ during the summer. Likewise, the larger region bounded by the $0.07 \text{ (}0.1\text{) mg m}^{-3}$ isoline experiences a 2.6-fold (2-fold) increase from a minimum wintertime area of $3.9 \pm 0.8 \times 10^6 \text{ km}^2$ ($7.5 \pm 0.7 \times 10^6 \text{ km}^2$) to a maximum summertime area of $1.0 \pm 0.1 \times 10^7 \text{ km}^2$ ($1.5 \pm 0.1 \times 10^7 \text{ km}^2$). The timing of this post-winter expansion, however, is somewhat different for the core than for the larger region. While the core expands quickly and maintains a relatively stable maximum size from late spring to late summer, the oligotrophic region as a whole undergoes a more protracted expansion all the way through the late summer. The entire region, along with its core, then rapidly contracts during the fall. This difference in timing suggests that productivity within the oligotrophic core is not driven by entirely the same processes that control productivity at the periphery of the oligotrophic region. The oligotrophic intensity also varies strongly seasonally (Figure 3-3b,d,f); average chl-*a* concentrations in the region are highest in January, coincident with its minimum size. The maximum intensity, interestingly, is not synchronous with the maximum oligotrophic size. Instead, average chl-*a* concentrations are lowest during June, ~2-3 months before the region reaches its greatest extent, again suggesting that the processes driving changes at the periphery are not exactly the same as within the core.

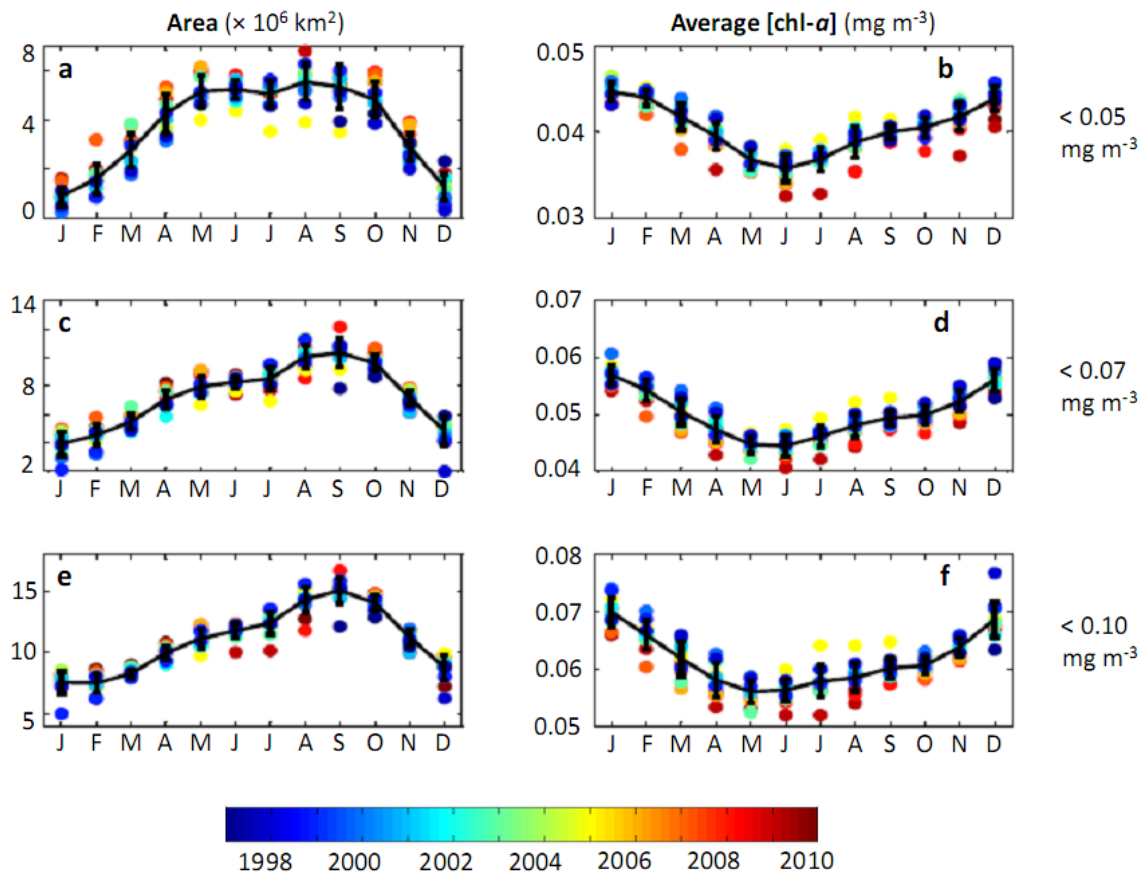


Figure 3-3: Time series showing seasonal variability in the size and intensity of the oligotrophic region in the subtropical North Atlantic, based on an examination of monthly SeaWiFS chl-*a* fields spanning the period 1997-2010. Left hand panels show the changing areal extent (in km^2) of the regions bounded by the (a) 0.05 mg m^{-3} , (c) 0.07 mg m^{-3} and (e) 0.1 mg m^{-3} chl-*a* isolines. Right hand panels show changing oligotrophic intensity, as indicated by the area-weighted average chl-*a* concentrations within regions bounded by the (b) 0.05 mg m^{-3} , (d) 0.07 mg m^{-3} and (f) 0.1 mg m^{-3} isolines. In each panel the colored points show the average value for each month of each year, with the color scale indicating the year of observation. The solid black line indicates the monthly climatological values calculated by averaging all observations for a given month, with the error bars indicating ± 1 standard deviation for each distribution. For all of these measures of the oligotrophic region, the magnitude of interannual variability is observed to be a fraction of the seasonal range.

The spatial patterns of monthly changes in the oligotrophic region (Figures 3-4 and 3-5) reveal that the largest changes in chl-*a* concentrations are focused at points along the periphery of the region as it expands and contracts. The most easily observable component of this expansion and contraction is the steady, zonally uniform migration of the northern boundary between 30°N and 40°N, towards and away from the subpolar region. The eastern boundary also expands outward, albeit less strongly or uniformly, reaching its farthest position in the late summer, coinciding with the seasonal weakening of the West African upwelling system [Marcello *et al.*, 2011]. During the interim period between the oligotrophic region's maximum intensity and maximum size, chl-*a* concentrations are observed to begin increasing within the interior of the oligotrophic region while its boundary is still expanding (Figure 3-5, see July-August panels).

One detail of note is the out-of-phase behaviour of the oligotrophic boundary near the Amazon/Orinoco outflow. During late spring and summer, elevated satellite chl-*a* values here deflect the boundary of the oligotrophic region inward towards the gyre center, just as the rest of the oligotrophic region is expanding outward almost everywhere else. This change coincides with the period of maximum discharge from both rivers [Hu *et al.*, 2004] and lends further support to the argument that the apparent summertime increase in chl-*a* in this region actually results from a misdiagnosis of riverine CDOM inputs.

3.4 Seasonal role of advective nutrient fluxes

The timing and spatial relationships of the seasonal changes in the oligotrophic region suggest that it is strongly impacted by processes at its periphery. In this section we examine the contribution of horizontal advection of nutrients to this seasonal variability. A

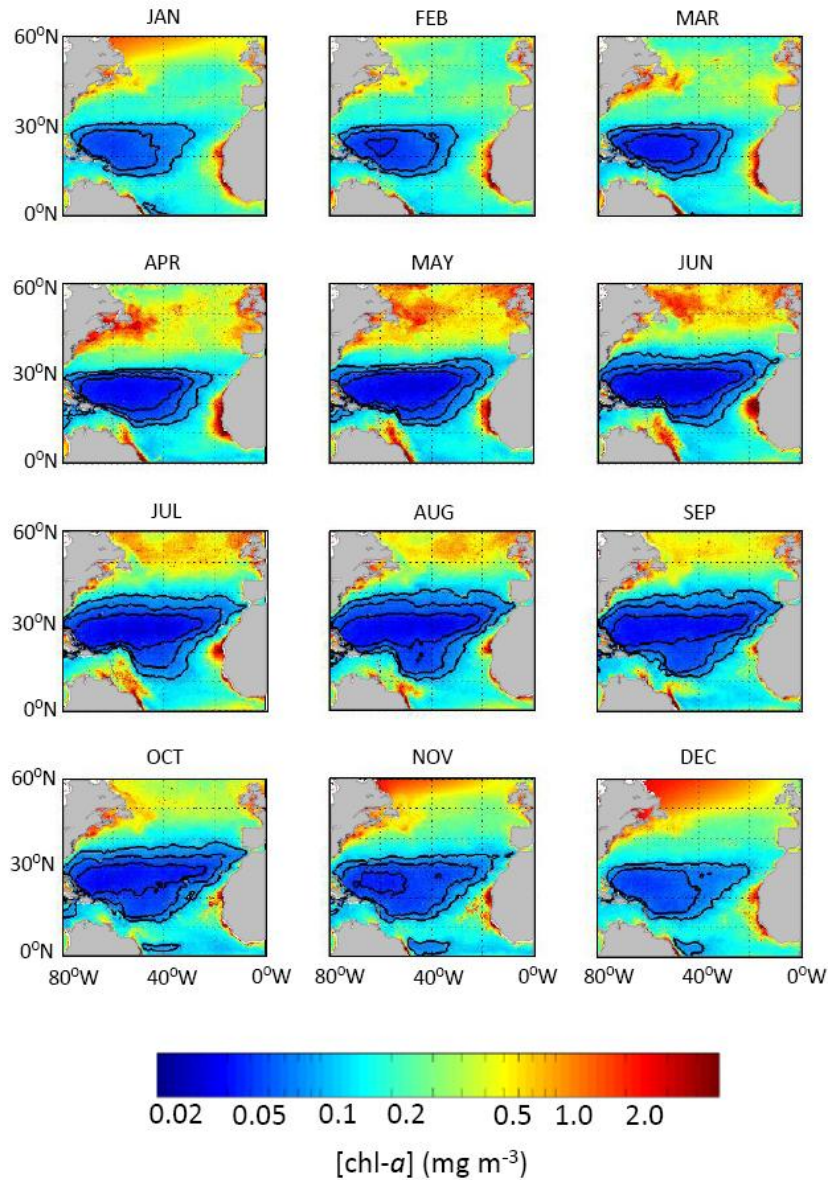


Figure 3-4: Seasonal cycle in the geometry of the oligotrophic region in the subtropical North Atlantic. The panels show monthly climatologies (January-December) of SeaWiFS chl-*a*, constructed by averaging monthly fields over the period September 1997 - December 2010. Black contours indicate the 0.05, 0.07, and 0.10 mg m⁻³ chl-*a* isolines. In each panel, the outermost contour corresponds to the 0.10 mg m⁻³ isoline. The oligotrophic region expands to its maximum extent during the late summer and contracts to its minimum extent during the winter. Note that the fields have been re-binned to 1° spatial resolution and so during the winter months the 0.05 mg m⁻³ contour is not observed.

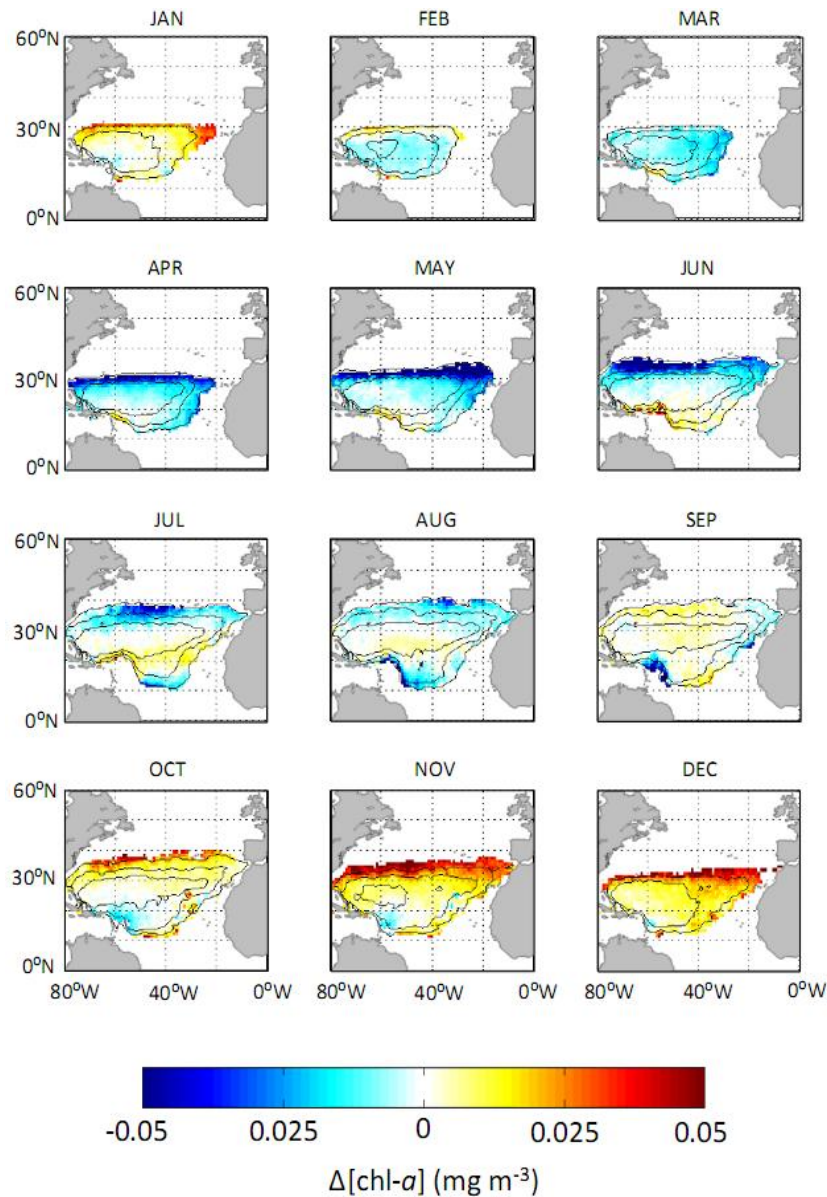


Figure 3-5: As with Figure 3-4, but here the panels show month-to-month differences in SeaWiFS chl-*a*. The color of each pixel indicates the absolute change in chl-*a* concentration from the previous month at that location. The black contours indicate the position of the 0.05, 0.07, 0.10 chl-*a* isolines. To highlight changes in the shape, position and internal ‘structure’ of the oligotrophic region, the color field is masked to remove all pixels that lie outside of whichever boundary (for the previous or current month) was most extensive. In other words, for any month in which the oligotrophic region is contracting, the corresponding panel includes pixels that lie within the previous month’s oligotrophic boundary.

comparison of summer and winter chl-*a* and Ekman layer nitrate ($[NO_3]_{Ek}$) fields shows that the oligotrophic region is at its maximum extent during the summer, when nutrient concentrations at its periphery are low and wind-driven Ekman transports in the basin are relatively weaker (Figure 3-6a,c). The situation in the winter is reversed (Figure 3-6b,d), with the oligotrophic region being at its smallest size at the same time that nutrient concentrations are generally higher along its periphery and Ekman transports in the basin are generally stronger, though these changes are more pronounced to the north than the south. We note that the summertime deflection of the oligotrophic boundary in the Amazon/Orinoco outflow region is not accompanied by significantly elevated nutrient concentrations, as might be expected if there were a strong seasonal increase in eddy pumping in this region. This detail is consistent with the argument that the summertime increase in chl-*a* in this region is biased by an increase in riverine CDOM.

Overall, these maps are consistent with the expectation that the diminishment of the oligotrophic region from its maximum size in summer to a minimum size in winter results from stronger winter winds and seasonal intensification of the negative wind stress curl, which increase Ekman transports of nutrients into the subtropical gyre from the nutrient-rich subpolar gyre, the tropics and the West African coastal upwelling zone. The subsequent expansion of the oligotrophic region is expected to occur when the Ekman transports, as well as the spatial nutrient gradients over which they operate, weaken from the winter into the summer. The seasonal evolution of the surface-ocean nutrient field (and potentially the geometry of the oligotrophic region), however, is also impacted by local (non-lateral) processes. For example, light-fueled biological uptake during the summer months would be expected to draw down surface nutrient concentrations, while vertical

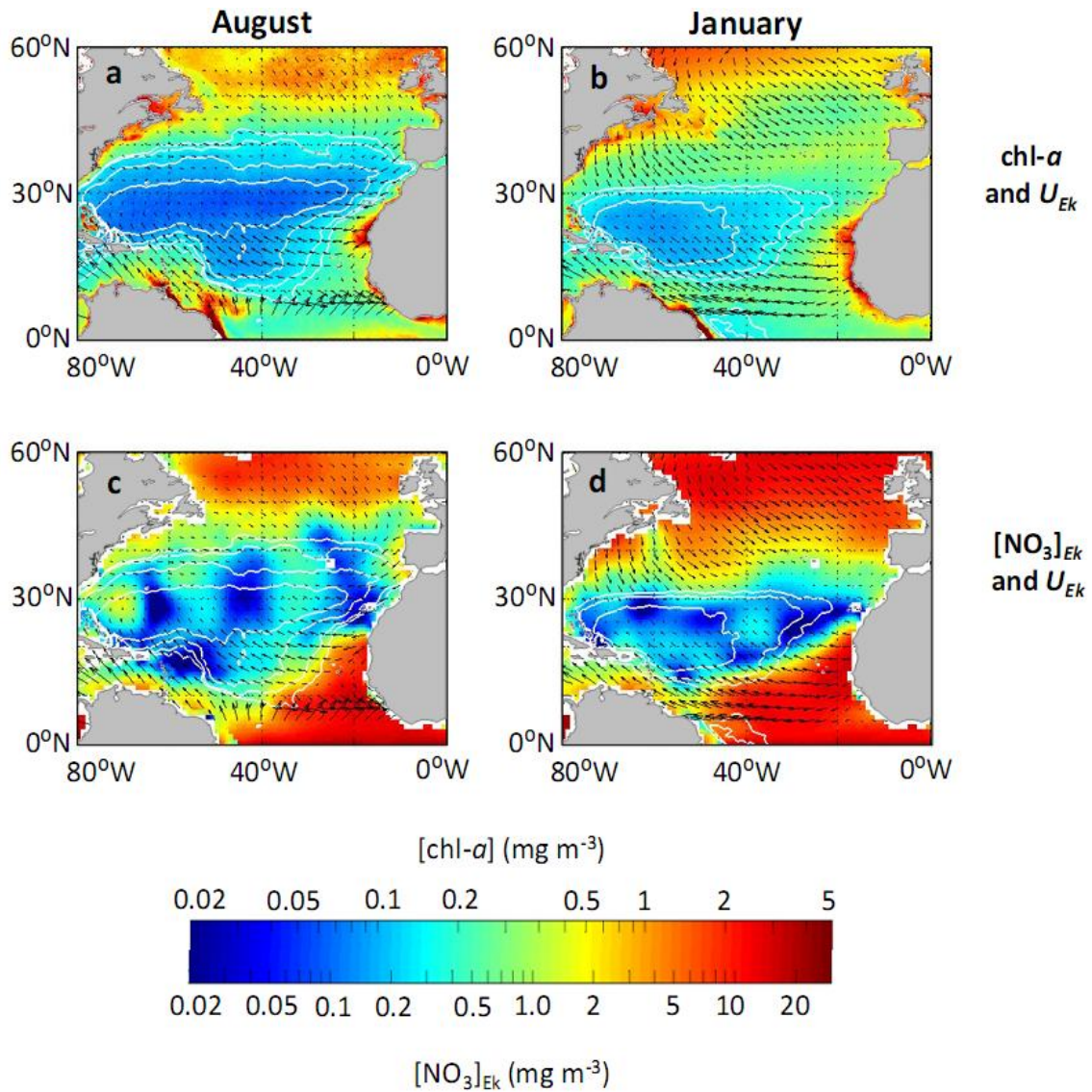


Figure 3-6: Maps showing the summer (August, left panels) and winter (January, right panels) distributions of SeaWiFS chl-*a* (mg m^{-3} , top panels) and average Ekman-layer nitrate concentration (mmol m^{-3} , bottom panels). In each panel the white contours show the positions of the 0.05, 0.07 and 0.10 chl-*a* isolines and the black arrows indicate the horizontal Ekman velocities. The Ekman currents are obtained from CTOH/LEGOS global fields, estimated from satellite scatterometry using an approach outlined by *Sudre and Morrow* [2008], while the Ekman-layer nutrient fields are derived from World Ocean Atlas 2009 data (see Appendix B). Both chl-*a* and nutrient fields are plotted on a log scale.

entrainment by enhanced overturning during winter months would recharge surface nutrients. An interesting future analysis would be to quantify the impacts of local and non-local nutrient dynamics to determine their relative importance in shaping surface nutrient concentrations around the subtropical basin. We note, however, that the geometry of the North Atlantic oligotrophic region does not closely match the spatial patterns of either winter mixed layer depth in this basin (see Figure 5 in *Palter et al.*, 2005) or the seasonal patterns of light levels at the surface of the ocean (assumed to be varying essentially meridionally). Our expectation, therefore, is that annual cycles of mixing and light availability in the North Atlantic will not be able to fully explain the observed changes in the size and shape of the oligotrophic region in this basin.

To examine the impact of seasonal variability in nutrient inputs by horizontal advection, we calculate the divergence of these fluxes within the Ekman layer as $\nabla \cdot \mathbf{U}_{HTot} [NO_3]_{Ek}$. We assess the horizontal nutrient fluxes using the total (Ekman + geostrophic) surface velocity field, \mathbf{U}_{HTot} , because geostrophic currents also contribute to horizontal nutrient fluxes and are primarily responsible for transporting nutrients around the gyre once they have been fluxed in. A comparison of the climatological oligotrophic region with the climatological divergence field for total horizontal advective fluxes of nitrate (Figure 3-7) suggests that, on an annual basis, the oligotrophic region occupies a space characterized by small inputs of horizontally advected nutrients, and that the oligotrophic boundaries are generally constrained by the regions of strong convergence (negative divergence) of horizontal nitrate fluxes – particularly along the northern boundary with the subpolar gyre and the eastern boundary with the upwelling zone. In the southern portion of the domain,

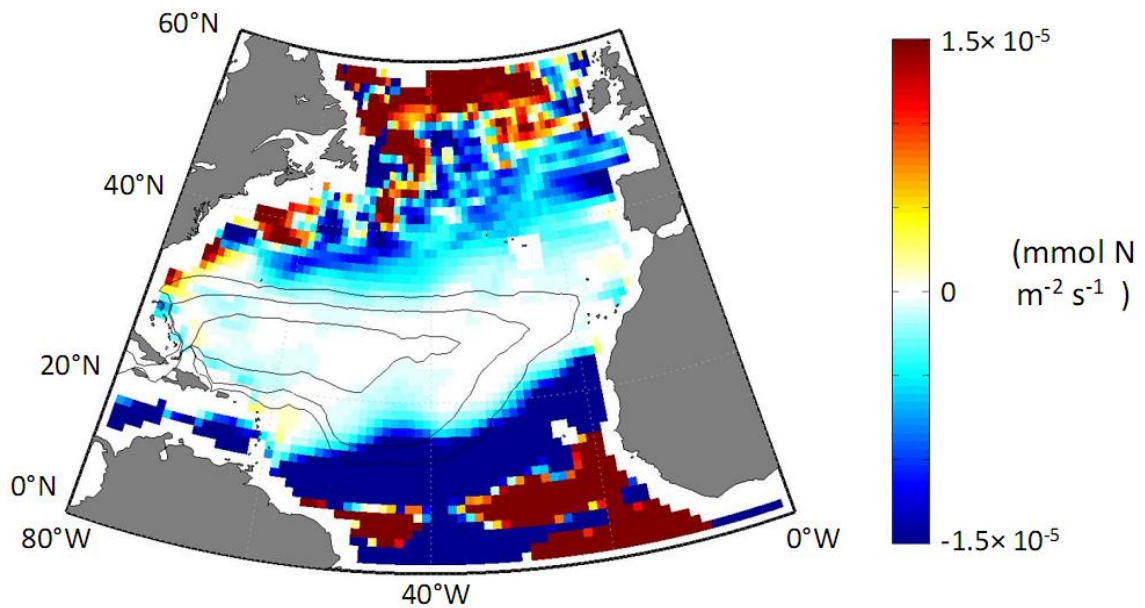


Figure 3-7: Annual mean divergence of the total (geostrophic + Ekman) horizontal advective NO₃ flux within the Ekman layer. The color field indicates the divergence (in mmol N m² s⁻¹), with cooler colors indicating a negative local divergence (or convergence) of NO₃ and warmer colors indicating a positive divergence. The black contours indicate the climatological positions of the 0.05, 0.07 and 0.10 mg m⁻³ chl-*a* isolines (as shown in Figure 3-1). The annual mean horizontal advective NO₃ fluxes are calculated by first pairing monthly climatologies of total surface currents obtained from NOAA OSCAR 1° velocity fields with monthly climatologies of Ekman-layer nitrate concentrations derived from World Ocean Atlas fields, then calculating the divergence of each monthly flux field and finally averaging the monthly divergence fields (see Appendix B).

however, the divergence field does not conform to the oligotrophic contours, with areas of very strong convergence overriding the boundaries of the oligotrophic region. The strength of this convergence here most probably reflects the deepening of the Ekman layer, and consequently increasing values of $[NO_3]_{Ek}$, at lower latitudes.

A comparison of the monthly climatologies of the oligotrophic contours and advective flux divergence allows us to visually compare seasonal variability in the two fields (Figure 3-8). Overall, the comparison is favorable. In each month the convergence of the advective nutrient fluxes generally conforms to the boundaries of the oligotrophic region. The convergence is most intense when the oligotrophic region is at its minimum extent (January, February) and weakest when the oligotrophic region is at its maximum extent (August, September). The very strong convergence in the southern portion of the domain described earlier still overlaps the oligotrophic boundaries, but also very clearly weakens during the late summer as the oligotrophic region expands southward. When the monthly advective flux divergences are re-calculated using a climatological (constant) nutrient field and variable Ekman transports, similar results are observed. These results suggest that the seasonal evolution of the horizontal nutrient fluxes is largely driven by changes in the advective field rather than in nutrient distributions, reinforcing our expectation that any changes in the surface nutrient field that arise from seasonal cycles of mixing and light availability are not a dominant factor driving the observed changes in the size and shape of the oligotrophic region.

The visual comparison of the seasonal divergence field with the oligotrophic boundaries suggests that the impact of horizontal advective nutrient inputs is limited to the

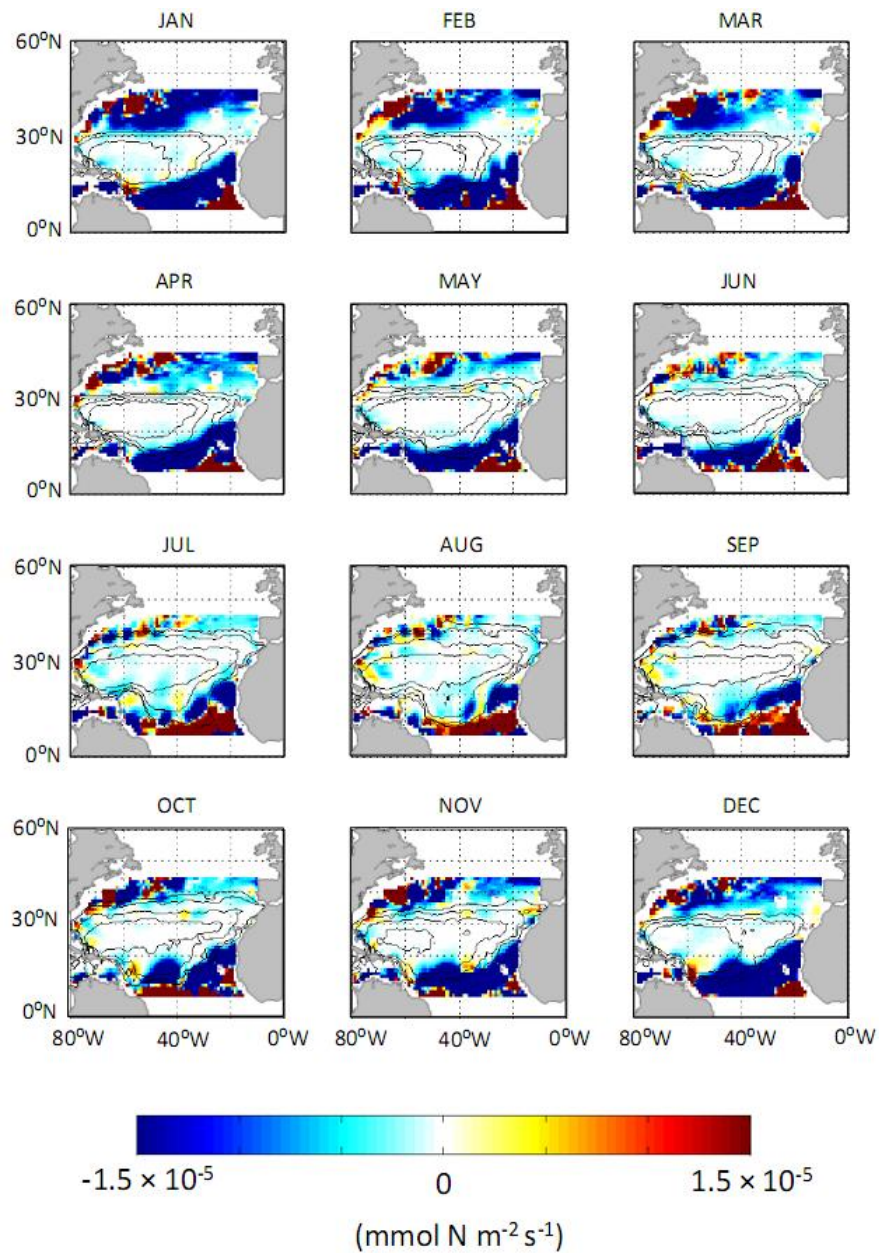


Figure 3-8: Seasonal cycle in the divergence field of the total (geostrophic + Ekman) horizontal advective NO₃ flux within the Ekman layer. The panels show the monthly climatological fields from January to December. As in Figure 3-7, the color scale indicates the strength and sign of the divergence, while the black contours show the positions of the 0.05, 0.07 and 0.10 chl-*a* isolines. To highlight changes in and around the oligotrophic region, pixels north of 45°N and south of 8°N are masked.

periphery of the oligotrophic region. This spatial signature is confirmed by time series showing the strength of the convergence of horizontal advective nutrient fluxes averaged within different climatological oligotrophic contours (Figure 3-9). Within the boundaries of the oligotrophic core, the convergence is close to zero and exhibits very little variability; for regions extending progressively outward from the core, the average magnitude of the convergence increases, as does its seasonality. Each individual time series still converges to very low values in August and September, a reflection of the strong weakening of the flux convergences across the basin during the late summer. As with the monthly divergence fields, when the time series is reproduced using divergence values calculated from a climatological nutrient field and variable advective field, a similar result is observed.

To examine the impact of the seasonal changes in the advective supply of nutrients on the geometry of the oligotrophic region, we correlate the local, temporal variability in chl-*a* concentrations with the divergence of the horizontal advective fluxes of nitrate in the Ekman layer and the mixed layer at every point in the domain (Figure 3-10). Whereas the previous calculations of the nutrient fluxes have been made over the Ekman layer to incorporate the full variability due to Ekman transports, the mixed layer is included for this correlation analysis since it is the layer for which satellite measures of chl-*a* can be considered representative and because the strong density gradients at its base restrict the access of surface photosynthesizers to nutrients that might be horizontally converged below it. The results of this analysis show broadly similar spatial patterns of correlation in both layers. The regions where chl-*a* variability is strongly negatively correlated with the divergence of the horizontal nitrate flux (that is, where chl-*a* concentrations increase with

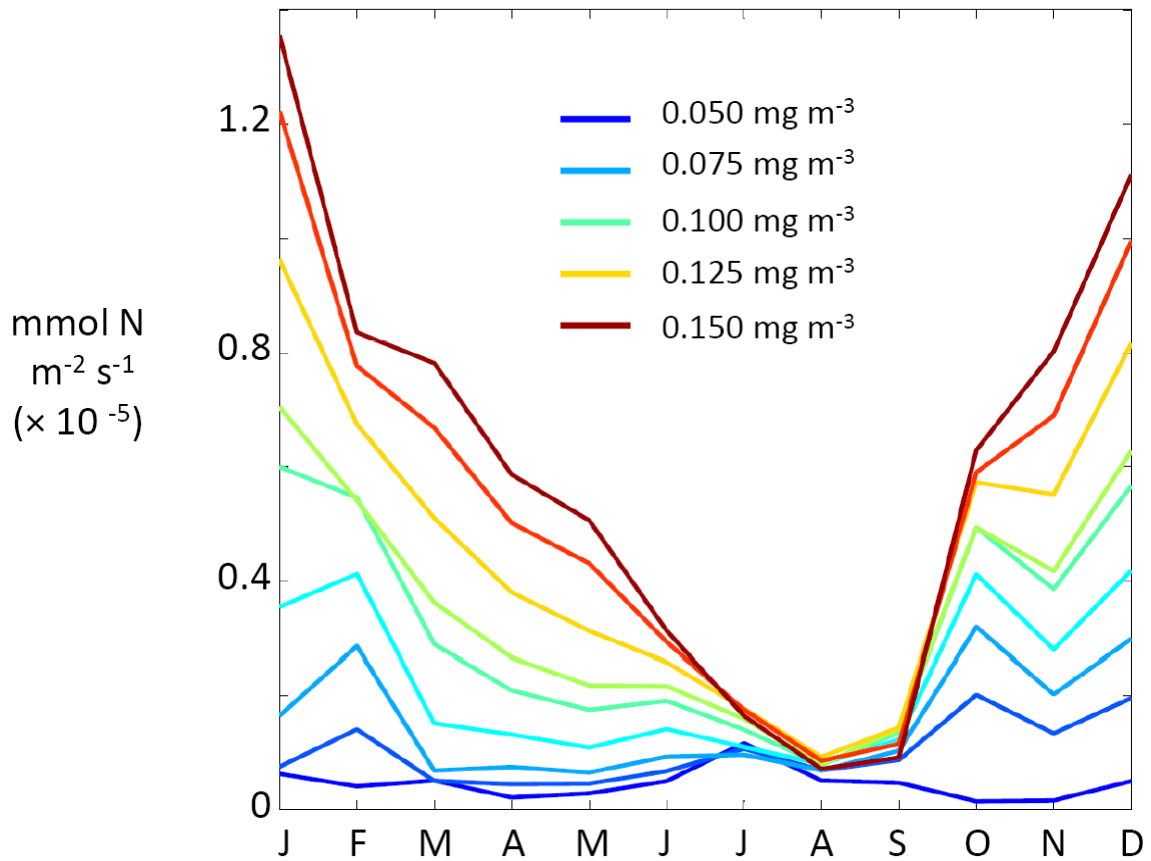


Figure 3-9: Time series showing the seasonal variability in divergences of total horizontal advective fluxes of NO_3 in the Ekman layer for different regions in the subtropical North Atlantic. At each month, the different lines show the spatial average of the divergences within regions bounded by different chl-*a* isolines, ranging from 0.05 - 0.15 mg m^{-3} . The cool colors indicate divergences averaged within regions characterized by lower chl-*a* concentrations (that is, within regions that lie closer to the oligotrophic 'core'), while warmer colors indicate divergences averaged over larger regions bounded by higher chl-*a* concentrations (that is, those that include the core, but extend closer to nutrient-rich regions on the periphery of the oligotrophic region).

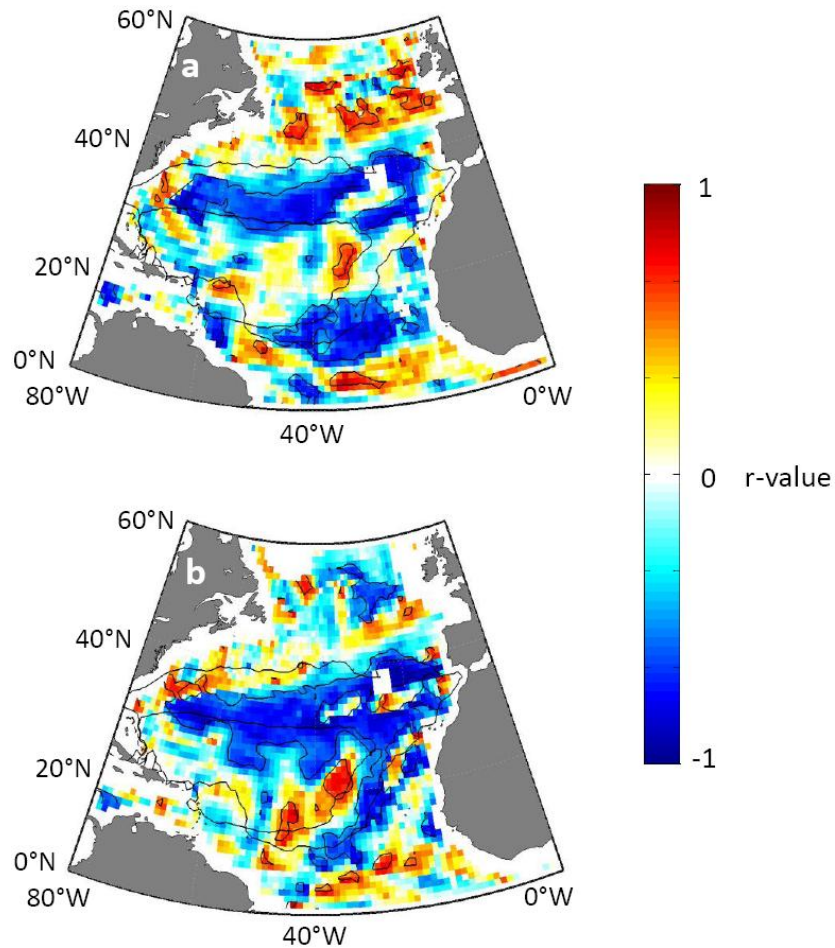


Figure 3-10: Map of the local, seasonal correlations between anomalies in SeaWiFS chl-*a* and anomalies in the divergence of the total horizontal advective fluxes of NO_3 in (a) the Ekman layer and (b) the surface mixed layer. The anomalies for each property are calculated by subtracting the corresponding annual mean at every pixel for each month. Warmer colors reflect a positive correlation (stronger divergence associated with increasing chl-*a*) while cooler colors reflect a negative correlation (stronger divergences associated with decreasing chl-*a*). Black contours indicate pixels where the correlation is statistically significant ($p < 0.05$). Regions of significant, negative correlations (i.e. enhanced chlorophyll with a stronger convergence of the horizontal advective nitrate flux) are focused in the intermediate zone between the maximum and minimum annual extents of the 0.1 mg m^{-3} chl-*a* isoline (indicated by the heavier black contours).

an advective gain of nitrate) overlap significantly with the region bounded by the smallest and largest extents of the 0.1 mg m^{-3} chl-*a* isoline. The spatial pattern of correlation supports the view that the expansion and contraction of the oligotrophic region is mediated by the waning and waxing, respectively, of horizontal advective fluxes from neighboring regions. We note that the region of strong correlations is close enough to the peripheries of the subtropical gyre to fall within the previously estimated length scale for the penetration of the horizontal nutrient fluxes from neighboring regions ($\sim 1000\text{km}$, *Williams and Follows, 1998*).

The total contribution of advective nutrient fluxes in the region lying between the maximum (August) and minimum (February) extent of the 0.1 mg m^{-3} chl-*a* isoline (hereafter referred to as the ‘intermediate zone’) can also be quantified by estimating the fraction of total new production in this region that could be supported by the average convergence of the advective fluxes over the period when the oligotrophic region is contracting (August-February). We estimate new productivity within the intermediate zone for this period using net primary productivity (NPP) values from the widely-used VGPM and CbPM models [*Behrenfeld and Falkowski, 1997; Behrenfeld, 2005*] and an *f* ratio of 0.06-0.13, used for waters in the oligotrophic region and in transitional regions with upwelling regimes [*Epply and Peterson, 1979*]. We estimate new production over August-February within the intermediate zone of $0.53\text{-}1.1 \text{ mol C m}^{-2} \text{ yr}^{-1}$ using values from the VGPM model and $0.58\text{-}1.2 \text{ mol C m}^{-2} \text{ yr}^{-1}$ using values from the CbPM model. We calculate that the convergence of the horizontal advective fluxes in the mixed layer during August-February supplies nitrate at a rate of approximately $0.059 \text{ mol N m}^{-2} \text{ y}^{-1}$, translating to $0.41 \text{ mol C m}^{-2} \text{ yr}^{-1}$ of productivity. Thus, between 34-71% of the new primary production inferred from

the CbPM model and 37-77% of the new production inferred from the VGPM model is potentially accounted for by the horizontal advection of nitrate during the period of oligotrophic contraction. In other words, the diminishment of the oligotrophic region from its maximum size in summer to a minimum size in winter appears to be significantly impacted by an increase in horizontal advection of nutrients into the subtropical gyre from neighboring nutrient-rich regions to the north and the east. We note that errors in these estimates could arise from negative biases in satellite-NPP that have been well documented with respect to *in situ* measurements in the North Atlantic [Saba *et al.*, 2010], as well as our assumption that Redfield stoichiometry for C/N is 106:16 and also from the use of the f ratio to convert NPP to new productivity. Still, our results clearly indicate that variability in the horizontal advection of nutrients plays an important role in driving the seasonal changes in oligotrophic geometry in the North Atlantic basin.

3.5 Conclusions

This study is motivated by recent reports of increases in the areal extent of the ocean's oligotrophic regions over the last decade, a finding that highlights the need for an understanding of the environmental factors that control the geometry of these ecologically and climatically significant regions. Oligotrophic variability is dominated by its seasonal component, and our analysis thus focuses on explaining the annual cycle in the size and shape of the oligotrophic region of the well-sampled North Atlantic basin. This region is set within the North Atlantic subtropical gyre and its associated wind-driven downwelling regime, which restricts the upward supply of deep nutrients and provides a first-order explanation for the low levels of biomass observed here. However, we observe that the

dramatic contraction of the oligotrophic region from summer to winter is not matched by a comparable reduction in the size or intensity of the wind-driven downwelling regime- instead the contraction coincides with a strengthening of spatial nutrient gradients along the oligotrophic periphery and a general strengthening of Ekman transports across the basin. These changes suggest that the diminishment of the oligotrophic region in the winter is impacted by an increase in the horizontal transfer of nutrients into the subtropical gyre from neighboring nutrient-rich regions.

To assess the relationship between oligotrophic variability and seasonal changes in the lateral inputs of nutrients, we calculate horizontal advective nitrate fluxes using the total (geostrophic + Ekman) surface velocity field. A comparison of the climatological divergence field of these fluxes with the climatological chl-*a* field shows that the oligotrophic region is bounded by areas of strong convergence of the advective nitrate flux. A comparison of the seasonal variability in both fields indicates that the strength of advective inputs of nutrients waxes and wanes with the contraction and expansion of the oligotrophic region, and that the spatial fingerprint of this advective variability is generally focused along the oligotrophic periphery.

We examine the impact of seasonal changes in horizontal nutrient advection on productivity within the oligotrophic region by comparing the local, temporal variability in chl-*a* and the divergence of the horizontal advective fluxes within the surface mixed layer. The resulting spatial pattern of correlation is characterized by strong negative associations (increased chl-*a* with more negative divergence) that are generally focused in an intermediate zone set between the maximum summertime (August) and minimum wintertime (February) extents of the oligotrophic boundary. In other words, chl-*a*

concentrations in most of the area over which the oligotrophic region is expanding and contracting are strongly impacted by changes in the horizontal advective input of nutrients. The one sector where this relationship is not observed is along the oligotrophic region's southwest boundary, where seasonal biomass variability is aliased by inputs of riverine CDOM from the Amazon/Orinoco outflow.

A calculation of the fraction of observed new production in the intermediate zone that can be supported by the horizontal advective nitrate flux from August-February suggests that horizontal advection of nitrate accounts for 34-71% (37-77%) of the new production estimated for this period by the CbPM (VGPM) model, with the range of values reflecting the choice of different f ratios to scale model NPP to new production. We note that our absolute estimate of intermediate zone new production that is supported by horizontal advective nitrate fluxes ($0.41 \text{ mol C m}^{-2} \text{ yr}^{-1}$) compares favorably to values attributed to Ekman nitrate supply for the winter in the North Pacific transition zone ($0.41 \text{ mol C m}^{-2} \text{ yr}^{-1}$; *Ayers and Lozier [2010]*) and annually along the northern flank of the North Atlantic subtropical gyre ($0.40\text{-}0.80 \text{ mol C m}^{-2} \text{ yr}^{-1}$; *Williams and Follows [1998]*).

The findings of this study may be generalizable to the other major subtropical basins. *McClain et al. [2004]* observe similarly large seasonal changes in the size and shape of all the major oligotrophic regions; they also calculate that the Ekman supply of nitrate and phosphate makes a net positive annual contribution to the nutrient budgets of all of the major subtropical gyres. We suggest the possibility, therefore, that the dynamics described in this study of the oligotrophic region of the North Atlantic play an important role in driving seasonal variability elsewhere. We also suggest that, because the seasonal cycles in horizontal nutrient advection are so pronounced, relatively modest changes from year to

year in the timing or strength this advection may drive a substantial portion of the interannual variability in oligotrophic regions that has been previously reported.

APPENDIX A (Chapter 2)

A.1 Data Description

A.1.1 Hydrographic profile data

To assess interannual variability in the hydrography of the subtropical North Pacific and equatorial Pacific, we use profile data obtained from the World Ocean Database (WOD) using the online WODselect retrieval system (<http://www.nodc.noaa.gov/OC5/SELECTdbsearch/dbsearch.html>). The selected profiles have been quality controlled and pre-interpolated to a set of standard depths. Data are acquired for the period September 4, 1997 to December 21, 2010, corresponding to the time span of the SeaWiFS dataset (160 months/ 4,847 days). Temperature data are far more numerous than salinity data, especially earlier in the record, and so stratification is assessed as the temperature difference between the surface (0, 50 m) and the sub-surface (50, 100, 150 or 200 m).

For the subtropical North Pacific the spatial domain is a rectangular box extending from 0°N - 40°N, 130°E - 110°W. Within this box, profiles are selected only for the oligotrophic region (delineated by climatological surface chlorophyll-a concentrations of less than 0.1 mg m⁻³, see Figure 2-1). In this manner a total of 201,574 profiles have been retrieved, from five observing platforms: CTD data (CTD – 9,695 profiles), moored buoys (MRB – 69,059 profiles) ship-based ocean station data (OSD – 5,666 profiles) , profiling floats (PFL – 71,295 profiles, consisting mostly of ARGO data) and expendable bathythermographs (XBT – 45,859 profiles).

For the equatorial Pacific the spatial domain is a rectangular box extending from 5°N-5°S, 150°E-90°W. This domain corresponds to the combined spatial bounds of the NINO 3 and NINO 4 regions, in which SST variability is closely tied to ENSO variability. A total of

188,500 profiles have been retrieved (CTD – 2,892 profiles; MRB – 150,815 profiles; OSD – 922 profiles; PFL – 23,534 profiles; XBT – 10,337 profiles). As in the subtropical North Pacific, the profiling data also consist mostly of ARGO data. However, the majority of data derive from the moored buoy arrays of ongoing the TOGA TAO observational programs.

A.1.2 Climatological Hydrographic Fields

To assess annual and monthly climatological fields of the hydrography of the subtropical North Pacific and equatorial Pacific domains we use gridded fields of T and S from the the World Ocean Atlas 2009 (WOA09) (available online at http://www.nodc.noaa.gov/OC5/WOA09/pr_woa09.html). Comparison of the WOA fields with the available hydrographic profile data demonstrates that our selected hydrographic profile measurements accurately record seasonal variability in both domains (Figures S1 and S2).

A.1.3 Re-analyzed Hydrographic Fields

We use monthly gridded 0.5° fields of re-analyzed temperature and density from the SODA datasets (Simple Ocean Data Assimilation, available online at <http://soda.tamu.edu>). We use output from the recently released SODA 2.1.6 experiment, which assimilates hydrographic data from WOD dataset into an eddy-permitting POP2.1 general circulation model forced by a combination of ERA-40 (ECMWF) and QuikSCAT winds. The model is integrated globally from 1958-2008, but we extract sub-domains that match the spatial boundaries of our WOD/ WOA data. The SODA data extend over the period September 1997 to December 2008, corresponding to the first 136 months of the SeaWiFS dataset. Our

analysis shows that stratification time-series constructed by sub-sampling the SODA fields using the individual profile locations accurately captures the interannual stratification variability described by the SODA dataset for both the subtropical North Pacific and equatorial Pacific domains. If we assume that the spatial gradients in the SODA fields are similar to that of the real ocean, these results suggest that the observed hydrographic profiles are able to accurately record interannual stratification variability in this domain (Figures S3 and S4).

A.1.4 Biogeochemical Data

A.1.4.1 Chlorophyll

To assess phytoplankton biomass at the same location as the individual hydrographic profiles we use daily and monthly fields of surface SeaWiFS chlorophyll-a concentrations (chl-a, in units of mg m^{-3}) for the subtropical North Pacific and equatorial Pacific domains. The data are gridded at 9km ($\sim 1/12^\circ$) resolution and available as global files online at <http://oceancolor.gsfc.nasa.gov>. From these global data, we extract spatial domains for the chl-a data that are padded by 1° with respect to the hydrographic domains described above, in order to accommodate capture radii of profiles at the boundaries of each domain. The daily data include 4501 separate fields (out of a total possible 4847 daily time steps spanning the period 9/4/1997 to 12/11/2010). The monthly data include 153 separate fields (out of a total possible 160 monthly time steps spanning the period 9/1997 to 12/2010).

A.1.4.2 Productivity Estimates

To assess primary productivity rates at the same location as the individual hydrographic profiles we use monthly fields of net primary productivity (NPP, in units of $\text{mg C m}^{-2} \text{ s}^{-1}$) estimated using the widely used Vertically Generalized Productivity Model (VGPM) [Behrenfeld and Falkowski, 1997a]. The data are gridded at 9km ($\sim 1/12^\circ$) resolution and available through the Oregon State ocean productivity website <http://www.science.oregonstate.edu/ocean.productivity/>. From these global data, we extract spatial domains for the NPP data in the same manner as described for the chl-*a* data above.

A.1.4.3 Nutrient Data

To assess spatial and temporal variability in the nutrient fields of the subtropical North Pacific and equatorial Pacific domains, and to calculate dynamic fluxes of nutrients in these domains, we use annual and monthly climatological fields of nitrate concentration ($[\text{NO}_3]$, in units of mmol m^{-3}) obtained from the World Ocean Atlas 2009 (as described above).

A.1.5 Wind data

To assess variability in the wind field of the equatorial Pacific we use gridded monthly fields of re-analyzed surface wind stress (zonal and meridional components evaluated at a height of 10m, in units of N m^{-2}) and surface wind speed (at 10 m, in units of m s^{-1}). The data are provided at (1.5°) resolution and are outputted from the ERA-interim atmospheric re-analysis dataset (provided by ECMWF and available via an online ordering

system at <http://www.ecmwf.int/research/era/do/get/index>). The data are downloaded as global fields over a user-defined time span; we selected the period 9/1997 to 12/2010 to provide full overlap with the SeaWiFS dataset.

A.1.6 Surface Current Data

To assess variability in surface ocean advection in the equatorial Pacific, we use gridded monthly fields of total surface currents (geostrophic + Ekman, evaluated at a depth of 15 m in units of cm s^{-1}) from NOAA's OSCAR (Ocean Surface Current Analyses – Real time) program. The velocity fields are derived from satellite altimetry and scatterometry measurements and are available via an online ordering system at http://www.oscar.noaa.gov/datadisplay/oscar_datadownload.php. The data are downloaded for a user-specified spatial and temporal domain at a user specified spatial resolution, with or without spatial filtering. A full description of this data product, and its validation with in-situ observations, is given in *Sudre and Morrow* [2008].

A.2 Basin-scale comparison of stratification and chl-a

A.2.1 Contemporaneous measures

Two techniques are used to match stratification values with contemporaneous measures of surface chl-a concentration: profile-capture and whole domain averaging.

A.2.1.1 Use of capture-radii

Each hydrographic profile is matched with an average value for all the SeaWiFS pixels that lie within one baroclinic Rossby radius of deformation of the profile's location. The Rossby radius defines a spatial domain over which a single profile measurement is considered representative. This averaging approach addresses concerns over potential biases created by small-scale heterogeneities (patchiness) in the ocean color fields for single-point interpolations of chl-a values. The Rossby radius at the location of each profile is calculated by interpolating values from a global climatological atlas produced by Chelton et al. [1998]. However, at very low latitudes the Rossby radii are sufficiently large (~250 km) that overlap between hydrographic profiles becomes an issue. To account for this, the capture radii of all profiles equatorward of 10°N or 10°S are capped to 100 km in length. Using this approach, in the subtropical North Pacific approximately 92% of profiles (185,468 out of 201,574) capture chl-a values from the monthly fields, with an average of ~98 individual chl-a values per profile. In the equatorial Pacific, approximately 89% of profiles (167,224 out of 188,500) capture chl-a values from the monthly fields, with an average of ~82 individual chl-a values per profile. The profiles and their associated chl-a values are able to accurately describe seasonal and interannual chl-a variability in the subtropical North Pacific domain and in the equatorial Pacific (Figures A-1 – A-6).

In addition to being paired with monthly SeaWiFS data, each hydrographic profile is also paired with two values derived from daily SeaWiFS fields: 1) the average of all chl-a within the Rossby radius and within +/- 1 day of each cast, and 2) the average of all chl-a within the Rossby radius after 6-8 days (i.e., ~1 week lag). This last temporal offset is used because it roughly corresponds to the expected response time of primary production to a

change in local stratification. In the subtropical North Pacific, approximately 64% of the total profiles (128,402 out of 201,574) capture chl-*a* values within +/- 1 day. Within this group an average of ~53 chl-*a* values per profile are contained within the local baroclinic Rossby radius and subsequently averaged to produce the contemporaneous chl-*a* value for that hydrographic profile. Approximately 61% (123,778) of profiles capture chl-*a* values in the 6-8 day interval, with an average of ~58 chl-*a* values per profile. In the equatorial Pacific, approximately 47% of the total profiles (89,019 out of 188,500) capture chl-*a* values within +/- 1 day. Within this group an average of ~52 chl-*a* values per profile are contained within the local baroclinic Rossby radius. Approximately 48% (91,394) of profiles capture chl-*a* values in the 6-8 day interval, also with an average of ~52 chl-*a* values per profile.

A.2.1.2 Whole-domain averaging

The stratification measures derived from profile measurements are also compared with whole-domain averages of the monthly chl-*a* and NPP monthly fields. This approach can be justified by the highly accurate reconstructions of interannual variability in chl-*a* for both of our domains, using profile captured data that show that the profiles are adequately sampling the domains (see Figures A-5, A-6). For the reproduction of the analysis of *Behrenfeld et al.* [2006] in the subtropical North Pacific, we use whole-domain averages of the monthly SODA stratification fields and the monthly NPP fields.

A.2.2 Calculating interannual variability

Local stratification anomalies are calculated by subtracting the local monthly mean from the profile stratification measure. The local monthly mean is found by interpolating values

from the climatological fields of the World Ocean Atlas to the location of each profile. Local chlorophyll anomalies are likewise calculated, yet here the local monthly means are obtained from the monthly climatological SeaWiFS fields using the profile capture radii. The local anomalies are then averaged across the spatial domain for each month of each year to produce an average anomaly for the domain as a function of time. Calculation of local anomalies in this manner avoids potential biases arising from changes in the spatial distribution of the profiles with time.

A.2.3 Additional comparisons of stratification and chl-*a*/ productivity

The comparison of profile measurements of stratification and profile-captured monthly chl-*a* values (Figure 2-2 in the main text) demonstrates that the two are not strongly negatively correlated over interannual time scales. The weakness of correlation is again observed when the comparison is made after substituting values from the daily chl-*a* fields captured within 1 day or after a 6-8 day lag for each profile measurement. The chl-*a* ‘tendency’ referred in the main text is a difference between the contemporaneous (+/- 1 day) and lagged (6-8 days) measurements and is calculated to see if a chl-*a* ‘response’ to a given stratification anomaly occurred.

In addition to examining profile-captured data, we compare the stratification record to the domain-averaged SeaWiFS chl-*a* and NPP fields. Neither of these comparisons demonstrate a strong correlation (Figure A-7a,b). The same weakness of correlation is observed when domain-averaged SODA stratification is compared with NPP fields (Figure A-7c).

A.3 Spatial correlations in the equatorial Pacific

Spatial maps of local, temporal correlations between the monthly chl-a and wind fields in the equatorial Pacific were created by first remapping the relatively coarser wind data (1.5°) and finer scale chl-*a* data ($1/12^\circ$) onto a grid of intermediate resolution ($1/4^\circ$). Anomalies were calculated by subtracting the corresponding local monthly mean from each pixel in each field. Temporal calculations were performed only at each pixel for which there were a sufficient number of measurements (at least 50 common months or both records, out of a total 160 months).

Creating spatial maps of temporal correlations between the hydrographic data and the monthly wind and chl-*a* fields requires objectively mapping the irregularly distributed profile measurements onto a grid before performing the correlation. This was achieved by calculating local anomalies in all of the profile data (see 2.2 above) and grouping these anomalies into subdomains before proceeding with the comparison. Although these subdomains were necessarily coarser than the grids wind or chl-*a* data, they are able to well represent the east west spatial patterns observed in the finer scale correlations.

A.4 Advective flux and divergence calculations

The advective fluxes of nitrate are calculated using a standard expression:

where \mathbf{U}_H is the horizontal velocity and $[\text{NO}_3]_{\text{MLD}}$ is the horizontal gradient in the nitrate concentrations within the mixed layer.

To calculate the total quantities of nitrate fluxed into and out of the mixed layer of the CWEPAC and EEPAC test regions due to horizontal advection, we treat each domain as a flux box across whose N,E,S,W faces the fluxes are integrated. Finally the fluxed quantities are summed to determine the net change within each box. The expression for the total nutrients fluxed across the east face of a given domain is:

Where y_1 and y_2 are the study region's southern and northern latitudes, respectively, x_2 is its eastern longitude. The terms $\mathbf{u}(x_2,y)$, $NO_3(x_2,y)$ and $MLD(x_2,y)$ represent the horizontal velocity, mixed layer nitrate and mixed layer depth values along the regions eastern face. This expression is evaluated numerically using the trapezoidal rule.

To calculate the total quantities of nitrate fluxed into and out of the mixed layer at within each region due to upwelling, we calculate vertical velocities at the base of the mixed layer for every grid point by calculating the divergence of the horizontal velocity at each grid point and using an assumption of continuity and zero vertical velocity at the surface. Vertical fluxes of nitrate were calculated by pairing the vertical velocity at each grid point with the a corresponding value for nitrate concentration interpolated to the depth of the climatological mixed layer at that location. The total vertically fluxed quantity in each region was calculated by integrating these vertical fluxes across the base of the mixed layer.

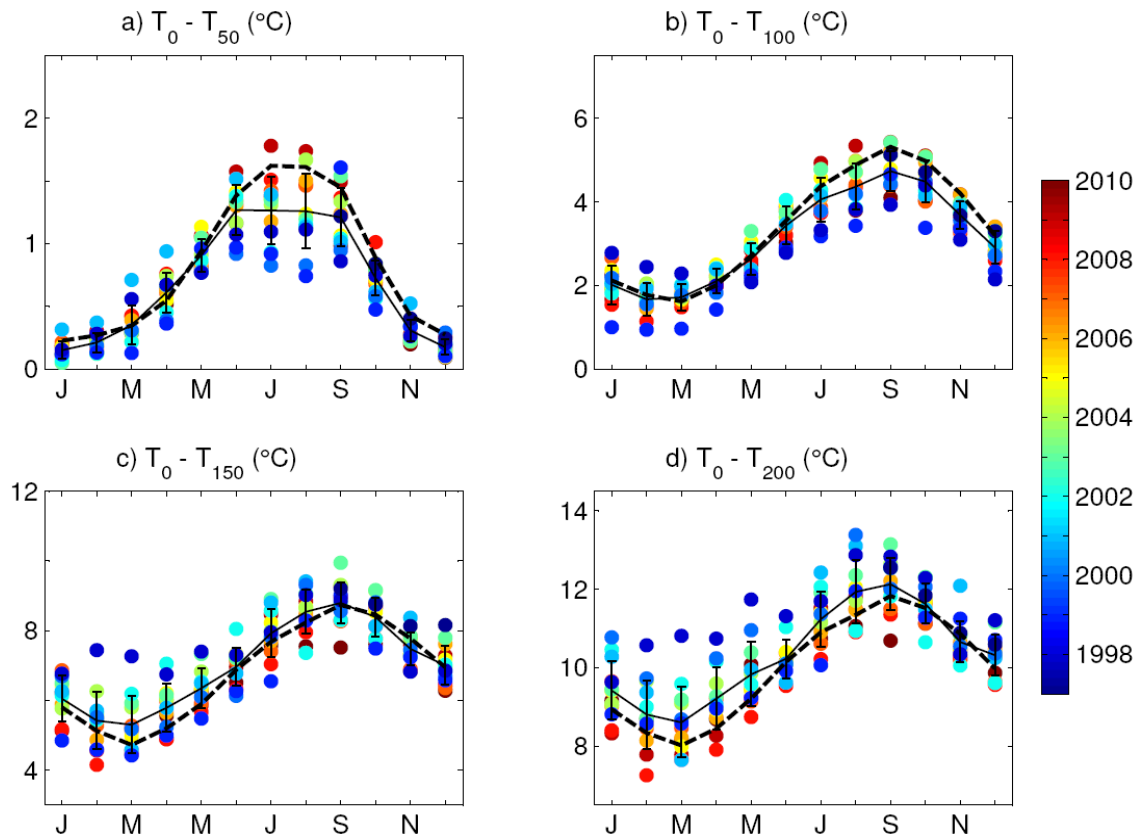


Figure A-1 Reconstruction of seasonal stratification variability in the subtropical North Pacific study domain by hydrographic profile data spanning 1997-2010. Annual cycles are shown for (a) $T_0 - T_{50}$, (b) $T_0 - T_{100}$, (c) $T_0 - T_{150}$ and (d) $T_0 - T_{200}$. In each panel, the colored points show the average of all profile measurements in each month of each year, with the color of each point indicating the year of observation. The solid black line shows the long term monthly means of profile observations in each month (that is, the reconstruction of the seasonal signal by the profiles). Error bars indicate ± 1 standard deviation. For comparison, the dashed line shows the seasonal cycle of $T_0 - T_{200}$ for this domain, as described by the complete WOA09 fields.

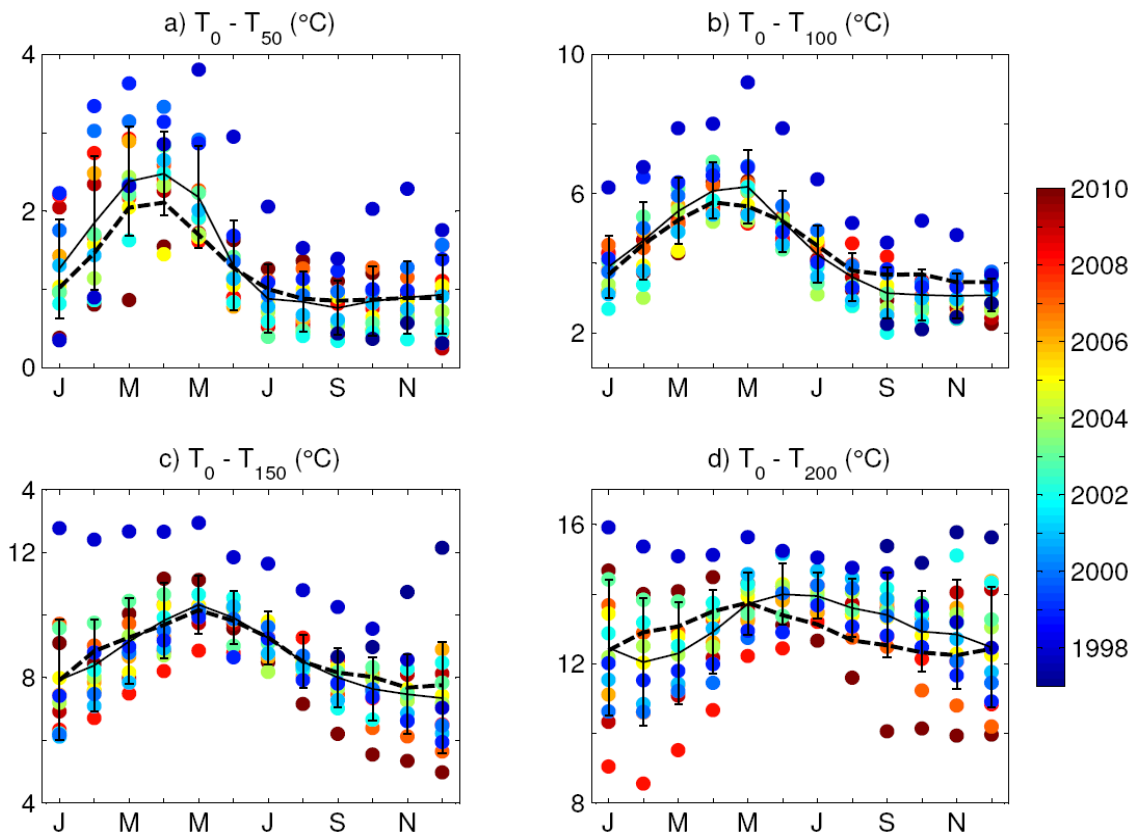


Figure A-2 As with Figure A-1, but for the equatorial Pacific study domain.

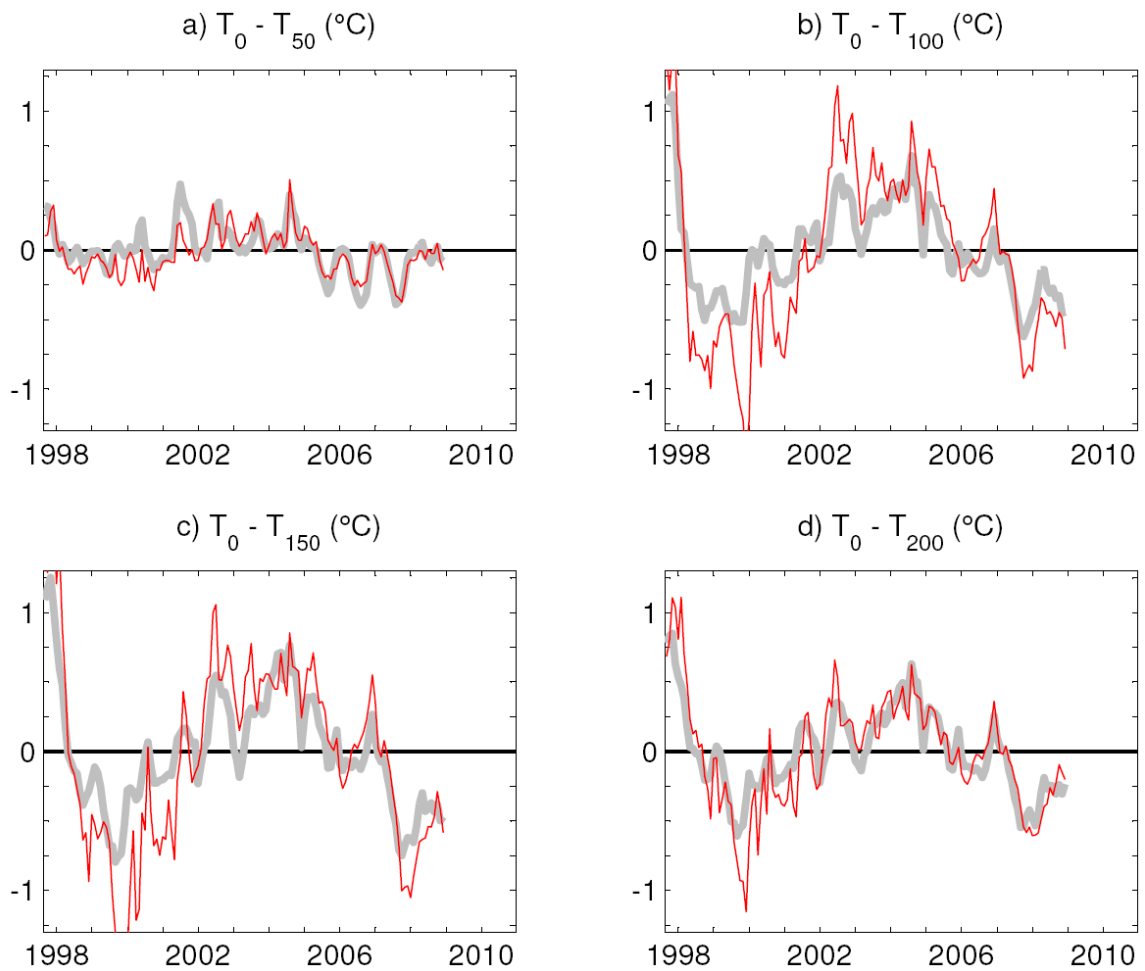


Figure A-3 Reconstruction of interannual stratification variability in the subtropical North Pacific domain by the hydrographic profiles from 1997-2010: Monthly mean-subtracted anomalies in (a) $T_0 - T_{50}$, (b) $T_0 - T_{100}$, (c) $T_0 - T_{150}$ and (d) $T_0 - T_{200}$ for the period 1997-2008. The bold grey line shows anomalies calculated from the complete SODA 2.1.6 field over this domain. The thin red line shows anomalies calculated by sub-sampling the SODA field using the profile locations in each month. For each measure of stratification, we only subsample the SODA field with profile measurements that extend to the deepest depth. In each case, the resulting time series are strongly correlated (for $T_0 - T_{50}$ / $T_0 - T_{100}$ / $T_0 - T_{150}$ / $T_0 - T_{200}$, the r -values are, respectively, +0.78/+0.89/+0.90/+0.88, with $p < 0.01$).

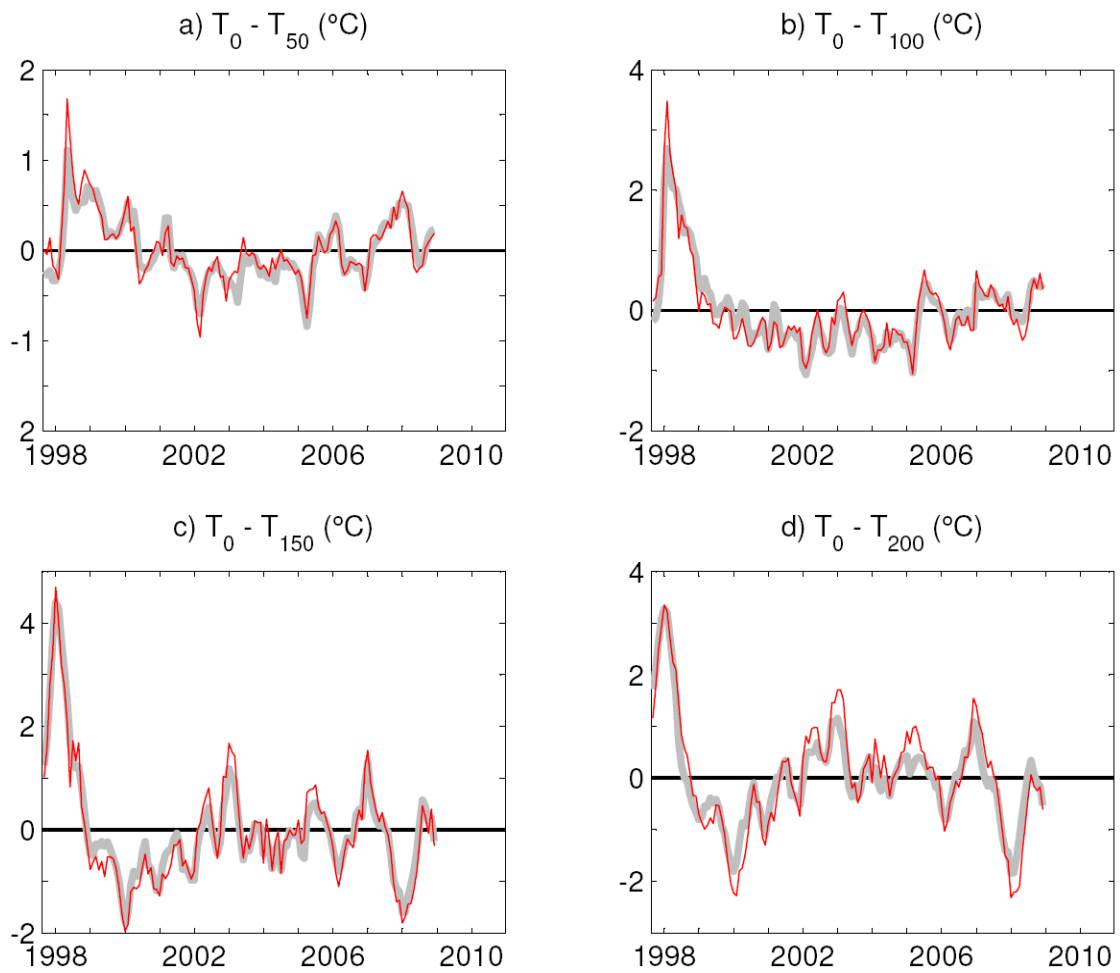


Figure A-4 As with Figure A-3, but for the equatorial Pacific study domain. In each case, the resulting time series are strongly correlated (for $T_0 - T_{50}$ / $T_0 - T_{100}$ / $T_0 - T_{150}$ / $T_0 - T_{200}$, the r -values are, respectively, +0.94 / +0.96 / +0.97 / +0.95, with $p < 0.01$).

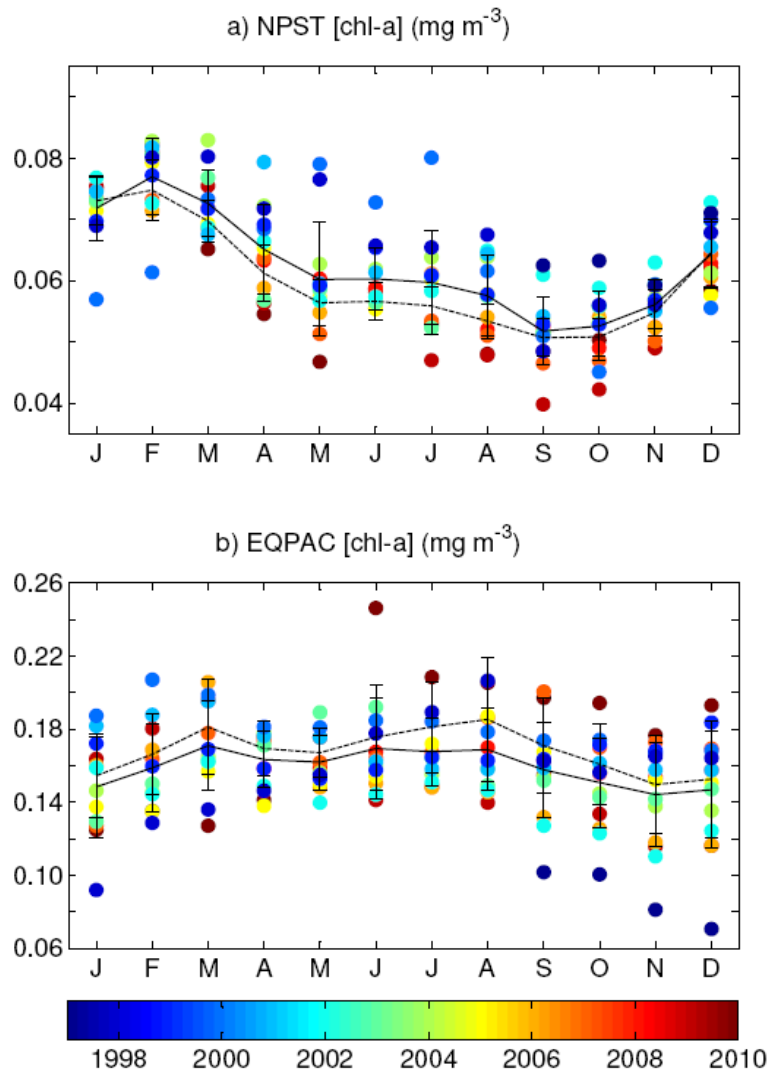


Figure A-5 Reconstruction of seasonal chl-*a* variability by profile-captured monthly SeaWiFS data spanning 1997-2010. Annual cycles are shown for (a) the subtropical North Pacific and (b) equatorial Pacific study domains. In each panel, the colored points show the average of all profile-captured chl-*a* values in each month of each year, with the color indicating the year of observation. The solid black line shows the long term monthly means of observations in each month (ie. the reconstruction of the seasonal signal by the profiles). Error bars indicate ± 1 standard deviation. For comparison, the dashed line shows the seasonal cycle of chl-*a* for the whole domain, as described by the complete monthly climatological SeaWiFS fields.

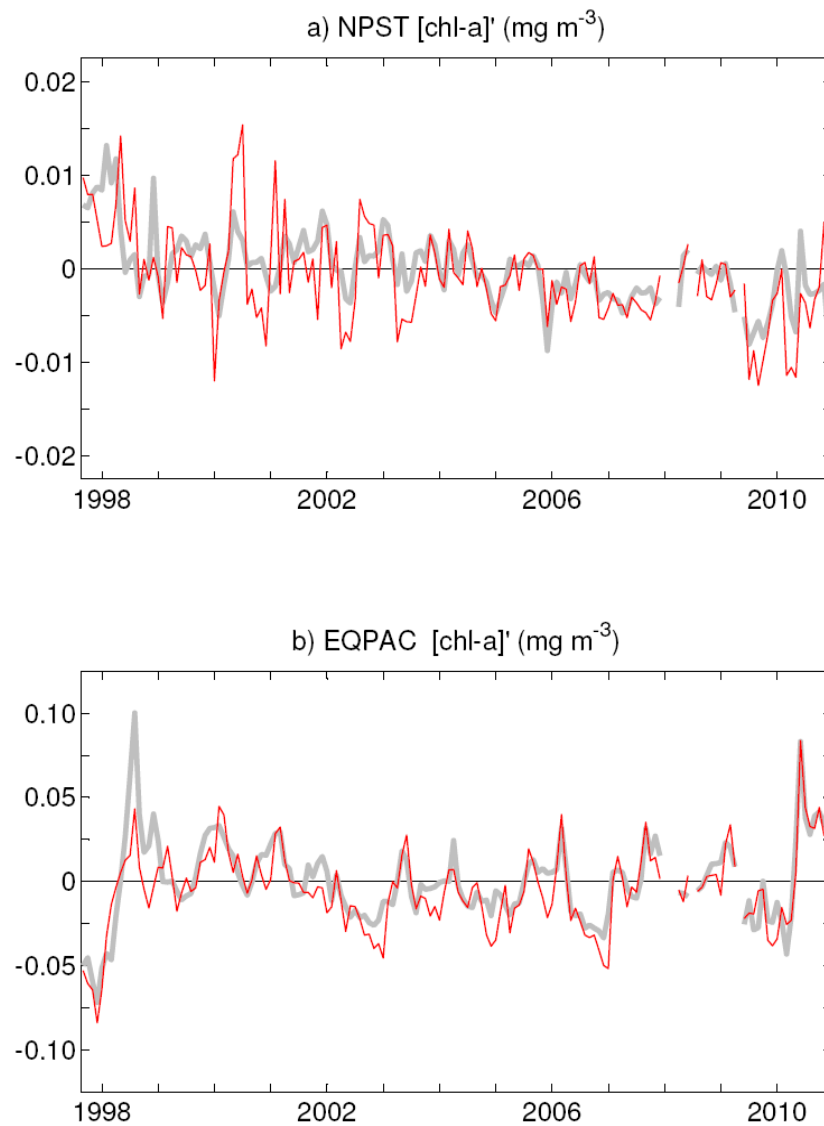


Figure A-6 Reconstruction of interannual chl-*a* variability by profile-captured monthly SeaWiFS data spanning 1997-2010. Monthly mean-subtracted anomalies in chl-*a* for the period 1997-2009 are plotted for (a) the subtropical North Pacific and (b) the equatorial Pacific. In each panel the bold grey line shows anomalies calculated from the complete SeaWiFS field over this domain. The thin red line shows anomalies calculated by subsampling the monthly SeaWiFS fields using the profile locations. The time series are strongly positively correlated in both the subtropical domain ($r=+0.63$, $p<0.05$) and the equatorial domain ($r=+0.85$, $p<0.05$).

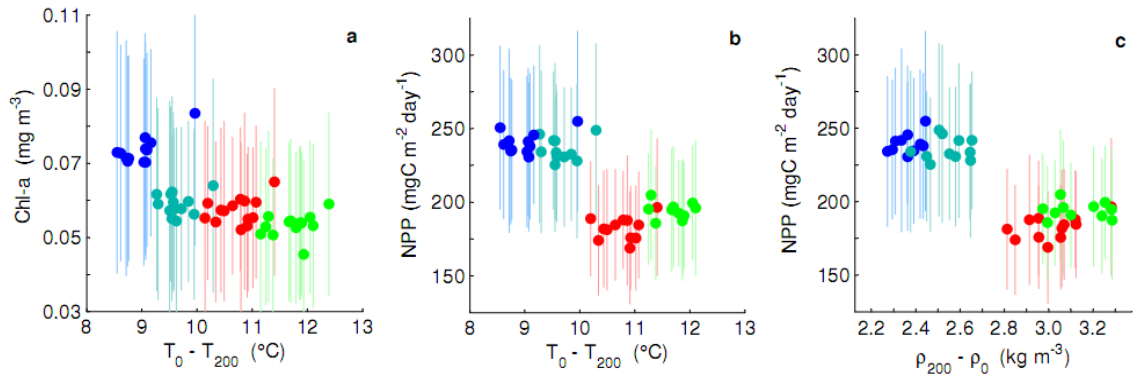


Figure A-7: Reproduction of Figure 2-2b showing three additional comparisons of seasonally averaged stratification, chl-*a* and productivity measures in the subtropical North Pacific: (a) whole-domain averaged SeaWiFS chl-*a* as a function of whole domain averaged profile measures stratification ; (b) as in (a), but with NPP data in place of SeaWiFS chl-*a*; (c) as in (b), but with whole domain averaged SODA stratification ($\rho_{200} - \rho_0$) in place of the profile stratification data. The standard errors bars for the seasonal chl-*a* and NPP values are too small to see, due to the large number of observations (i.e. $n > 200,000$ for a $1/12^\circ$ field).

Appendix B (Chapter 3)

B.1 Data

B.1.1 Chlorophyll, productivity and nutrients

Seasonal changes in the oligotrophic regions are assessed using monthly climatologies constructed from synoptic, global 9km ($\sim 1/12^\circ$) fields of SeaWiFS surface chlorophyll-*a* concentrations (chl-*a*, in units of mg m^{-3}) that have been sub-sampled for the North Atlantic domain ($0^\circ\text{N} - 60^\circ\text{N}$, $0^\circ\text{W} - 80^\circ\text{W}$). The data span the period 9/1997 to 12/2010 and are downloaded from <http://oceancolor.gsfc.nasa.gov>. To assess seasonal changes in primary productivity we use the same approach to construct monthly climatologies from synoptic, global fields of net primary productivity rates (NPP, in units of $\text{mg C m}^{-2} \text{ s}^{-1}$) estimated using the widely used Vertically Generalized Productivity Model (VGPM) and Carbon-based Productivity Model (CbPM). The NPP data are mapped on the same grid as the SeaWiFS data and are available as through the Oregon State ocean productivity website <http://www.science.oregonstate.edu/ocean.productivity/>. To assess the spatial and temporal variability in nutrient fields of the subtropical North Atlantic, and to calculate dynamic fluxes of nutrients, we use monthly climatological fields of nitrate concentration ($[\text{NO}_3]$, in units of mmol m^{-3}) obtained from the World Ocean Atlas 2009 (WOA09). The data are mapped onto rectangular grids of 1° horizontal resolution and are available online at http://www.nodc.noaa.gov/OC5/WOA09/pr_woa09.html.

B.1.2 Winds and currents

To assess variability in the wind field of the subtropical North Atlantic we construct monthly climatologies from synoptic fields of QuikSCAT surface wind stress (at 10 m, in

units of N m^{-2}) and wind stress curl (units of N m^{-3}). The data are rectangularly gridded at 0.5° resolution and span the period 7/1999 - 11/2009. The data are available online from CERSAT: <http://www.ifremer.fr.cersat/en/>. One potential disadvantage of using Quik-SCAT dataset is that it does not fully overlap with the SeaWiFS record. As a check, we also repeat our analyses of wind data using an additional surface wind dataset from the ERA-interim atmospheric re-analysis (provided by ECMWF and available via an online ordering system at <http://www.ecmwf.int/research/era/do/get/index>). These data are downloaded as global fields over a user-defined time span; we selected the period 9/1997 to 12/2010 to provide full overlap with the SeaWiFS dataset. The data are provided at 1.5° resolution.

To assess variability in surface ocean advection in the subtropical North Atlantic, we use 2 different data products, each consisting of rectangular gridded fields of total surface currents (geostrophic + Ekman, evaluated at a depth of 15 m in units of cm s^{-1}) for our study domain. These velocity fields are derived from satellite altimetry and scatterometry measurements. The first dataset is obtained from NOAA's OSCAR (Ocean Surface Current Analyses - Real time) program and is available via an online ordering system at http://www.oscar.noaa.gov/datadisplay/oscar_datadownload.php. The data are downloaded as monthly fields of total velocity for a user-specified spatial and temporal domain at a user specified spatial resolution, with or without spatial filtering. For this study, we use the 1° resolution, spatially filtered product. As with the other data, monthly climatologies are created from the synoptic fields. A description of this data product, along with a validation and error analysis, is given in *Johnson et al.* [2007]. The second surface current product is obtained from CTOH/LEGOS and is downloaded as separate annual files consisting of weekly velocity fields using an online order form at <http://ctoh.legos.obs->

mip.fr/products/global-surface-currents. We construct synoptic monthly files by taking weighted averages of the weekly data. Monthly climatologies are then constructed in the same manner as the other data. CTOH velocity data are provided as separate components: Ekman, geostrophic anomalies (based on sea level anomalies) and a single climatological mean (based on mean a dynamic topography field). A full description of this data product, and its validation with in-situ observations, is given in *Sudre and Morrow* [2008].

B.2 Methods

B.2.1 Delineation of the oligotrophic region and the subtropical gyre

Previous studies examining productivity variability in the subtropics have used a variety of metrics to delineate their study regions, including climatological hydrography [*Behrenfeld et al.*, 2006], simple isolines of chlorophyll-*a* (a proxy for phytoplankton biomass) [*McClain et al.*, 2004; *Gregg et al.*, 2005; *Polovina et al.*, 2008] and more complex biogeographical provinces [*Irwin and Oliver*, 2009]. Irwin and Oliver also make a distinction between extreme- ($<0.06 \text{ mg m}^{-3}$) and hyper-oligotrophic ($<0.08 \text{ mg m}^{-3}$) regions. This analysis identifies the oligotrophic region at any month in the North Atlantic as all waters that have surface chlorophyll concentrations of less than 0.05 (we term this region the oligotrophic 'core') and 0.07 mg m^{-3} and which fall within the wind-driven downwelling regime and/or the anti-cyclonic velocity field of the subtropical gyre. The study also references the isoline for 0.1 mg m^{-3} , which has been a value used in delineating oligotrophic (0-0.1 mg m^{-3}), mesotrophic (0.1-1.0 mg m^{-3}) and eutrophic ($>1 \text{ mg m}^{-3}$) environments [*Gruber and Sarmiento*, 2006].

To assess the spatial and temporal variability in the geometry of the subtropical gyre we perform an inversion of geostrophic velocity data to obtain a geostrophic streamfunction, ψ , for our study domain. This is accomplished through an iterative approach for minimizing the total error of successive estimates of the streamfunction. The algorithm to accomplish this is based on a Tikhonov regularization and is described in detail by *Li et al.* [2006]. Once the streamfunction is calculated, we use the separatrix line, ψ_0 , to delineate the boundaries of the subtropical gyre.

B.2.2 Horizontal advective nutrient fluxes

The calculation of the divergence of horizontal advective fluxes of nitrate in the Ekman layer uses the standard formulation:

where U_H is the vertically integrated surface Ekman layer transport (in units of $\text{m}^2 \text{s}^{-1}$) total horizontal velocity and $[NO_3]_{Ek}$ is the average nitrate concentration within the Ekman layer (in units of mmol m^{-3}). To calculate the fluxes themselves, the velocity and nutrient fields are first mapped onto a common 1° grid before being multiplied together at every grid point.

To calculate the fractional contribution of the horizontal advective nutrient fluxes to observed new production in the transition region, we convert the satellite productivity estimates from net primary productivity (in units of $\text{mg C m}^{-2} \text{d}^{-1}$) to new primary production (in units of $\text{mol C m}^{-2} \text{d}^{-1}$) using the molar mass of carbon ($12.011 \text{ g mol}^{-1}$) and f

ratio values ranging from 0.06 (for waters within the oligotrophic region) to 0.13 (for waters in transitional zones between the oligotrophic regions and upwelling area, such as the subpolar gyre and the equatorial upwelling zone) [Epply and Peterson, 1979]. To convert the nutrient flux divergences (in units of $\text{mmol N m}^{-2} \text{s}^{-1}$) to new production (same units as above), we use Redfield stoichiometry ($\text{C/N} = 106/16$).

References

- Ayers, J. M., and M. S. Lozier (2010), Physical controls on the seasonal migration of the North Pacific transition zone chlorophyll front, *Journal of Geophysical Research-Oceans*, 115, doi: 10.1029/2009jc005596.
- Ayers, J. M., and M. S. Lozier (2010), Physical controls on the seasonal migration of the North Pacific transition zone chlorophyll front, *Journal of Geophysical Research-Oceans*, 115, doi: 10.1029/2009jc005596.
- Barber, R. T., and F. P. Chavez (1991), Regulation of Primary Productivity Rate in the Equatorial Pacific, *Limnol Oceanogr*, 36(8), 1803-1815.
- Behrenfeld, M. J., and P. G. Falkowski (1997), Photosynthetic rates derived from satellite-based chlorophyll concentration, *Limnol Oceanogr*, 42(1), 1-20.
- Behrenfeld, M. J., E. Boss, D. A. Siegel, and D. M. Shea (2005), Carbon-based ocean productivity and phytoplankton physiology from space, *Global Biogeochem Cy*, 19(1).
- Behrenfeld, M. J., R. T. O'Malley, D. A. Siegel, C. R. McClain, J. L. Sarmiento, G. C. Feldman, A. J. Milligan, P. G. Falkowski, R. M. Letelier, and E. S. Boss (2006), Climate-driven trends in contemporary ocean productivity, *Nature*, 444(7120), 752-755, doi: 10.1038/nature05317.
- Behrenfeld, M. J. (2010), Abandoning Sverdrup's Critical Depth Hypothesis on phytoplankton blooms, *Ecology*, 91(4), 977-989.
- Bidigare, R. R., F. Chai, M. R. Landry, R. Lukas, C. C. S. Hannides, S. J. Christensen, D. M. Karl, L. Shi, and Y. Chao (2009), Subtropical ocean ecosystem structure changes forced by North Pacific climate variations, *Journal of Plankton Research*, 31(10), 1131-1139, doi: 10.1093/plankt/fbp064.
- Bonnet, S., I. C. Biegala, P. Dutrieux, L. O. Slemmons, and D. G. Capone (2009), Nitrogen fixation in the western equatorial Pacific: Rates, diazotrophic cyanobacterial size class distribution, and biogeochemical significance, *Global Biogeochem Cy*, 23.
- Bopp, L., P. Monfray, O. Aumont, J. L. Dufresne, H. Le Treut, G. Madec, L. Terray, and J. C. Orr (2001), Potential impact of climate change on marine export production, *Global Biogeochemical Cycles*, 15(1), 81-99.
- Boyce, D. G., M. R. Lewis, and B. Worm (2010), Global phytoplankton decline over the past century, *Nature*, 466(7306), 591-596.

- Boyd, P. W., and S. C. Doney (2002), Modelling regional responses by marine pelagic ecosystems to global climate change, *Geophysical Research Letters*, 29(16), doi: 10.1029/2001gl014130.
- Brix, H., N. Gruber, D. M. Karl, and N. R. Bates (2006), On the relationships between primary, net community, and export production in subtropical gyres, *Deep-Sea Research Part II-Topical Studies in Oceanography*, 53(5-7), 698-717, doi: 10.1016/j.dsr2.2006.01.024.
- Bryden, H. L. and E. C. Brady (1989), Eddy momentum and heat fluxes and the effects on the circulation of the equatorial Pacific Ocean, *J Marine Sci*, 47(1), 55-79.
- Carr, M-E. N.S. Oakey, and M. R. Lewis (1996), Vertical mixing in the equatorial Pacific along 150W in March 1988, *J Phys Oceanogr* 27(3), 373-387.
- Cermeno, P., S. Dutkiewicz, R. P. Harris, M. Follows, O. Schofield, and P. G. Falkowski (2008), The role of nutricline depth in regulating the ocean carbon cycle, *Proceedings of the National Academy of Sciences of the United States of America*, 105(51), 20344-20349, doi: 10.1073/pnas.0811302106.
- Chelton, D. B., R. A. DeSzoeke, M. G. Schlax, K. El Naggar, and N. Siwertz (1998), Geographical variability of the first baroclinic Rossby radius of deformation, *J Phys Oceanogr*, 28(3), 433-460.
- Chelton, D. B., M. G. Schlax, M. H. Freilich, and R. F. Milliff (2004), Satellite measurements reveal persistent small-scale features in ocean winds, *Science*, 303(5660), 978-983.
- Church, M. J., C. Mahaffey, R. M. Letelier, R. Lukas, J. P. Zehr, and D. M. Karl (2009), Physical forcing of nitrogen fixation and diazotroph community structure in the North Pacific subtropical gyre, *Global Biogeochemical Cycles*, 23, doi: 10.1029/2008gb003418.
- Corno, G., D. M. Karl, M. J. Church, R. M. Letelier, R. Lukas, R. R. Bidigare, and M. R. Abbott (2007), Impact of climate forcing on ecosystem processes in the North Pacific Subtropical Gyre, *Journal of Geophysical Research-Oceans*, 112(C4), doi: 10.1029/2006jc003730.
- Corno, G., R. M. Letelier, M. R. Abbott, and D. M. Karl (2008), Temporal and vertical variability in photosynthesis in the North Pacific Subtropical Gyre, *Limnology and Oceanography*, 53(4), 1252-1265.
- Cravatte, S., G. Madec, T. Izumo, C. Menkes, and A. Bozec (2007), Progress in the 3-D circulation of the eastern equatorial Pacific in a climate ocean model. *Ocean Modelling*, 17(1), 28-48.
- Dave, A. C., and M. S. Lozier (2010), Local stratification control of marine productivity in the subtropical North Pacific, *Journal of Geophysical Research-Oceans*, 115(C12), C12032.

- Di Lorenzo, E., et al. (2008), North Pacific Gyre Oscillation links ocean climate and ecosystem change, *Geophysical Research Letters*, 35(8) , doi: 10.1029/2007gl032838.
- Doney, S. C. (2006), Oceanography - Plankton in a warmer world, *Nature*, 444(7120), 695-696, doi: 10.1038/444695a.
- Dore, J. E., J. R. Brum, L. M. Tupas, and D. M. Karl (2002), Seasonal and interannual variability in sources of nitrogen supporting export in the oligotrophic subtropical North Pacific Ocean, *Limnology and Oceanography*, 47(6), 1595-1607.
- Dore, J. E., R. M. Letelier, M. J. Church, R. Lukas, and D. M. Karl (2008), Summer phytoplankton blooms in the oligotrophic North Pacific Subtropical Gyre: Historical perspective and recent observations, *Progress in Oceanography*, 76(1), 2-38, doi: 10.1016/j.pocean.2007.10.002.
- Duarte, C. M., and J. Cebrian (1996), The fate of marine autotrophic production, *Limnology and Oceanography*, 41(8), 1758-1766.
- Dugdale, R. C. (1967), Nutrient Limitation in Sea - Dynamics Identification and Significance, *Limnology and Oceanography*, 12(4), 685-&.
- Dugdale, R. C., F. P. Wilkerson, and H. J. Minas (1995), The Role of a Silicate Pump in Driving New Production, *Deep-Sea Res Pt I*, 42(5), 697-719.
- Dugdale, R. C., A. G. Wischmeyer, F. P. Wilkerson, R. T. Barber, F. Chai, M. S. Jiang, and T. H. Peng (2002), Meridional asymmetry of source nutrients to the equatorial Pacific upwelling ecosystem and its potential impact on ocean-atmosphere CO₂ flux; a data and modeling approach, *Deep-Sea Res Pt Ii*, 49(13-14), 2513-2531.
- Emery, W. J., and J. S. Dewar (1982), Mean Temperature-Salinity, Salinity-Depth and Temperature-Depth Curves for the North-Atlantic and the North Pacific, *Progress in Oceanography*, 11(3), 219-&.
- Eppley, R. W., E. H. Renger, E. L. Venrick, and M. M. Mullin (1973), Study of Plankton Dynamics and Nutrient Cycling in Central Gyre of North Pacific Ocean, *Limnology and Oceanography*, 18(4), 534-551.
- Eppley, R. W., and B. J. Peterson (1979), Particulate organic-matter flux and planktonic new production in the deep ocean, *Nature*, 282(5740), 677-680.
- Evans, W., P. G. Stratton, and F. P. Chavez (2009), Impact of tropical instability waves on nutrient and chlorophyll distributions in the equatorial Pacific, *Deep-Sea Res Pt I*, 56(2), 178-188.
- Falkowski, P. G., R. T. Barber, and V. Smetacek (1998), Biogeochemical Controls and Feedbacks on Ocean Primary Production, *Science*, 281(5374), 200-206.

- Falkowski, P. G., and M. J. Oliver (2007), Mix and match: how climate selects phytoplankton, *Nature Reviews Microbiology*, 5(10), 813-819, doi: 10.1038/nrmicro1751.
- Fennel, K., and E. Boss (2003), Subsurface maxima of phytoplankton and chlorophyll: Steady-state solutions from a simple model, *Limnology and Oceanography*, 48(4), 1521-1534.
- Follows, M., and S. Dutkiewicz (2002), Meteorological modulation of the North Atlantic spring bloom, *Deep-Sea Research Part II-Topical Studies in Oceanography*, 49(1-3), 321-344.
- Fong, A. A., D. M. Karl, R. Lukas, R. M. Letelier, J. P. Zehr, and M. J. Church (2008), Nitrogen fixation in an anticyclonic eddy in the oligotrophic North Pacific Ocean, *Isme Journal*, 2(6), 663-676, doi: 10.1038/ismej.2008.22.
- Gao, Y., S. M. Fan, and J. L. Sarmiento (2003), Aeolian iron input to the ocean through precipitation scavenging: A modeling perspective and its implication for natural iron fertilization in the ocean, *J Geophys Res-Atmos*, 108(D7).
- Grabowski, M. N. W., M. J. Church, and D. M. Karl (2008), Nitrogen fixation rates and controls at Stn ALOHA, *Aquatic Microbial Ecology*, 52(2), 175-183, doi: 10.3354/ame01209.
- Gregg M.C. 1991. The study of mixing in the ocean: a brief history. *Oceanography* 4 (1): 39-45.
- Gregg, W. W., N. W. Casey, and C. R. McClain (2005), Recent trends in global ocean chlorophyll, *Geophysical Research Letters*, 32(3), doi: 10.1029/2004gl021808.
- Gruber, N., C. D. Keeling, and N. R. Bates (2002), Interannual variability in the North Atlantic Ocean carbon sink, *Science*, 298(5602), 2374-2378.
- Hasse, L., and S. D. Smith (1997), Local sea surface wind, wind stress, and sensible and latent heat fluxes, *Journal of Climate*, 10(11), 2711-2724.
- Henson, S. A., J. P. Dunne, and J. L. Sarmiento (2009), Decadal variability in North Atlantic phytoplankton blooms, *J Geophys Res-Oceans*, 114, -.
- Hu, C. M., E. T. Montgomery, R. W. Schmitt, and F. E. Muller-Karger (2004), The dispersal of the Amazon and Orinoco River water in the tropical Atlantic and Caribbean Sea: Observation from space and S-PALACE floats, *Deep-Sea Res Pt II*, 51(10-11), 1151-1171.
- Huisman, J., N. N. P. Thi, D. M. Karl, and B. Sommeijer (2006), Reduced mixing generates oscillations and chaos in the oceanic deep chlorophyll maximum, *Nature*, 439(7074), 322-325, doi: 10.1038/nature04245.

- Irwin, A. J., and M. J. Oliver (2009), Are ocean deserts getting larger?, *Geophysical Research Letters*, 36, doi: 10.1029/2009gl039883.
- Johnson, G. C. (2001), Equatorial Pacific Ocean horizontal velocity, divergence, and upwelling (vol 31, pg 839, 2001), *J Phys Oceanogr*, 31(7), 1936-1936.
- Johnson, E. S., F. Bonjean, G. S. E. Lagerloef, J. T. Gunn, and G. T. Mitchum (2007), Validation and error analysis of OSCAR sea surface currents, *Journal of Atmospheric and Oceanic Technology*, 24(4), 688-701.
- Kahru, M., S. T. Gille, R. Murtugudde, P. G. Strutton, M. Manzano-Sarabia, H. Wang, and B. G. Mitchell (2010), Global correlations between winds and ocean chlorophyll, *J Geophys Res-Oceans*, 115.
- Karl, D. M., R. Letelier, D. Hebel, L. Tupas, J. Dore, J. Christian, and C. Winn (1995), Ecosystem Changes in the North Pacific Subtropical Gyre Attributed to the 1991-92 El-Nino, *Nature*, 373(6511), 230-234.
- Karl, D. M., and R. Lukas (1996), The Hawaii Ocean Time-series (HOT) program: Background, rationale and field implementation, *Deep-Sea Research Part II-Topical Studies in Oceanography*, 43(2-3), 129-156.
- Karl, D. M., J. R. Christian, J. E. Dore, D. V. Hebel, R. M. Letelier, L. M. Tupas, and C. D. Winn (1996), Seasonal and interannual variability in primary production and particle flux at Station ALOHA, *Deep-Sea Research Part II-Topical Studies in Oceanography*, 43(2-3), 539-568.
- Karl, D., R. Letelier, L. Tupas, J. Dore, J. Christian, and D. Hebel (1997), The role of nitrogen fixation in biogeochemical cycling in the subtropical North Pacific Ocean, *Nature*, 388(6642), 533-538.
- Karl, D. M. (1999), A sea of change: Biogeochemical variability in the North Pacific Subtropical Gyre, *Ecosystems*, 2(3), 181-214.
- Karl, D. M., R. R. Bidigare, and R. M. Letelier (2001), Long-term changes in plankton community structure and productivity in the North Pacific Subtropical Gyre: The domain shift hypothesis, *Deep-Sea Research Part II-Topical Studies in Oceanography*, 48(8-9), 1449-1470.
- Karl, D. M., E. A. Laws, P. Morris, P. J. L. Williams, and S. Emerson (2003), Global carbon cycle - Metabolic balance of the open sea, *Nature*, 426(6962), 32-32.
- Kessler, W. S. (2006), The circulation of the eastern tropical Pacific: A review, *Prog Oceanogr*, 69(2-4), 181-217.

- Lagerloef, G. S. E., G. T. Mitchum, R. B. Lukas, and P. P. Niiler (1999), Tropical Pacific near-surface currents estimated from altimeter, wind, and drifter data, *J Geophys Res-Oceans*, 104(C10), 23313-23326.
- Le Borgne, R., R. A. Feely, and D. J. Mackey (2002), Carbon fluxes in the equatorial Pacific: a synthesis of the JGOFS programme, *Deep-Sea Res Pt I*, 49(13-14), 2425-2442.
- Ledwell, J. R., A. J. Watson, and C. S. Law (1993), Evidence for Slow Mixing across the Pycnocline from an Open-Ocean Tracer-Release Experiment, *Nature*, 364(6439), 701-703.
- Lengaigne, M., G. Madec, C. Menkes, and G. Alory (2003), Impact of isopycnal mixing on the tropical ocean circulation, *J Geophys Res-Oceans*, 108(C11).
- Letelier, R. M., R. R. Bidigare, D. V. Hebel, M. Ondrusek, C. D. Winn, and D. M. Karl (1993), Temporal Variability of Phytoplankton Community Structure-Based on Pigment Analysis, *Limnology and Oceanography*, 38(7), 1420-1437.
- Letelier, R. M., J. E. Dore, C. D. Winn, and D. M. Karl (1996), Seasonal and interannual variations in photosynthetic carbon assimilation at Station ALOHA, *Deep-Sea Research Part I-Topical Studies in Oceanography*, 43(2-3), 467-490.
- Letelier, R. M., D. M. Karl, M. R. Abbott, P. Flament, M. Freilich, R. Lukas, and T. Strub (2000), Role of late winter mesoscale events in the biogeochemical variability of the upper water column of the North Pacific Subtropical Gyre, *Journal of Geophysical Research-Oceans*, 105(C12), 28723-28739.
- Letelier, R. M., D. M. Karl, M. R. Abbott, and R. R. Bidigare (2004), Light driven seasonal patterns of chlorophyll and nitrate in the lower euphotic zone of the North Pacific Subtropical Gyre, *Limnology and Oceanography*, 49(2), 508-519.
- Lewis, M. R., W. G. Harrison, N. S. Oakey, D. Hebert, and T. Platt (1986), Vertical Nitrate Fluxes in the Oligotrophic Ocean, *Science*, 234(4778), 870-873.
- Li, Z., Y. Chao, and J. C. McWilliams (2006), Computation of the streamfunction and velocity potential for limited and irregular domains, *Monthly Weather Review*, 134(11), 3384-3394.
- Lien, R. C., D. R. Caldwell, M. C. Gregg, and J. N. Moum (1995), Turbulence Variability at the Equator in the Central Pacific at the Beginning of the 1991-1993 El-Nino, *J Geophys Res-Oceans*, 100(C4), 6881-6898.
- Longhurst, A. (1993), Seasonal cooling and blooming in tropical oceans, *Deep-Sea Res Pt I*, 40(11-12), 2145-2165.
- Longhurst, A. (1995), Interpreting CZCS images of the Amazon Plume: Reply, *Deep-Sea Res Pt I*, 42(11-12), 2139-2141.

- Lozier, M. S., W. B. Owens, and R. G. Curry (1995), The climatology of the North Atlantic, *Progress in Oceanography*, 36(1), 1-44.
- Lozier, M. S., A. C. Dave, J. B. Palter, L. M. Gerber, and R. T. Barber (2011), On the relationship between stratification and primary productivity in the North Atlantic, *Geophys Res Lett*, 38.
- Lukas, R. (2001), Freshening of the upper thermocline in the North Pacific subtropical gyre associated with decadal changes of rainfall, *Geophysical Research Letters*, 28(18), 3485-3488.
- Lukas, R., and F. Santiago-Mandujano (2008), Interannual to Interdecadal Salinity Variations Observed Near Hawaii: Local and Remote Forcing by Surface Freshwater Fluxes, *Oceanography*, 21(1), 46-55.
- Macdonald, A. M., T. Suga, and R. G. Curry (2001), An isopycnally averaged North Pacific climatology, *Journal of Atmospheric and Oceanic Technology*, 18(3), 394-420.
- Mahaffey, C., C. R. Benitez-Nelson, R. R. Bidigare, Y. Rii, and D. M. Karl (2008), Nitrogen dynamics within a wind-driven eddy, *Deep-Sea Research Part II-Topical Studies in Oceanography*, 55(10-13), 1398-1411, doi: 10.1016/j.dsr2.2008.02.004.
- Mantua, N. J., S. R. Hare, Y. Zhang, J. M. Wallace, and R. C. Francis (1997), A Pacific interdecadal climate oscillation with impacts on salmon production, *Bulletin of the American Meteorological Society*, 78(6), 1069-1079.
- Marcello, J., A. Hernandez-Guerra, F. Eugenio, and A. Fonte (2011), Seasonal and temporal study of the northwest African upwelling system, *International Journal of Remote Sensing*, 32(7), 1843-1859.
- Martinez, E., D. Antoine, F. D'Ortenzio, and B. Gentili (2009), Climate-Driven Basin-Scale Decadal Oscillations of Oceanic Phytoplankton, *Science*, 326(5957), 1253-1256.
- McClain, C. R., S. R. Signorini, and J. R. Christian (2004), Subtropical gyre variability observed by ocean-color satellites, *Deep-Sea Research Part II-Topical Studies in Oceanography*, 51(1-3), 281-301, doi: 10.1016/j.dsr2.2003.08.002.
- McGillicuddy, D. J., A. R. Robinson, D. A. Siegel, H. W. Jannasch, R. Johnson, T. Dickey, J. McNeil, A. F. Michaels, and A. H. Knap (1998), Influence of mesoscale eddies on new production in the Sargasso Sea, *Nature*, 394(6690), 263-266.
- Meinen, C. S., M. J. McPhaden, and G. C. Johnson (2001), Vertical velocities and transports in the equatorial Pacific during 1993-99, *J Phys Oceanogr*, 31(11), 3230-3248.
- Menzel, D. W., and J. H. Ryther (1961), Annual Variations in Primary Production of the Sargasso Sea Off Bermuda, *Deep-Sea Res*, 7(4), 282-288.

- Meskhidze, N., W. L. Chameides, A. Nenes, and G. Chen (2003), Iron mobilization in mineral dust: Can anthropogenic SO₂ emissions affect ocean productivity?, *Geophys Res Lett*, 30(21).
- Mills, M. M., and K. R. Arrigo (2010), Magnitude of oceanic nitrogen fixation influenced by the nutrient uptake ratio of phytoplankton, *Nat Geosci*, 3(6), 412-416.
- Moore, J. K., S. C. Doney, J. A. Kleypas, D. M. Glover, and I. Y. Fung (2002), An intermediate complexity marine ecosystem model for the global domain, *Deep-Sea Res Pt II*, 49(1-3), 403-462.
- Moum, J. N., and J. D. Nash (2009), Mixing Measurements on an Equatorial Ocean Mooring, *J Atmos Ocean Tech*, 26(2), 317-336.
- Muller-Karger, F. E., C. R. McClain, and P. L. Richardson (1988), The dispersal of the Amazon's water, *Nature*, 333(6168), 56-59.
- Muller-Karger, F. E., C. R. McClain, T. R. Fisher, W. E. Esaias, and R. Varela (1989), Pigment distribution in the Caribbean sea - observations from space, *Prog Oceanogr*, 23(1), 23-64.
- Muller-Karger, F. E., P. L. Richardson, and D. McGillicuddy (1995), On the offshore dispersal of the Amazon's Plume in the North Atlantic: Comments, *Deep-Sea Res Pt I*, 42(11-12), 2127-&.
- Nicholson, D., S. Emerson, and C. C. Eriksen (2008), Net community production in the deep euphotic zone of the subtropical North Pacific gyre from glider surveys, *Limnology and Oceanography*, 53(5), 2226-2236.
- Palter, J. B., M. S. Lozier, and R. T. Barber (2005), The effect of advection on the nutrient reservoir in the North Atlantic subtropical gyre, *Nature*, 437(7059), 687-692 doi: 10.1038/nature03969.
- Pena, M. A., M. R. Lewis, and J. J. Cullen (1994), New Production in the Warm Waters of the Tropical Pacific-Ocean, *J Geophys Res-Oceans*, 99(C7), 14255-14268.
- Pennington, J. T., K. L. Mahoney, V. S. Kuwahara, D. D. Kolber, R. Calienes, and F. P. Chavez (2006), Primary production in the eastern tropical Pacific: A review, *Prog Oceanogr*, 69(2-4), 285-317.
- Peters, H., M. C. Gregg, and J. M. Toole (1988), On the Parameterization of Equatorial Turbulence, *J Geophys Res-Oceans*, 93(C2), 1199-1218.
- Polovina, J. J., E. A. Howell, and M. Abecassis (2008), Ocean's least productive waters are expanding, *Geophysical Research Letters*, 35(3), doi: 10.1029/2007gl031745.

- Richards, K.J., and N. R. Edwards (2003), Lateral mixing in the equatorial Pacific: the importance of inertial instability. *Geophys. Res. Lett.* 30(17), 1888
- Riebesell, U., A. Kortzinger, and A. Oschlies (2009), Sensitivities of marine carbon fluxes to ocean change, *P Natl Acad Sci USA*, 106(49), 20602-20609.
- Rii, Y. M., S. L. Brown, F. Nencioli, V. Kuwahara, T. Dickey, D. M. Karl, and R. R. Bidigare (2008), The transient oasis: Nutrient-phytoplankton dynamics and particle export in Hawaiian lee cyclones, *Deep-Sea Research Part II-Topical Studies in Oceanography*, 55(10-13), 1275-1290, doi: 10.1016/j.dsr2.2008.01.013.
- Rixen, T., C. Goyet, and V. Ittekkot (2006), Diatoms and their influence on the biologically mediated uptake of atmospheric CO₂ in the Arabian Sea upwelling system, *Biogeosciences*, 3(1), 1-13.
- Ryan, J. P., I. Ueki, Y. Chao, H. C. Zhang, P. S. Polito, and F. P. Chavez (2006), Western Pacific modulation of large phytoplankton blooms in the central and eastern equatorial Pacific, *J Geophys Res-Biogeophys*, 111(G2).
- Saba, V. S., et al. (2010), Challenges of modeling depth-integrated marine primary productivity over multiple decades: A case study at BATS and HOT, *Global Biogeochem Cy*, 24.
- Sakamoto, C. M., D. M. Karl, H. W. Jannasch, R. R. Bidigare, R. M. Letelier, P. M. Walz, J. P. Ryan, P. S. Polito, and K. S. Johnson (2004), Influence of Rossby waves on nutrient dynamics and the plankton community structure in the North Pacific subtropical gyre, *Journal of Geophysical Research-Oceans*, 109(C5), doi: 10.1029/2003jc001976.
- Sarmiento, J. L., et al. (2004), Response of ocean ecosystems to climate warming, *Global Biogeochemical Cycles*, 18(3), GB3003, doi:10.1029/2003GB002134.
- Schmittner, A. (2005), Decline of the marine ecosystem caused by a reduction in the Atlantic overturning circulation, *Nature*, 434(7033), 628-633, doi: 10.1038/nature03476.
- Smith, R. B., and V. Grubisic (1993), Aerial Observations of Hawaii Wake, *J Atmos Sci*, 50(22), 3728-3750.
- Stammer, D., S. Park, A. Kohl, R. Lukas, and F. Santiago-Mandujano (2008), Causes for large-scale hydrographic changes at the Hawaii Ocean time series station, *Journal of Physical Oceanography*, 38(9), 1931-1948, doi: 10.1175/2008jpo3751.1.
- Stanley, R. H. R., J. B. Kirkpatrick, N. Cassar, B. A. Barnett, and M. L. Bender (2010), Net community production and gross primary production rates in the western equatorial Pacific, *Global Biogeochem Cy*, 24.

- Strutton, P. G., J. P. Ryan, and F. P. Chavez (2001), Enhanced chlorophyll associated with tropical instability waves in the equatorial Pacific, *Geophys Res Lett*, 28(10), 2005-2008.
- Sudre, J., and R. A. Morrow (2008), Global surface currents: a high-resolution product for investigating ocean dynamics, *Ocean Dynam*, 58(2), 101-118.
- Suga, T., A. Kato, and K. Hanawa (2000), North Pacific Tropical Water: its climatology and temporal changes associated with the climate regime shift in the 1970s, *Progress in Oceanography*, 47(2-4), 223-256.
- Suga, T., K. Motoki, Y. Aoki, and A. M. Macdonald (2004), The North Pacific climatology of winter mixed layer and mode waters, *Journal of Physical Oceanography*, 34(1), 3-22.
- Sverdrup, H. U. (1953), On Conditions for the Vernal Blooming of Phytoplankton, *ICES J. Mar. Sci.*, 18(3), 287-295, doi: 10.1093/icesjms/18.3.287.
- Ueyama, R., and B. C. Monger (2005), Wind-induced modulation of seasonal phytoplankton blooms in the North Atlantic derived from satellite observations, *Limnology and Oceanography*, 50(6), 1820-1829.
- Vantrepotte, V., and F. Melin (2009), Temporal variability of 10-year global SeaWiFS time-series of phytoplankton chlorophyll a concentration, *Ices J Mar Sci*, 66(7), 1547-1556.
- Venrick, E. L. (1982), Phytoplankton in an Oligotrophic Ocean - Observations and Questions, *Ecological Monographs*, 52(2), 129-154.
- Venrick, E. L. (1993), Phytoplankton Seasonality in the Central North Pacific - the Endless Summer Reconsidered, *Limnology and Oceanography*, 38(6), 1135-1149.
- Visbeck, M., J. Marshall, T. Haine, and M. Spall (1997), Specification of eddy transfer coefficients in coarse-resolution ocean circulation models, *J Phys Oceanogr*, 27(3), 381-402.
- Wells, M. L., G. K. Vallis, and E. A. Silver (1999), Tectonic processes in Papua New Guinea and past productivity in the eastern equatorial Pacific Ocean, *Nature*, 398(6728), 601-604.
- White, A. E., Y. H. Spitz, and R. M. Letelier (2007), What factors are driving summer phytoplankton blooms in the North Pacific Subtropical Gyre?, *Journal of Geophysical Research-Oceans*, 112(C12), doi: 10.1029/2007jc004129.
- Williams, R. G., and M. J. Follows (1998), The Ekman transfer of nutrients and maintenance of new production over the North Atlantic, *Deep-Sea Research Part I-Oceanographic Research Papers*, 45(2-3), 461-489.

- Wilson, C., and D. Adamec (2002), A global view of bio-physical coupling from SeaWiFS and TOPEX satellite data, 1997-2001, *Geophys Res Lett*, 29(8).
- Winn, C. D., L. Campbell, J. R. Christian, R. M. Letelier, D. V. Hebel, J. E. Dore, L. Fujieki, and D. M. Karl (1995), Seasonal Variability in the Phytoplankton Community of the North Pacific Subtropical Gyre, *Global Biogeochemical Cycles*, 9(4), 605-620.
- Xie, S. P., W. T. Liu, Q. Y. Liu, and M. Nonaka (2001), Far-reaching effects of the Hawaiian islands on the Pacific Ocean-atmosphere system, *Science*, 292(5524), 2057-2060.

Biography

Apurva Dave was born in London in the United Kingdom on the 2nd of November, 1972. He earned a B.Sc. in Chemistry from the University of Florida in 1995 and an M.A. in Geology (Paleoceanography/ Chemical Oceanography) from the University of California at Santa Barbara in 2000. He has published two articles: as first author on “Local stratification control of marine productivity in the subtropical North Pacific” appearing in the Journal of Geophysical Research in 2010, and as second author on “On the relationship between stratification and primary productivity in the North Atlantic” appearing in Geophysical Research Letters in 2011. He was awarded an NC SpaceGrant Graduate Student Fellowship for the year 2007-2008 and was a Duke Preparing Future Faculty Fellow for the year 2009-2010. He is married and has two children.